Utrecht University

Publiek energiebedrijf van en voor Nederland

Rotliegend in the North Sea 5 Nations Area

Understanding the deposition of the Rotliegend and the possible potential

Driel, S.F. van (Sofie), studentnummer: 1641182,
UU supervisor : Dr. Fred Beekman
EBN supervisor: Daan den Hartog Jager
8/1/25

Abstract

The Rotliegend is a key reservoir play in Western Europe, yet the Rotliegend in the far Dutch offshore and in the neighbouring countries is poorly understood and relatively unexplored due to the lack of available data. This problem is further complicated by the sporadic distribution of the Lower Rotliegend Volcanics and its poorly understood relationship with the Upper Rotliegend sediments. This study was conducted to investigate the distribution, deposition, and interplay of the Upper and Lower Rotliegend, aiming to identify unrealised reservoir potential in the far Dutch offshore by analysing data across the Netherlands, Germany, Denmark, Norway, and the UK. Using well data, cores, porosity-permeability measurements, and literature, I constructed well correlation panels, thickness maps, gross depositional maps, and poro-perm-depth plots. Well correlations and thickness mapping showed that the Volcanics varied in components and appeared in all five nations. Thick Volcanics were usually associated with a thin or absent Upper Rotliegend, and deposition of the Volcanics was likely paired with faulting. Coeval with magmatism was the formation of half-graben-like structures, aiding in the deposition of sediments in the Lower and Upper Rotliegend. Thickening trends showed that Upper Rotliegend sands in the Northern Permian Basin (NPB) were thicker closer to the Rotliegend Volcanics than the Sands and sediments in the Southern Permian Basin (SPB). This difference is possibly related to the wind direction or differential subsidence. In the Netherlands, the wind direction from the Northeast may have caused sand to become contaminated with Volcanic material limiting reservoir potential in areas close to these volcancs. Porosity-permeability and depth data showed that the alluvial depositional environments had poor porosity and permeability, whilst fluvial, alluvial-aeolian, and aeolian sediments had a clear porosity-permeability trend. Overall, the results indicate that the far Dutch offshore holds reservoir potential, especially in blocks A11, A12, A15 & B13.

Keywords: Rotliegend, five-nation area, Rotliegend Volcanics, Reservoir, well correlation, Gross Depositional Environment, Porosity-Permeability, and depth.

Table of Contents

Table of Figures:

Main Report figures & tables:

Appendix figures and tables:

1. Introduction:

The red beds that underlie the Zechstein, commonly known as the Rotliegend or Rotliegendes (Heeremans et al., 2004a; K. W. Glennie, 1972), has historically been and continues to be an important play in Europe and particularly in the Netherlands. This is exemplified by the fact that by 2010 ~10.000 wells across the Southern Permian basin had been drilled into the Rotliegend (Gast et al., 2010). The Rotliegend's notoriety comes from the fact that it has both an excellent seal in the form of the Zechstein salts and proven fluvial and aeolian reservoir sandstones in the upper clastic part of the Rotliegend (Doornenbal et al., 2019; Remmelts et al., 2025). The Lower Rotliegend also contains sands, but is primarily defined by the presence of Volcanic rock. These features also make the Upper Rotliegend an important play for future use, due to the increasing energy uncertainty in Europe's energy security and climate change (Remmelts et al., 2025).

In the offshore of the Netherlands, exploration began in 1968 in the K and L blocks (Verdier, 1996). For most of the onshore area of the Netherlands, exploration into the Rotliegend play has been very extensive. One part of the offshore that has been relatively unexplored to this day is the Dutch northern offshore (de Bruin et al., 2015), particularly in the A and B blocks of the Dutch offshore. As of now, ~10 wells have been drilled that penetrate the Rotliegend in the Dutch A-B blocks, most of which do not reach the lower boundary of the Rotliegend. The scarcity of good-quality seismic data further exacerbates this problem. Nevertheless, findings from the EBN exploration team's 2023 focus week suggested that the Dutch offshore may still have significant sand deposits.

A possible way to further our understanding of the northern offshore of the Netherlands, despite the limited data, is to connect it within a broader context by looking across borders. Most studies performed are regional exploration studies focused on a single country, which result in maps that terminate against national borders (Houben et al., 2020). Studies that do look across borders do exist, but are usually zoomed out to cover either the entirety of the Southern Permian Basin (SPB) or the Northern Permian Basin (NPB), resulting in a lack of detail. Maps that cross borders are challenging due to different nations defining their stratigraphy and structures differently, and a regional framework for the North Sea is not fully developed (Houben et al., 2020; Patruno et al., 2022), which often leads to a mismatch on maps. One study that has successfully looked across borders was the Paleo Five project from TNO, in which they looked at the pre-Westphalian stratigraphy(Houben et al., 2020). But such extensive studies are, as of now, lacking for the Permian interval.

This project aims to improve the perception of the distribution of the Rotliegend and particularly the sandstones in the far Dutch offshore in the five-nation area to hopefully identify new areas with reservoir potential. Through well correlation, thickness mapping,

Gross Depositional Environment mapping (GDE), and porosity-permeability-depth analyses in the Five-Nation area, this report will address the distribution of the Rotliegend, how it was deposited, and the transport direction. In addition, this report will explore where in the Dutch offshore area, good reservoir sands are located and the influence of the Lower Rotliegend Volcanics on the distribution of the sediments of the Upper Rotliegend. This report will show the most important findings in the main report, showcasing the most representative panels, photos, and plots. Supplementary figures and tables to support the main body of text are available in the Appendix. The Appendix contains a table showing all wells that were used, additional plots, core photos, well panels, and supplementary figures.

2. Geological Background:

2.1 Area of Interest: Five-Nation area

This cross-border study focuses on an area covering five countries, covering both parts of the SPB and NPB in the North Sea area. Due to the North Sea being an economically important body of water, it has been divided by maritime boundaries (Marsh, 2023). In the central-southern part of the North Sea, the borders of the Netherlands (NL), Germany (GER), Denmark (DK), Norway (NOR), and the United Kingdom (UK) come together in an area referred to as the five-nation area. This project will specifically look at the far outer edges of those five countries (424563,6297255), (674090,6295350), (425003,6096520) & (668669,6097838) (coordinate system=EPSG 23031)(Fig. 1). This area will include the A and B blocks in the Dutch offshore, the A & B blocks in the German offshore area, also referred to as the Entenschnabel. For the Danish area, its eastern margin runs along a straight N-S line from North Sea blocks B5503/02 to B5505/19. For Norway, the blocks cover the southern margin of the Norwegian offshore, including blocks 1-4. For the UK offshore, the area covers blocks 30, 31, 38, and 39 entirely, and the eastern parts of blocks 29 and 37. The most important Highs in the research area are the Mid North Sea High (MNSH), Ringkøbing-Fyn High (RKFH), and the Elbow Spit High (ESH). The area is also abundant with small and large faults, with the most important faults being the Paleo 5 fault, the Coffee Soil Fault, and the Søgne basin fault (Fig. 1B)

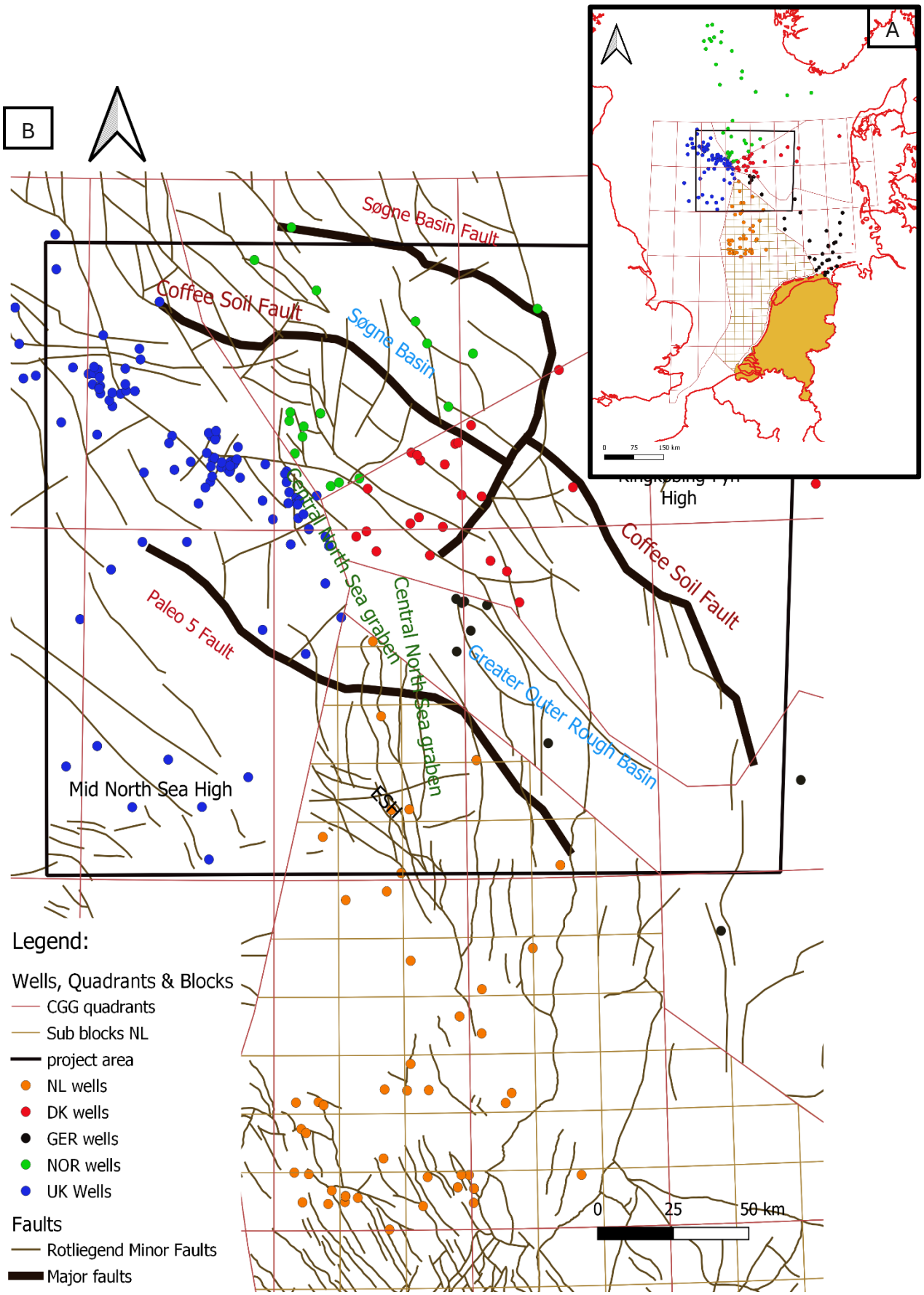

Figure 1 (A) Figure showing the location of the research area in the Dutch offshore area, with the Netherlands marked in brown and landmasses bordered by red. (B). Zoomed in on the area of interest and the most important structures, and all wells used in this project.

2.2 Tectonic history of the five-nation area:

The Rotliegend was deposited from the start of the Permian up to the middle to late Permian between ~300 and 258 Ma, and is present in much of the subsurface of Northwestern Europe (Glennie, 1998; Patruno et al., 2022). The deposition of these sediments coincides with the existence of the supercontinent Pangea (Heeremans, et al., 2004a), which formed due to the collision of Gondwana, Laurussia, and multiple microcontinents paired with the closure of the Rheic Ocean (~330 Ma) (de Jager et al., 2025; McCann et al., 2006) . This resulted in the Netherlands becoming landlocked (McCann et al., 2006). This convergence resulted in the pre-existing Dinantian basin, which started as being controlled by faults, to start deepening and drowning due to the thermal subsidence becoming dominant (Ter Borgh et al., 2018). The thermal subsidence led to the deepening of the Dinantian basin, with sediment input from the Variscan Mountains (de Jager et al., 2025; Ter Borgh et al., 2018). As the collision and compressive deformation continued and compressional forces overcame extensional forces, inversion occurred, causing the basin to be filled by the end of the Carboniferous (Westphalian), with the inversion intensity decreasing towards the north. This inversion was paired with reverse faults becoming active in the southern North Sea (Ter Borgh et al., 2018). This event is known as the Asturic Phase of deformation (Corfield et al., 1996; Heeremans et al., 2004a; Maynard & Dunay, 1999), and led to NWS-SE oriented faults and basins in the Southern North Sea reactivating with an uplift (Corfield et al., 1996; de Jager et al., 2025).

At the transition from the Carboniferous to the Permian, inversion had largely ceased, and much of western Europe became affected by wrench faulting, paired with extensive intrusive and extrusive magmatism and thermal uplift (de Jager et al., 2025; Ter Borgh et al., 2018). The Carboniferous-Permian tectonic event led to the reactivation of the NW-SE zone of weakness (Tornquest zone) and the development of a conjugate set of NE-SW-oriented faults and marks the change from foreland basin development to a thermal and extensional event (de Jager et al., 2025; Heeremans, et al., 2004a; Heeremans et al., 2004b).

The magmatic event varied in composition between alkaline to tholeiitic, with large-scale emplacement of basaltic and doleritic lavas and minor emplacement of felsic lavas (Heeremans et al., 2004b). For the most part, this activity was relatively short-lived, but, for example, in the Oslo Graben, it continued up to the Triassic period (Heeremans, et al., 2004b). Previous age determinations propose that the magmatic activity extended from 305 – 245 Ma, with the earliest event restricted to 305-290 Ma. However, other geochronological age dating suggest that the Volcanics were emplaced in the North Sea in multiple events based on findings in the Danish offshore (Heeremans et al., 2004b; Stemmerik et al., 2000; van Bergen et al., 2025). The origin of the

magmatism is still debated, with decompression paired with thinning of the lithosphere and a mantle plume both being proposed (Neumann et al., 2004; Van Wees et al., 2000).

The thermal uplift has been proposed to be induced by a combination of wrench tectonic, magmatic inflation, and thinning of the lithosphere (McCann et al., 2006). The uplift caused widespread deep erosion, resulting in the event best known as the Base Permian Unconformity (BPU) (Bouroullec et al., 2025; McCann et al., 2006; Ter Borgh et al., 2018). It was proposed that volcanism in the Netherlands, in what is now the offshore North Sea area, mainly took place in the Central Graben (Bouroullec et al., 2025). Sediments from this period (Autunian/ Early Permian) are rare and suggest that most of the southern and northern Permian basin was uplifted (Heeremans et al., 2004a; Van Wees et al., 2000). The sediments deposited in this period were dominated by Volcaniclastic rocks and alluvial deposits.

After the main magmatic event, a period of non-deposition took place, which is often referred to as the Saalian unconformity (Heeremans, et al., 2004a). During the Saalian event (~20 Ma), the Mid North Sea High (MNSH) and the Ringkøbing-Fyn High (RKFH) experienced uplift (de Jager et al., 2025). The Elbow Spit High, by comparison, was already pre-existing high in Devonian and/Carboniferous times (Ter Borgh et al., 2018) Here, the Saalian unconformity is associated with the northward development of the Variscan orogeny (Glennie, 2005; Heeremans., 2004a). After this event of non-deposition, the thermal anomaly introduced during the start of the Permian-Carboniferous event started to decay, resulting in thermal subsidence, the formation of basins, and the widespread sedimentation of the Upper Rotliegend group (de Jager et al., 2025; Heeremans., 2004a; Ter Borgh et al., 2018).

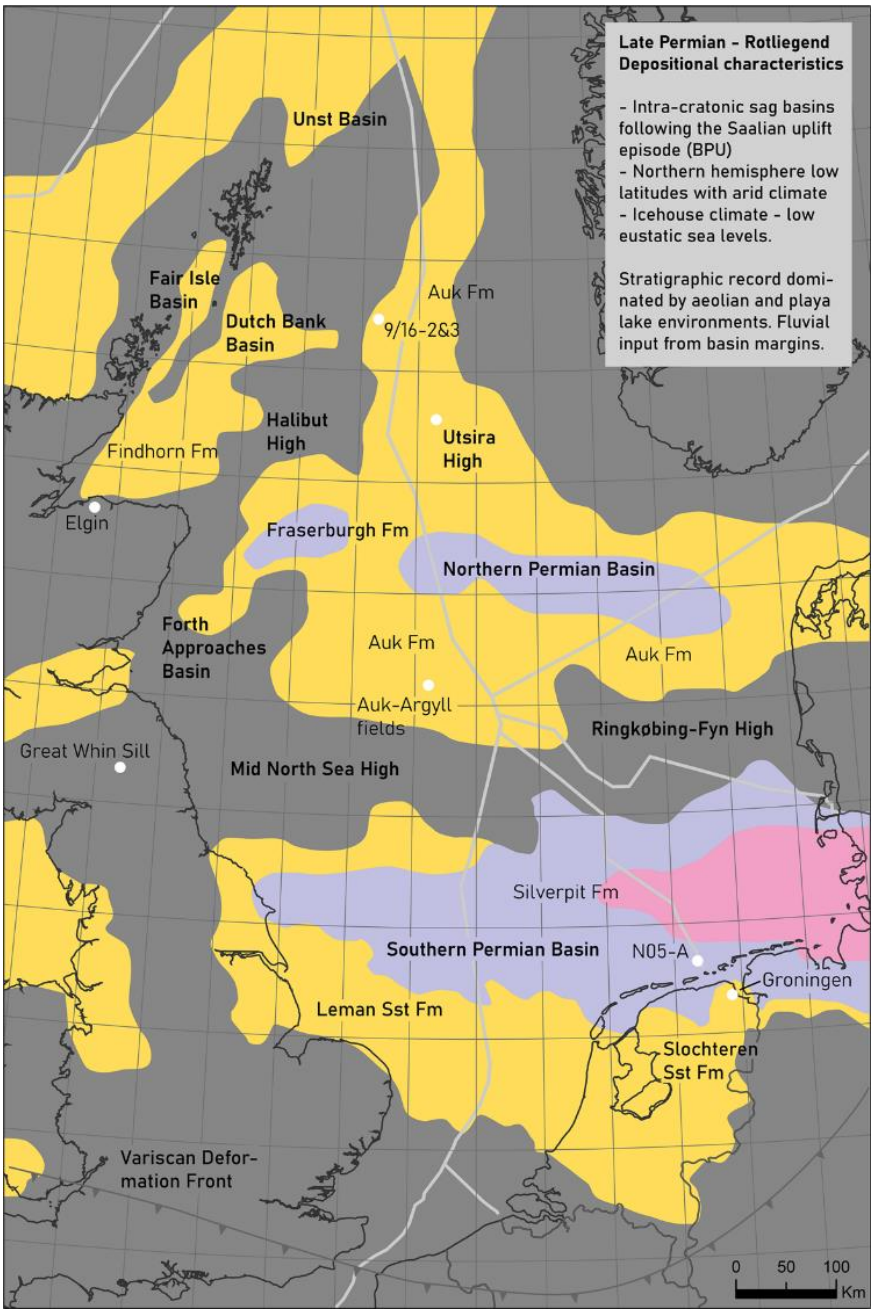

Figure 2.Figure showing the area of interest on the locations of the NPB and the SPB as interpreted by Patruno et al., (2022).

Due to thermal subsidence, two E-W oriented basins developed, known as the Southern and Northern Permian (SPB & NPB) ~263 Ma (Glennie, 2005)(Fig.2). The Southern Permian Basin or the Southern North Sea Permian Basin (SNPB) stretched from the UK to Poland, and its margins were made of the London-Brabant Massif and the Rhennish Massif in the south and the MNSH and the RKFH in the north (Bouroullec et al., 2025). The SPB is an amalgamation of three basins, of which the Anglo-Dutch basin is the most important concerning the study area. The depositional area within the SPB gradually expanded from the middle to late Permian towards its Southern and Northern margins (Bouroullec et al., 2025). The Northern Permian basin extends in an E-W direction from the shores of Scotland into Northern Denmark and is the smaller of the two basins (Van Wees et al., 2000). During the Rotliegend, the basin was filled with sediments whilst the basins continued to subside, and once subsidence rates exceeded sedimentation rates, the basins started to be filled by the sea, marking the end of the deposition of the Rotliegend and the onset of the Zechstein (de Jager et al., 2025).

2.3 Palaeoenvironment-and-climate

Towards the end of the Carboniferous, the study area was situated just north of the equator and had humid equatorial conditions (Glennie, 1998). During the Permian, the study area was situated in the northern hemisphere between 10-30 N° (Gast et al., 2010). It is thought that the study area had a semi-desert climate like modern Arabia or the Sahara (Armour et al., 2004; Bouroullec et al., 2025) . The southern margin of the SPB was kept dry due to the Variscan mountains in the south, which likely acted as a rain shadow for the southern part of the southern Permian basin (McKie, 2011). During the deposition of the Upper Rotliegend, the research area was still drifting north, affecting the climate at the time. Based on the palaeogeography, it is likely that the Rotliegend basins were affected by the Northeasterly trade winds (Glennie, 1998). Glennie (1998) also proposed that these winds were likely much faster than modern-day winds. Glennie (1998) argues that most of the Rotliegend was deposited during glacial periods with large ice caps, resulting in low-pressure and high-pressure air systems being closer together and the wind, in turn, being much stronger than modern-day winds. Furthermore, due to these winds having a continental route, they were likely to be very dry, further promoting the formation of dunes (Glennie, 1998). On the other hand, during interglacial periods, the wind systems would have been weaker and wetter conditions due to convection-induced rainfalls (Glennie, 1998).

Others have also interpreted north-westerly winds in part of the UK (Heward, 1991). To explain these multidirectional winds Glennie, (1982) proposed that, instead, the Mid North Sea high coincided with the area of high atmospheric pressure at the Horse latitude(30° North of the equator). On the other hand, it was also proposed that the dunes in the UK area are linear dunes formed by winds from two directions, but it also gives weight to the dominant wind direction still being from the NE (Besly et al., 2018)

2.4 Stratigraphy:

The majority of the Rotliegend was deposited during the Permian. Most of the Rotliegend overly the Namurian to Stephanian deposits (Gast et al., 2010). This hiatus represents 35-80 Myr and is best known as the Base Permian Unconformity (BPU) and is better described as an amalgamation of several smaller unconformities (Bouroullec et al., 2025) . Traditionally, the Permian can be divided into 3 stratigraphic groups, of which the oldest two comprise the Rotliegend. The two Rotliegend units are divided into the Upper and Lower Rotliegend, of which the Upper Rotliegend is sometimes divided into the Rotliegend 1 and Rotliegend 2 (Gast et al., 2010; Glennie, 1998) (Fig. 3).

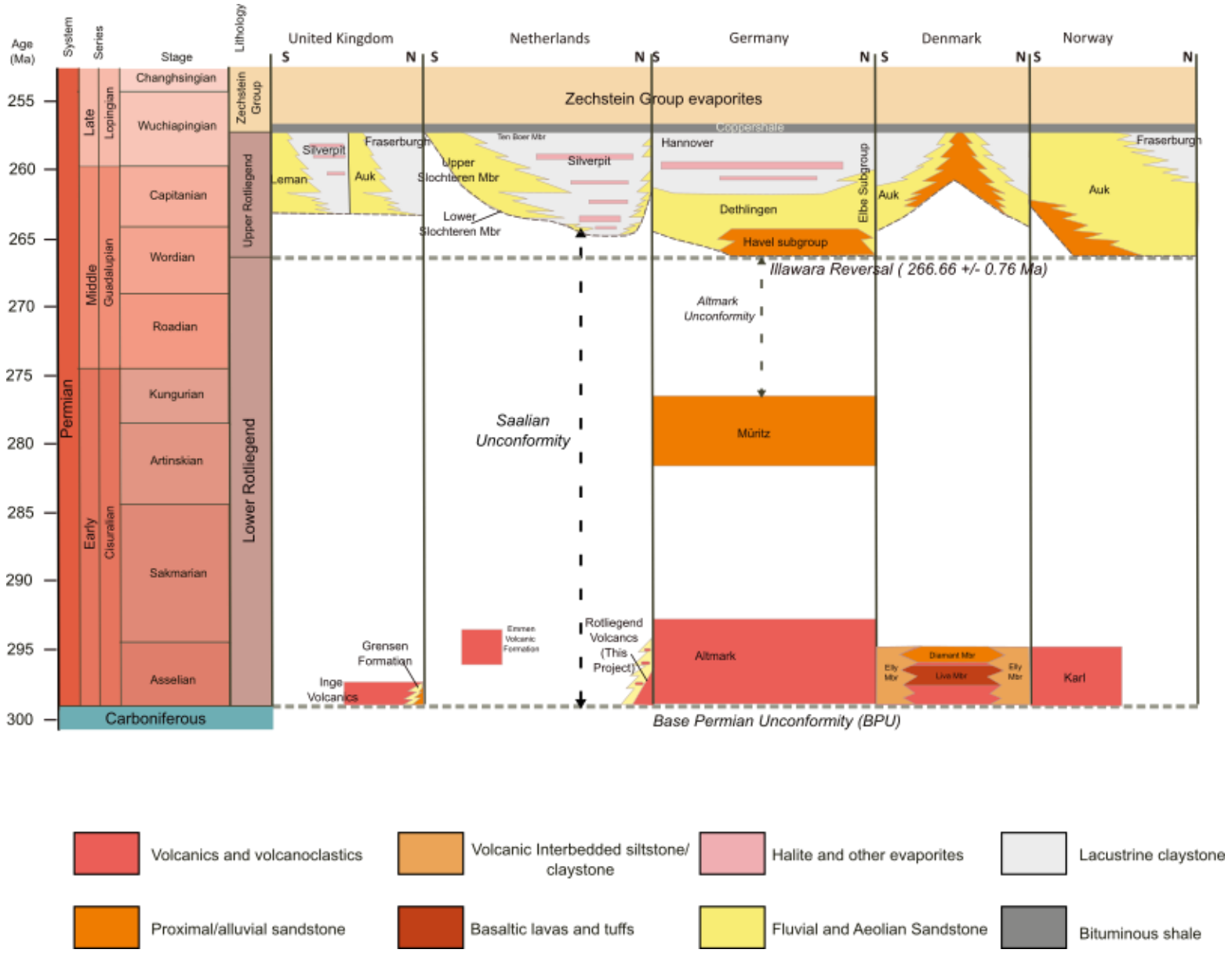

Figure 3. Stratigraphic column of the Rotliegend in the five-nation area was inspired by Armour et al.,(2004) & Bouroullec et al., (2025).

2.4.1 Lower Rotliegend Group:

The Lower Rotliegend Group consists of a succession of Volcanic, volcanoclastic, and clastic rocks with limited distribution (Bouroullec et al., 2025) . This group is dated to the late Carboniferous-early Permian, with the lavas primarily consisting of basaltic lavas with some rhyolitic lavas (Heeremans et al., 2004a). The deposition of the Lower Rotliegend group is limited in its distribution, being restricted in the offshore to the Central Graben, Norwegian-Danish basin, and Step Graben (Bouroullec et al., 2025; Patruno et al., 2022). Three Volcanic pulses have been identified, the first of which occurred in the western Central Graben and Horn Graben ~300-288 Ma, the two younger pulses occurred in the eastern Central Graben and the Norwegian-Danish basin and have been dated to 291-276 and 269-261 Ma (Bouroullec et al., 2025; Gast et al., 2010; Patruno et al., 2022). These two younger igneous events are divided by the Altmark unconformity (Gast et al., 2010; Patruno et al., 2022). The older pulses are andesitic and rhyolitic in composition, and the younger pulse was basaltic in composition (Bouroullec et al., 2025). In the Dutch offshore, these Volcanics are referred to as the Lower Rotliegend or the Rotliegend Volcanics (RV) and share a similar lithology to the Karl formation found in both Denmark and Norway (Armour et al., 2004). The Karl formation in Denmark can be further subdivided into the Elly member, which possesses lacustrine siltstones that interfinger with Volcanic rock from the Liva member (Armour et al., 2004). The Danish Karl formation can be further subdivided into the Liva member and the Diamant member, which consist of basaltic lavas and alluvial material, respectively (Pedersen, 2012). In Germany, the Volcanics are known as the Altmark subgroup and are coeval with the two oldest Volcanic pulses (303-290 Ma) (Gast et al., 2010). In the UK, the Volcanics are known as the Inge Volcanics, which have been correlated with the Karl formation but are dated coeval with the oldest Volcanic pulses (~299 ±3 Ma) (Heeremans et al., 2004a). The Inge Volcanics and Karl formation are also time equivalent with the Grensen formation in the UK (299± 1.6 Ma) (Bouroullec et al., 2025). Large parts of the Rotliegend Volcanics are capped by the Saalian unconformity; however, this unconformity is also partly overlapped by the Karl Formation (Gast et al., 2010; Patruno et al., 2022).

2.4.1.1 Identifying igneous rocks.

Igneous rock characteristics on a well log

Classifying igneous rocks based on well logs can be difficult, with one major problem being the identification of the lithology and type of lava due to the complex lithology (Ning et al., 2009). Volcanic rock can be classified in a multitude of ways. Mafic rock is usually low in Silica and K_2O+Na_2O but high in FeO + MgO, whilst the opposite is true for felsic rocks (Figures 4 & 5). Furthermore, intrusive and extrusive rocks can have the same composition. However, due to the difference in cooling rate, extrusive rocks will have smaller crystals than intrusive magmatic rocks. For extrusive rock, a TAS diagram is used for rock identification (Fig. 5).

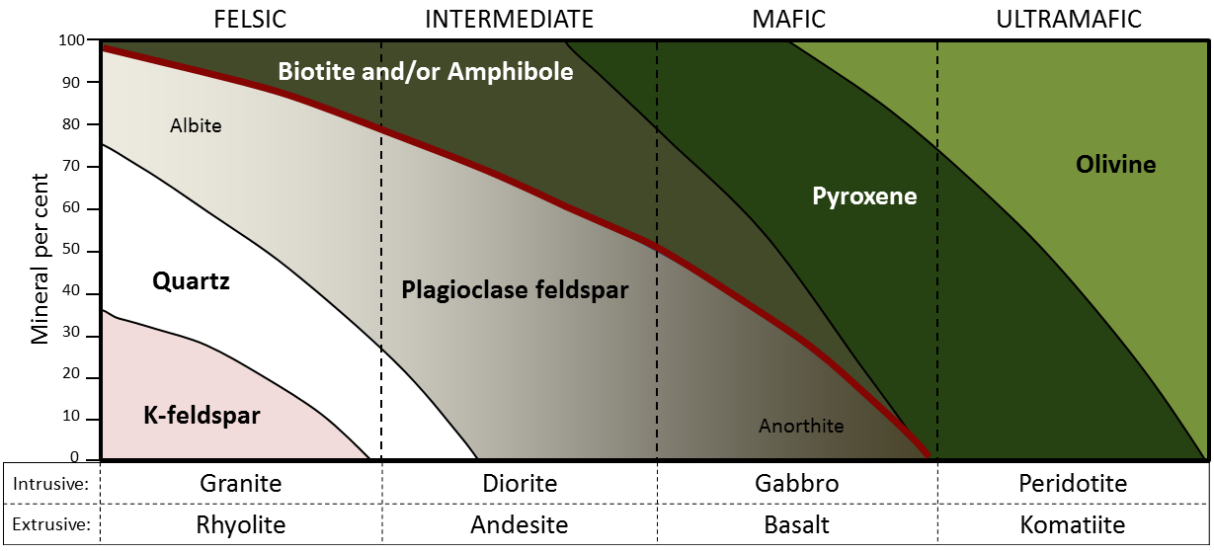

Figure 4. Diagram showing the classification of igneous rock based on mineral percentages (Earle & Earle, 2015).

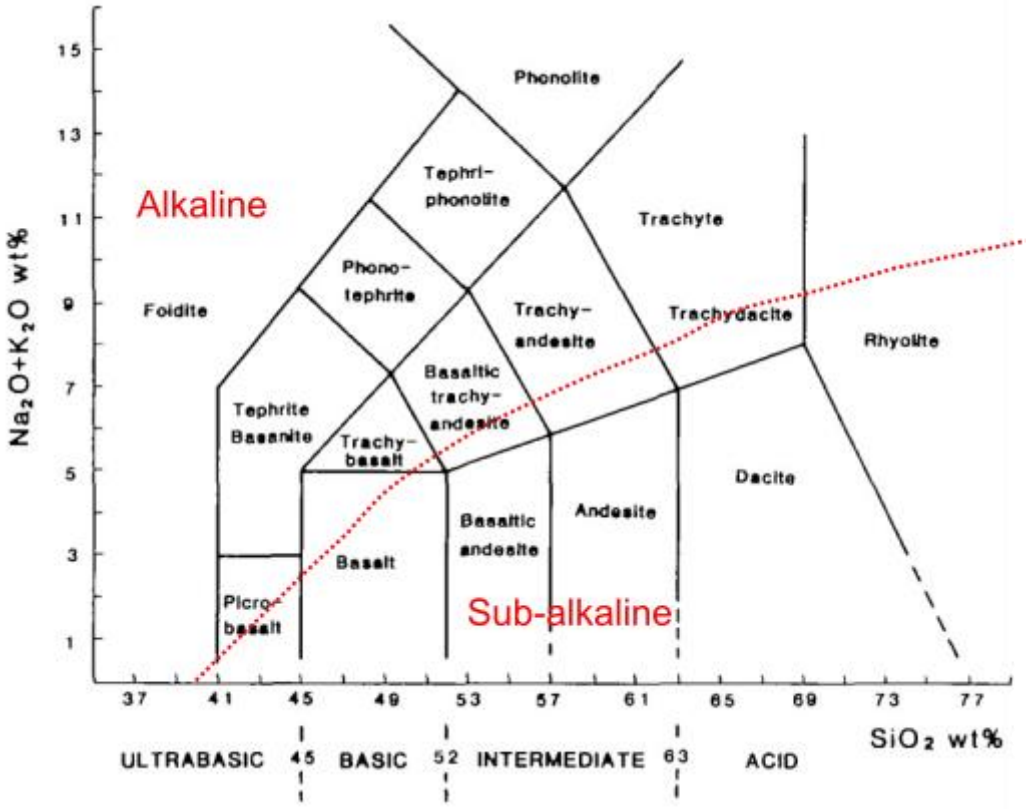

Figure 5. The Total Alkali versus Silica diagram is used for classifying extrusive igneous rocks by their chemistry when their mineralogy is not visible (Bas et al., 1986).

Interpreting igneous rock based on well data is difficult due to the complex mineralogy (*KGS--Geological Log Analysis--Igneous and Metamorphic Rocks*, n.d.). For Unaltered Volcanic rock, the natural gamma ray increases from basic to felsic, whilst the density, velocity, and resistivity are reduced (Fig. 6) (Hou et al., 2013). Though it should be noted that whether the rock is alkalic or sub-alkalic (Fig. 5) may influence the natural gamma ray due to the large wt% of K_2O. If the rocks are weathered, the density and velocity may be reduced, with the weathering intensity increasing from basic rocks to acidic rocks (Hou et al., 2013; Fig. 6). Igneous rock can further be differentiated with the photoelectric factor, which is high in mafic rocks due to possessing minerals that are high in iron and magnesium, whilst the opposite applies to felsic rocks (*KGS--Geological Log Analysis--Igneous and Metamorphic Rocks*, n.d.). Lastly, the neutron porosity can be expected to be low for both basic and felsic igneous rocks. Volcanoclastic material or tuffs may have properties like the igneous rock, but may also have lower density and neutron porosity.

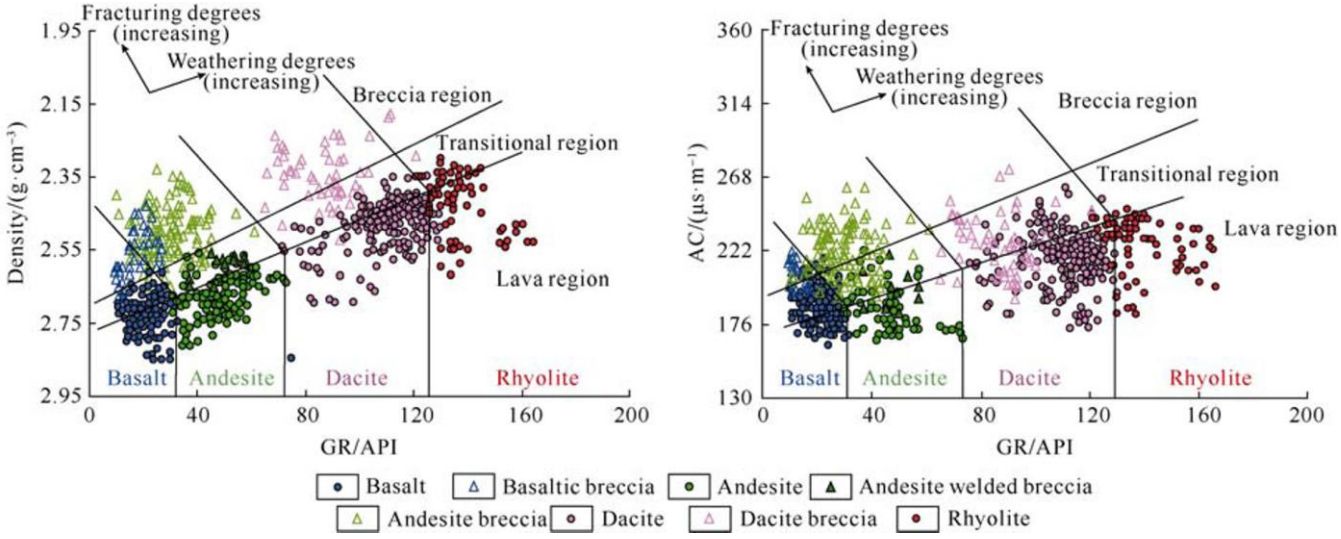

Figure 6. Log response to igneous rocks depending on type and weathering degree. (Hou et al., 2013); density vs gamma ray, and sonic vs. gamma ray. AC = sonic transit time.

2.4.1.2 Gravity and magnetic anomaly

Due to igneous rocks generally having a high density, centres of volcanism can be identified with mass anomalies (Malahoff, 1969). For this, the complete Bouguer gravity anomaly is commonly used. The Bouguer anomaly size is the measure of the mass deficit or mass excess (*Gravity and Magnetic Field | NLOG*, n.d.). The value of the gravity anomaly depends on the type of Volcanics. In practice, tuffaceous or volcanoclastic material will not have a notable anomaly, thick basalts will cause a positive anomaly, and felsic igneous rocks like rhyolite or granite may cause a negative gravity anomaly (Malahoff, 1969). Another anomaly is the total Earth's magnetic field, which indicates the concentration of ferromagnetic minerals (predominantly magnetite)(*Gravity and Magnetic Field | NLOG*, n.d). This anomaly is larger at high concentrations of magnetic components, with high concentrations often occurring in igneous and metamorphic

rocks. (*Gravity and Magnetic Field | NLOG*, n.d.). This means that rocks that are rich in magnetite or iron-rich minerals would be expected to cause larger magnetic anomalies (Clark, 1997). The Southern Permian Basin Atlas published maps for both the Bouguer and total magnetic field anomaly for the SPB (Guterch et al, 2010; Figures 7A & 7B).

2.4.2 Upper Rotliegend Group:

The Upper Rotliegend Group is dominated by sedimentary rocks, including sandstones, claystones, with some halite beds (Bouroullec et al., 2025). In the Netherlands, this group is subdivided into the Slochteren Formation, which mainly consists of sandstones and conglomerates of fluvial or aeolian origin, and the interfingering Silverpit Formation, composed of claystone, siltstone, and evaporites (Bouroullec et al., 2025). Volcanic fragments have been recorded in the sandstone and conglomerates (Gast et al., 2010). In the UK, the Upper Rotliegend correlates with the Auk Formation and Fraserburgh in the central North Sea, or the Leman Formation and Silverpit Formation in the southern North Sea. In Denmark and Norway, the Auk formation is also used to refer to the Upper Rotliegend. In addition, in Norway, the term Fraserburgh formation is used, which interfingers with the Auk formation and is equivalent to the Leman Sandstone Formation (Armour et al., 2004). This formation consists mainly of lacustrine and sabkha sediments that were deposited in topographic lows. In Germany, the equivalent of the Upper Rotliegend is the Elbe Subgroup (Gast et al., 2010). The oldest sediment in Germany, which predate the Elbe Subgroup, is the Müritz Subgroup consisting of volcanic fanglomerate, fluvial sandstones, and playa deposits, and partly overlaps with Volcanic activity in the central North Sea and Horn Graben (Gast et al., 2010). After the Müritz Subgroup, the Havel Subgroup was deposited in fault-bound depressions in which breccia was deposited first, but mostly consists of aeolian and fluvial desert sediments (Gast et al., 2010). The Dethlingen Formation is the equivalent of the Slochteren Formation, whilst the Hannover Formation partly correlates with the Silverpit Formation and specifically with the Ten Boer Member in the Netherlands (Gast et al., 2010).

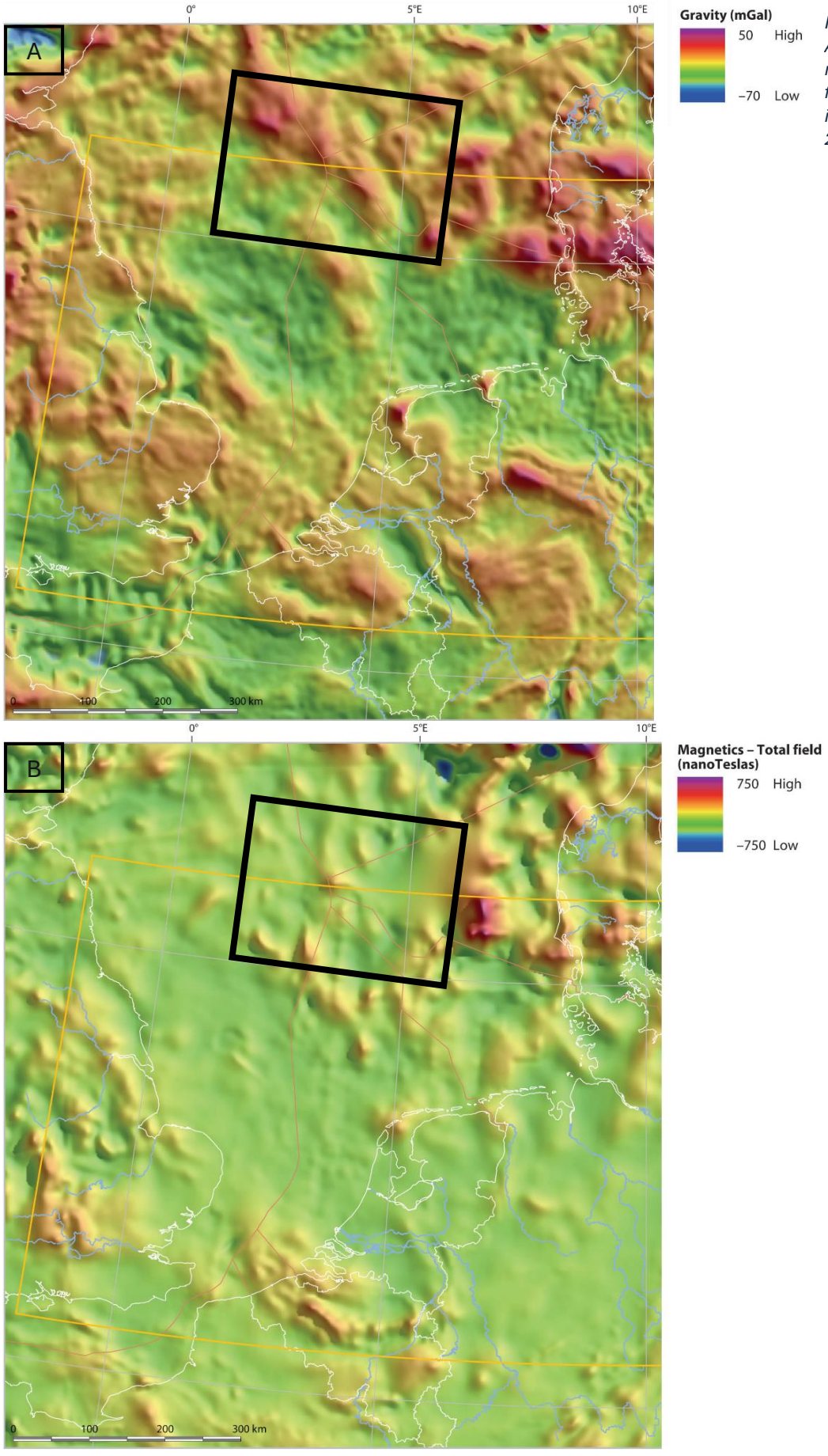

Figure 7.(A). Bouguer gravity Anomaly map of the SPB in mGal and (B) Total magnetic field anomaly map of the SPB in nanotesla (Guterch et al., 2010).

3. Methods:

3.1 Data:

For this report, data was gathered from several sources. Composite logs, log files (in LAS or LIS format), well deviation files, core-photos, core-reports with porosity & permeability measurements, core-descriptions, and geological reports on the wells were gathered as far as available. The wells selected for use in this project met at least one of the following requirements:

1. If the well was confirmed to have reached the bottom of the Rotliegend.
2. Had reached a unit below the Rotliegend without Rotliegend present.
3. Or had reached the top of the Rotliegend but not the bottom of the Rotliegend.

The well selection was based on data available in the EBN database on wells in the five-nation area. After the data was gathered, all wells were imported into Petrel as LAS files, and if available, with their well deviation path file (WDD). When the well deviation path file was not available, it was assumed that the well was nearly vertical unless it showed a large deviation from the surrounding wells. In the latter case, the well was disregarded in the interpretation. The quality of the data also depended on the country of origin.

Data were sourced from a variety of platforms (Table 1). Furthermore, due to working with different countries, the availability of core-photos, porosity, and permeability data varied per country (A1). Data on the Dutch offshore was obtained from the EBN database or the NLOG website. Here, a total of 62 wells were used to make the thickness maps. For the making of the GDE map, a total of eight were used in the Dutch A-B block, but a total of 62 were used for GDE mapping. Only one well in the project area had porosity-permeability data (A16-01). To bolster the Dutch porosity permeability data and data on the playa-sabkha environment, additional wells from the E and F blocks were taken into consideration when making the porosity permeability analyses. The porosity-permeability data were obtained from the EBN database.

Table 1. Table showing the data country of origin (Netherlands (NL), Germany (GER), United Kingdom (UK), Denmark (DK) & Norway (NOR)), platform used, data availability, cost associated with it, alternative databases available, and the general quality of the data.

Country	Platform	Data available	Cost	Alternative?	Data quality?
NL	NLOG	Yes	Free	EBN dataset	Good
GER	BGR geoportal	No (Not published yet)	Free	Paleo 5 project, EBN database, Well summaries	Poor
UK	NDR	Yes	NDR license	UU received data	Good
DK	GEUS	YES	Free	x	Good
NOR	Dyskos	Yes	Membership ~16.000 €/y	NOD sodir, - reports - paleo 5 project	Moderate

German data was the scarcest due to much of the necessary data still being unpublished. An attempt was made to consider eleven wells for well correlation, thickness map making, and GDE map making. Data on two wells outside the research area were taken from the BGR Geoportal. Data on wells inside the research area was unable to be obtained from the BGR, as at the time of this project, any data concerning the Entenschnabel had yet to be published. For wells inside the Entenschnabel, data from 1 well was taken from the Paleo Five project, three wells were directly provided from the BGR, and well B-1x duc was obtained from the Danish databank, as this well was originally drilled when that part of the North Sea was still part of the Danish sector of the North Sea. For all other wells, well correlations were based on the well summary sheets available at the BGR. In total, eight wells were used for well correlation and GDE mapping, and data from two wells were considered in the porosity-permeability analyses.

Danish data was obtained from GEUS. GEUS is the Danish information platform with an extensive database on the subsurface of Denmark. 27 wells were selected in the well correlating process, and the thickness maps were made with three wells lying just outside the study area. Only one well core had porosity-permeability data on the Rotliegend, and two wells had core photos.

Norwegian data, similar to German data, was difficult to obtain. Unlike German data, all Norwegian data is available on the Dyskos platform. However, data from this service could be used during this project due to the costs associated with the service (Table 1). Instead, the website SODIR of the Norwegian offshore directorate and any available data from there were used. This included geological reports and composite logs of all the wells. Furthermore, core photos and core data were available. This data was supplemented with 10 wells from the Paleo Five project. In the end, a total of twelve wells were used for the well correlating and thickness making process, and two of those had porosity and permeability data. All LAS and WDD files from Norway were taken from the paleo-five project.

Lastly, data from the UK was obtained from the EBN database, whose data was received from the University of Utrecht. This data was supplemented by data from NDR. A total of 107 UK wells were used in the well correlating and thickness map-making process, of which fourteen wells had core photos and seventeen had porosity-permeability data. Some of the UK wells' log files were only available as LIS files and were converted into LAS files before use. This was done with the help of an EBN petro-physicist.

3.2 Well correlation & Thickness maps

To analyse the distribution, lithology, and thickness of the Rotliegend, the Rotliegend was first subdivided into sub-units. Here, the Rotliegend was first subdivided into the Upper Rotliegend (ROT sed or RO), which is dominated by sediments, and the Lower Rotliegend (RV), which is dominated by volcanics. This is in line with the official stratigraphic nomenclature for the Netherlands, as published on NLOG. No further classification was applied to better correlate across borders. Inside the Upper Rotliegend, the thickness of the sand was also determined and sand well top were assigned. Next, the wells were correlated, and thickness maps were created based on the well tops. During the well correlation process, a lithological log was created to help visualise differences in rock type. To accomplish this, the subsurface software Petrel was utilised. Petrel Software, marketed by SLB, allows people to visually analyse subsurface data from exploration to production.

The wells were correlated using several different types of logs. The logs that were primarily used were the Gamma ray[API], the density [g/cm^3] & neutron porosity [m^3/m^3]. However, due to many of the wells being old, they often lacked this information. To combat this, the Spontaneous potential (SP) [mv], Sonic [us/ft], deep Resistivity [ohm*m], potassium concentration (%), and photo-electronic factor (PEF) [b/e] were also used.

During correlation, EBN, University Utrecht(UU), and the well tops from the Paleo five project were used as an initial guideline, but new well tops were also interpreted, and old ones were reinterpreted. The EBN well tops were in accordance with the, at the time,

tops defined in NLOG. The UU and Paleo five-well tops were used due to a lack of available well tops from across the border. The Rotliegend was identified by the base of the Zechstein Kupferschiefer/ Coppershale member (ZEZ1K) at the top and the Base Permian Unconformity (BPU) at the base, with underlying rocks of Carboniferous or Devonian age. The Upper Rotliegend was identified by the rocks, consisting mainly of sedimentary material like sands, clays, silt, and pebbles with no tuffs or igneous rock in between them. The Lower Rotliegend, which consisted mainly of volcanics, was identified by the Saalian unconformity on top and the BPU below, and the presence of either lavas, tuffs, or volcanoclastic material. Volcanic is a very broad term that brings difficulty when identifying it on well logs (see Chapter 2.4.1.1). Mafic lavas were identified by having a low gamma ray, similar to sands, with high density, low porosity, high sonic, and a high photo-electronic factor or a near vertical SP. It should be noted that the gamma ray may vary depending on the type of mafic extrusive; for example, feldspar-rich trachybasalts will have a high potassium content and high gamma ray. Tuffs and Volcaniclastic rocks were defined as having similar gamma ray values as the igneous rocks they are associated with, but with lower density and limited porosity. Felsic lavas still had low porosity like their mafic counterparts, but had higher gamma ray values, lower density, and photo-electronic factor. The sands were identified as having low gamma ray, low density, high porosity & low sonic though variations may occur if the sands were to be contaminated with volcanic material. For the sandstone intervals, separate well tops were created for different units. All well log interpretations were verified with lithological interpretations from cuttings or core, available in mud logs or lithology logs.

Based on the well tops, thickness maps were created by first converting them to the isochore point and using the “make surface” option in Petrel. Thickness maps were made for;

1. The total Rotliegend,
2. The Upper Rotliegend,
3. The Lower Rotliegend, and
4. The sandstones within the Upper Rotliegend.

These thickness maps were chosen to provide a broad perspective on the relationship between sediments, volcanics, and sands. All thickness maps were made based on the wells that reached at least the base of the Rotliegend, and were supplemented with wells that had a considerable Rotliegend thickness to create minimum thickness maps. The thickness maps were solely based on well correlations and may lack essential detail due to the lack of wells in the area. The thickness maps were created by defining the boundary with the project area, with grid increments of 50 x 50, using the convergent interpolation gridding algorithm. This algorithm was chosen due to the negative values automatically being discarded.

3.3 GDE Mapping

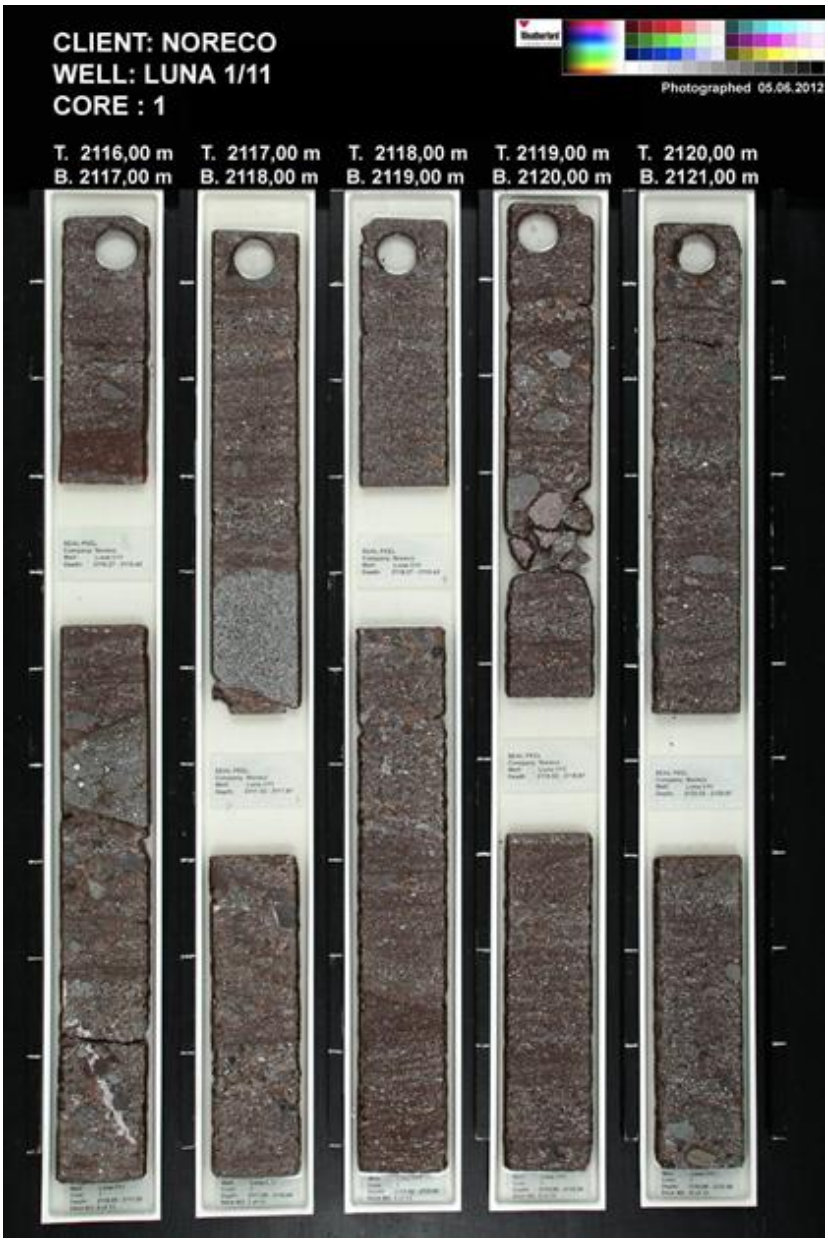

Figure 8. Example core photo of the Danish well Luna-1 showing Alluvial fan deposits with large Mafic Volcanic clasts. Source: GEUS.

For the making of the Gross Depositional Environment (GDE) map, first, for each well, the gross depositional environment of the Upper Rotliegend and the Lower Rotliegend was determined. The depositional environment was determined based on core-photos (Figures 8, 9, Appendix S7-S10 & table A1)- descriptions of the core, composite well logs, mud logs, thickness of sands, geological reports, and literature review. To simplify the map, the Volcanics were divided into 4 categories and the sediments into 7 main categories and 3 additional mixed categories. The Volcanics were defined as being either mafic lavas, felsic lavas, tuffs/Volcaniclastic rocks, or undifferentiated Volcanics. Undifferentiated Volcanics can be any of the three other categories, but lack conclusive data. Mapping of the mafic lavas and felsic rocks was enhanced by using the Bouguer gravity anomaly map from the Southern Permian basin Atlas (Guterch et al., 2010) (Fig. 7A). In addition, areas that had overlapping Rotliegend Volcanics, positive Bouguer gravity anomaly [mGal], and positive total magnetic field anomaly [nanotesla] were marked on the map. The main categories for the Rotliegend sediments are: aeolian, sandflat, alluvial, playa&/or sabkha, saline lake, fluvial, and non-deposition. The other three categories were a mix of depositional environments or did not have enough evidence to distinguish one environment from the other. These included alluvial&/or aeolian, alluvial&/or fluvial & fluvio-lacustrine. Transport direction and wind directions were based on dipmeter logs, GDE, thickness mapping, and literature review. Lastly, an attempt was made to define the watershed boundary between the SPB and NPB based on the transport direction and thickness of the sands and sediments.

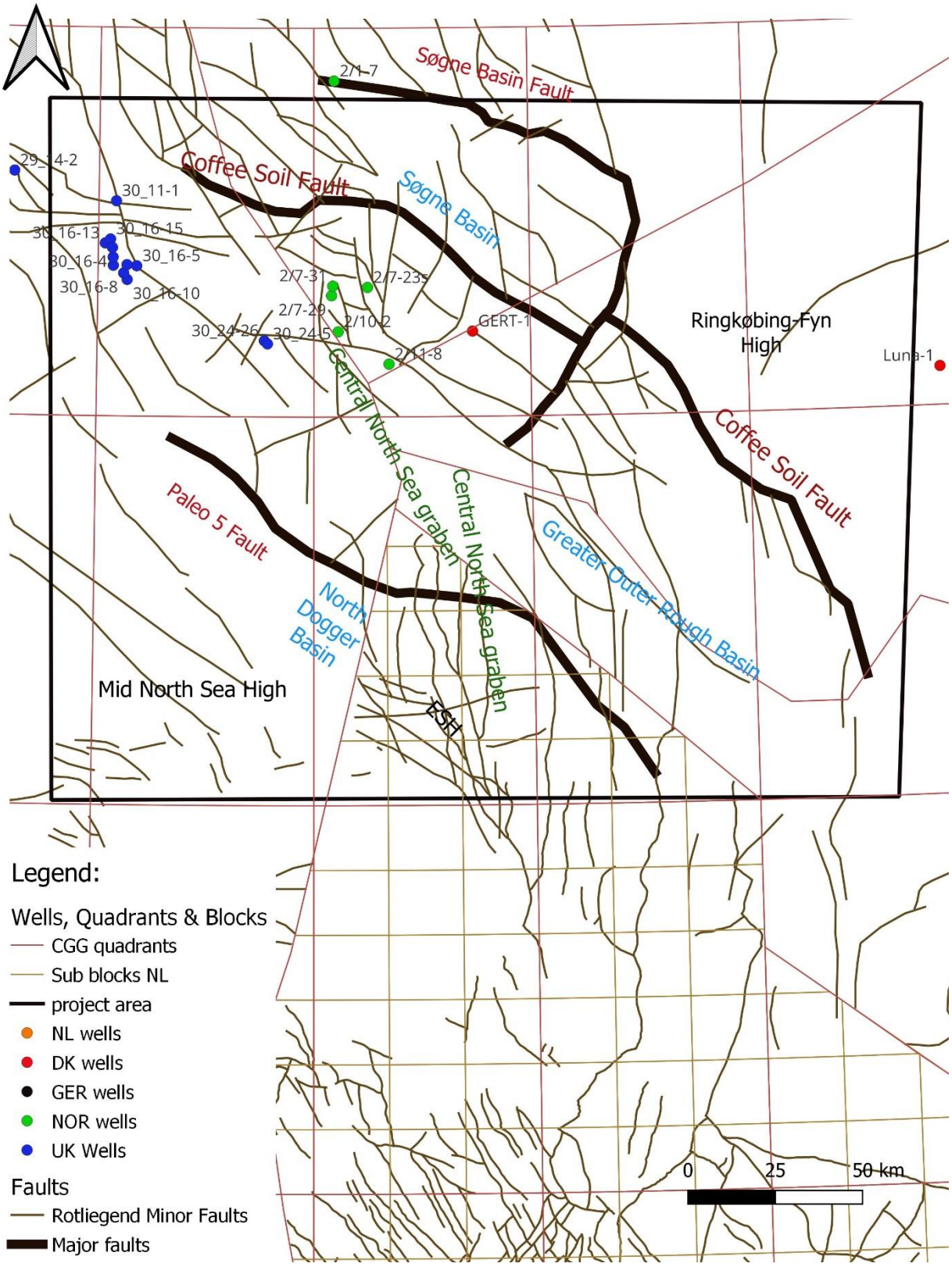

Figure 9. Map of the study area showing the location of all the wells with Core-photos.S7-10. Additional core photos can be found in: https://docs.google.com/presentation/d/18phprij_AlmL3q-Afq81BePHSAFPLH5CX8QjLhAKdgQ/edit?slide=id.g3736aec42a6_0_2#slide=id.g3736aec42a6_0_2

3.4 Porosity-Permeability-Depth analyses

In total, 2147 data points of cores were gathered from the area of twenty-seven wells with the goal to analyse reservoir potential in different depositional environments (Fig. 10)(Appendix A1). These wells had a poor distribution in the study area and in depth, which may cause biased results. For the depth [m] was either the true vertical depth (TVD) used or the MD if the azimuth was below 10°, and no TVD was mentioned to ensure the truest representation of the depth. The permeability used was the horizontal permeability [md], the porosity was the helium porosity [%], and all depths are given in meters. This analysis focused on the trend between depositional environment, porosity, permeability, and depth. First, all data points were divided into their corresponding depositional environment.

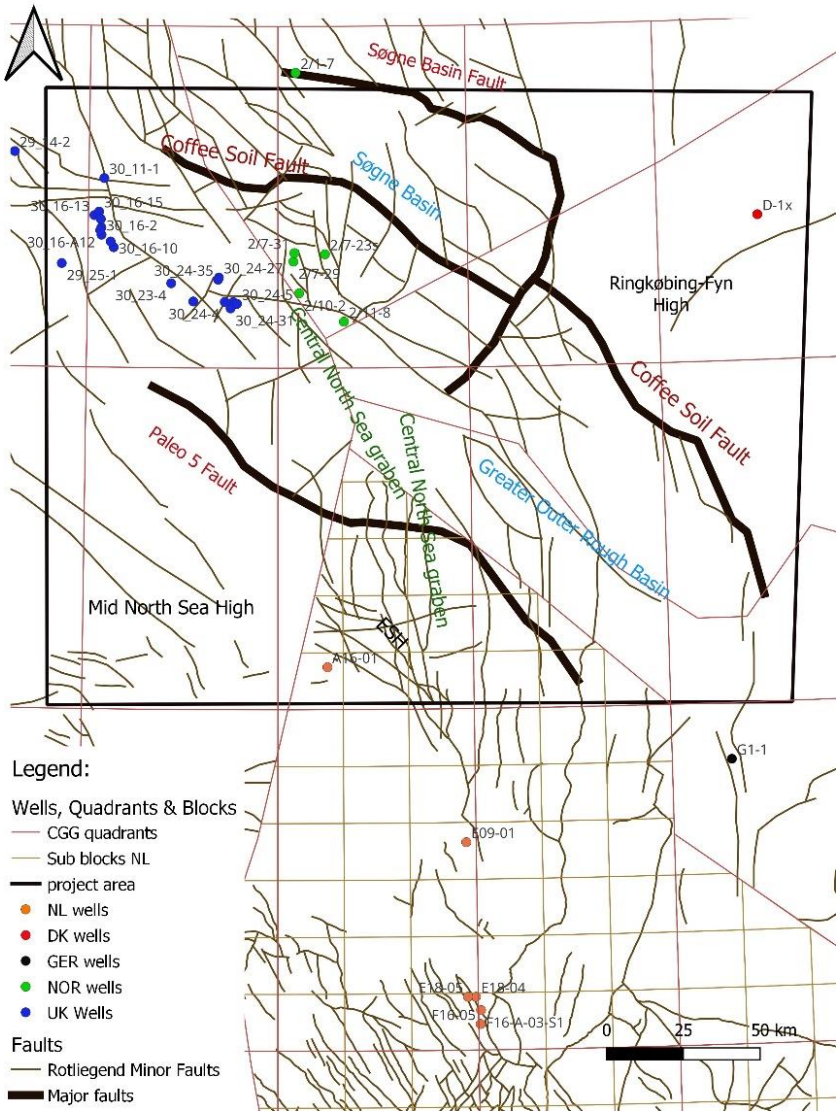

Figure 10. Map showing the research area, the most important structures, and all wells which had porosity and permeability measurements (A1).

Plots were created plotting porosity versus permeability, porosity versus depth, and permeability versus depth to see if there were any significant trends with the purpose of evaluating the reservoir quality. It should be noted that all permeability values were plotted on a logarithmic scale, whilst porosity and depth were always plotted on a linear scale. To determine the trend lines, binning was applied over the porosity axis and depth axis (Table 2) using the arithmetic averaging method. This averaging method was chosen due to the majority of the depositional environments consisting of laminated sandstones. For all trendlines, the coefficient of determination R^2 values were added, with R^2 being the proportion of variation.

Table 2. Table showing the bins used during the making of the trendlines for the porosity-permeability, porosity-depth, and permeability-depth plots. For large datasets (aeolian, playa-sabkha & aeolian-alluvial the large bins were used, whilst for fluvial, sandflat & alluvial, the small bins were used.

Porosity bins (large datasets)	Porosity bin (small data sets	Depth bins
0 ≤x <0.5	0≤x <0.5	2100 ≤x 2200
0.5 ≤x <1	0.5≤x 1	2200≤ x <2300
1≤x<5	1≤x<2.5	2300 ≤x <2400
5 x<10	2.5≤x<5	2400 ≤x <2500
10 ≤x<15	5≤x<7.5	2500 ≤x <2600
15 ≤x<20	7.5≤x<10	2600 ≤x <2700
20 ≤x<25	10≤x<12.5	2700 ≤x <2800
25 ≤x<30	12.5≤x<15	2800 ≤x <2900
		2900 ≤x <3000
		3000 ≤x <3100
		3100 ≤x <3200
		3200 ≤x <3300
		3300 ≤x <3400
		3400 ≤x <3500
		3500 ≤x <3600
		3600 ≤x <3700
		3700 ≤x <3800
		3800 ≤x <3900
		3900 ≤x <4000
		4000 ≤x< 4100
		4100≤ x <4200
		4200 ≤x <4300
		4300 ≤x <4400
		4400 ≤x <4500
		4500 ≤x <4600
		4600 ≤x <4700
		4700 ≤x <4800
		4800 ≤x <4900
		4900 ≤x <5000
		5000 ≤x <5100
		5100≤ x <5200

4. Results:

4.1 Distribution and Thickness of the Rotliegend

4.1.1 Total Rotliegend: Well correlation and thickness

In most of the study area, the Rotliegend was covered by the Coppershale (ZEZ1K) and bounded by the BPU or Saailian unconformity. Exceptions to this are in a few select areas where the Base Cretaceous unconformity (BCU) cuts into the Rotliegend and Jurassic overlies the Rotliegend (Fig. 11). Most of the Rotliegend was found throughout the study area. Areas where the Rotliegend unit was absent were associated with paleo-highs, mainly the MNSH (Fig. 12) and RFKH. On the MNSH, Zechstein is directly deposited onto Carboniferous rock, with proven absence of Rotliegend due to non-deposition. Whether this is the case for the RFKH was not observed due to the lack of wells on the RFKH. The Rotliegend is also absent in the Central part of the Entenschnabel in the Central Graben System in Germany (Figures 11B & 12). The Total Rotliegend is at its thickest in areas where there are either large volumes of volcanics, volcanics with a sediment cover, or areas with continuous sandstone depositions. Generally, the thickness of the Total Rotliegend varies between 0-600m. The lithology varied depending on the location with respect to the Lower Volcanics within the Netherlands; the sediments consisted of clay or shale layers alternating with more sandy layers. (Figures 12 & 13).

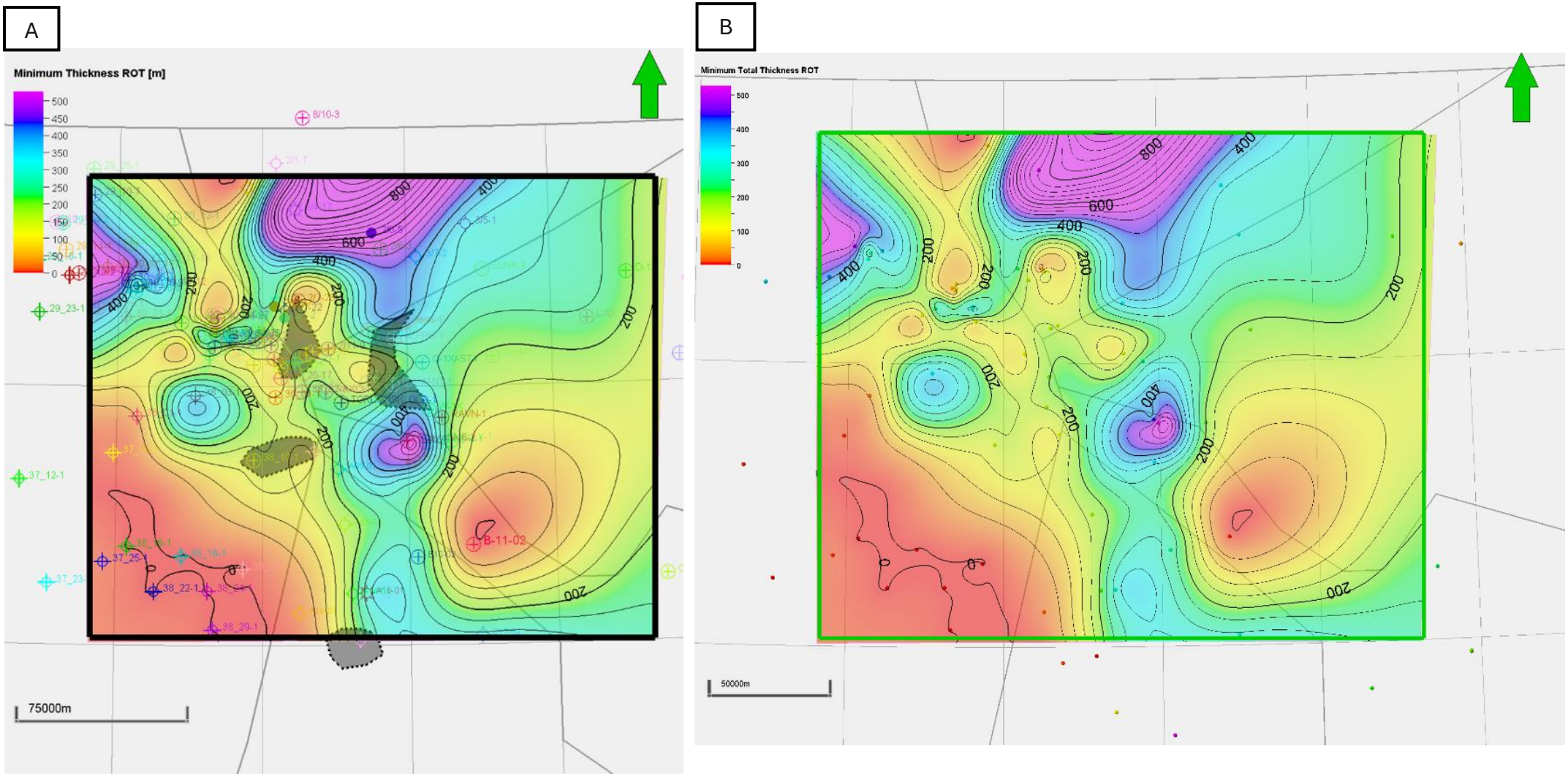

Figure 11. (A) Thickness map with all wells and in grey all areas where the base cretaceous unconformity (BCU) cuts into the Rotliegend. Colour scale 0-500m. (B) Minimum Thickness map of the Total Rotliegend in meters with a scale from 0-500m.

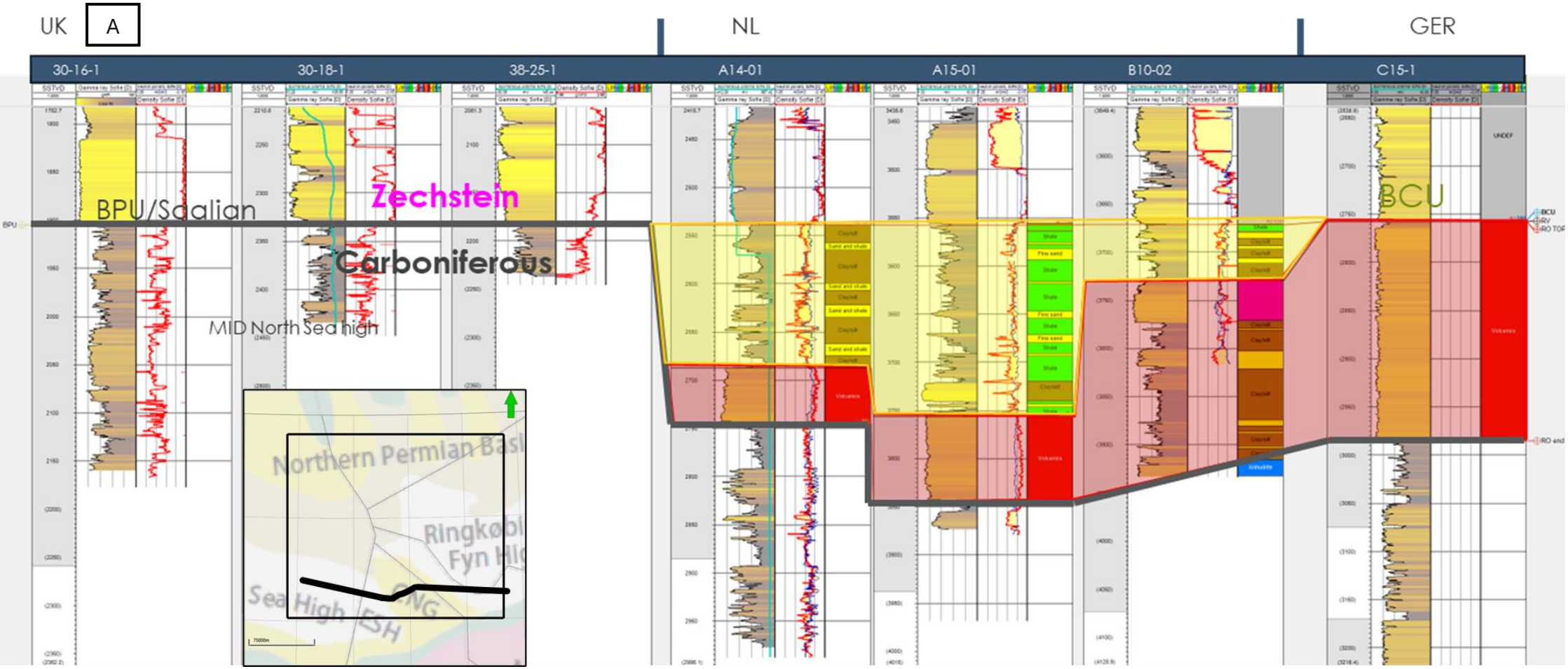

Figure 12.(A). Well correlation panel (E-W from the UK MNSH through NL and ending at Germany). The location of the well panel (12B). Figures show the absence of Rotliegend on the MNSH the presence of the upper Rotliegend in the Netherlands and the lack in Germany.. The panel shows the Gamma ray, the SP, Density neutron porosity and lithology (Fig. 13). The background map for 12B is from Bouroullec et al., 2025).

Code	Name	Parent	Background	Lines	Pattern
0	Sand and conglomerate				
1	Fine sand				
2	Medium fine sand				
3	Medium coarse sand				
4	Coarse sand				
5	Sand and shale				
6	Carbonate and sand				
7	Carbonate				
8	Carbonate and Shale				
9	Shale, some carbonate				
10	Shale				
11	Organic shale				
12	Halite				
13	Sulphate				
14	Coal				
15	Volcanics				
16	Intrusives				
17	Dolomite				
18	Siderite				
19	Basalt/altered basalt				
20	Trachybasalt/andesite				
21	Rhyloite				
22	tuff/ volcanoclastics				
23	Volcanic breccia				
24	Sand with halite				
25	Sand with gypsum				
26	Clay/silt				
27	Sand with & sediments rocks				
28	Anhudrite				
29	limestone				
30	sand with anhydrite				
31	Salt				

Figure 13 Lithology legend for all well correlation panels. Additional well panels can be found in the appendix (S11-S20).

4.1.2 Rotliegend Volcanics: Distribution, Thickness, and Character

The older Rotliegend Volcanics have a limited distribution and were at their thickest near the German-Danish border and the Danish-Norwegian offshore (Fig. 14). However, they do appear in some form in all five nations. From east to west, the RV unit thickens towards the Danish-German border, with the layers in between volcanic material becoming increasingly rich in clay, and thins again further west (Figures 15 & 16). From north to south, the volcanics are thickest in the centre but become thinner towards the edges in Norway and in the Netherlands (Fig. 17).

The Rotliegend volcanics expressed themselves in various ways depending on their location. Most of the Rotliegend volcanic rocks consisted of mafic igneous rock as either basalt or trachybasalt. In Denmark, Norway, and in block 39 of the UK, the Volcanics consisted of layers of mafic igneous rock interbedded with clay, silt, or sand, with their interbedded material increasing towards Denmark. In the UK, some wells show alternating sand and clay layers beneath the Volcanics, which is likely the Grensen formation, which is interfingered with the volcanics in the UK. The volcanics in the A blocks of the Netherlands likely have a similar expression as the volcanics in Denmark, which are part of the Karl/Inge Volcanics. Tuffs and volcanoclastic material have a sporadic distribution, but wells with tuffs and volcanoclastic material are usually situated between or near wells with volcanic deposition (Fig. 16). Just outside the project area, the Rotliegend Volcanics in Germany (well C15-1) consist of a thick sequence of Volcanics with little to no sediments interbedded in between. In the Netherlands, the volcanics either consist of tuffs or volcanoclastic or thin intervals of igneous rock. Examples of igneous rock around the Carboniferous-Permian boundary occur in wells A14-01, A15-01, B17-04, and F04-02A (Van Bergen et al, 2025). They may be of extrusive origin, and in that case, represent a correlatable interval. Felsic igneous rocks were not found inside the area of interest, with them being limited to a few wells in the Dutch F blocks. The Rotliegend volcanic top boundary is either the Saalian unconformity and Rotliegend sediments, the BCU with either Triassic or chalk on top or the Zechstein Unit.

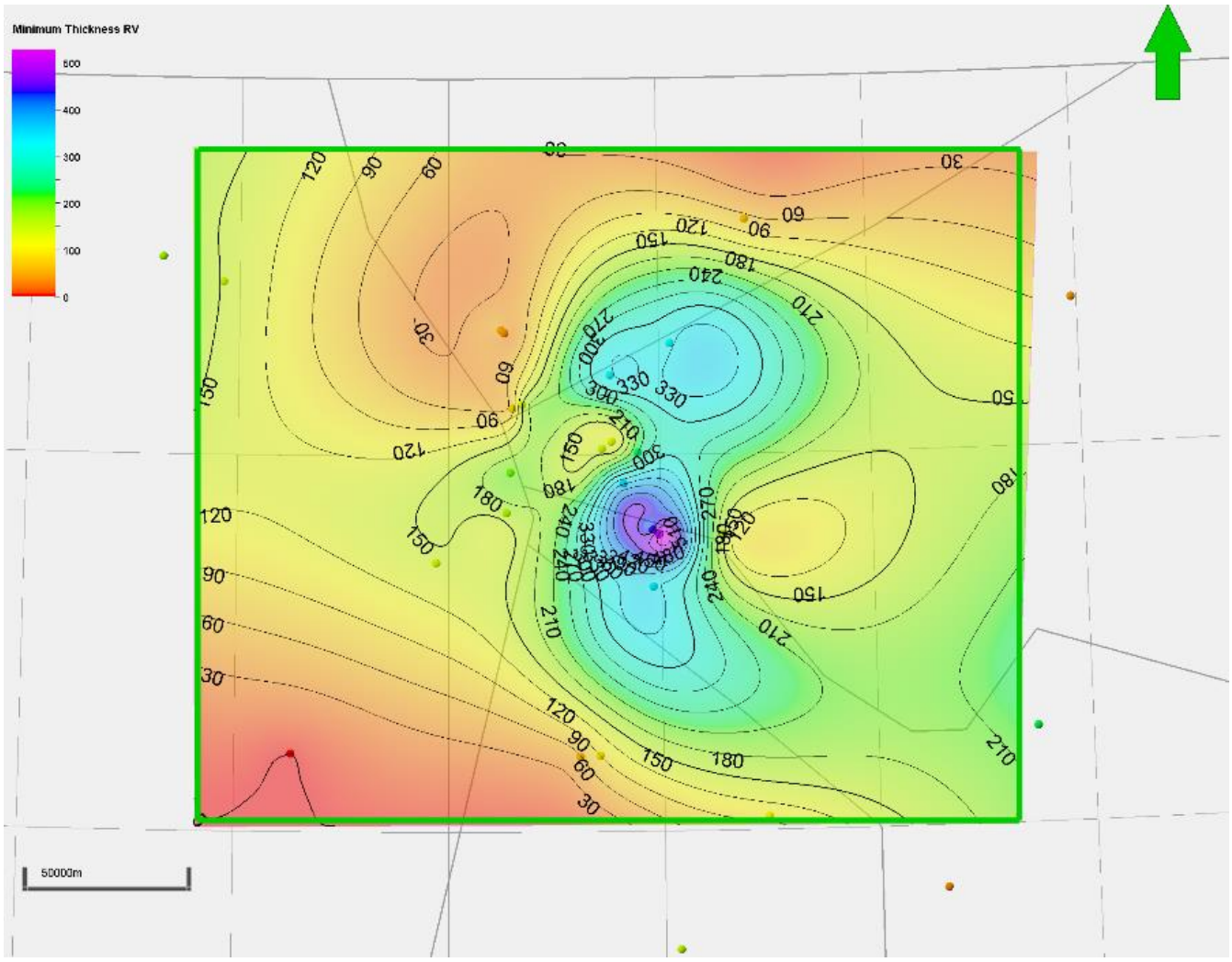

Figure 14. Minimum Thickness map of the Rotliegend Volcanics (Lower Rotliegend) in meters. Colour scale 0-500m.

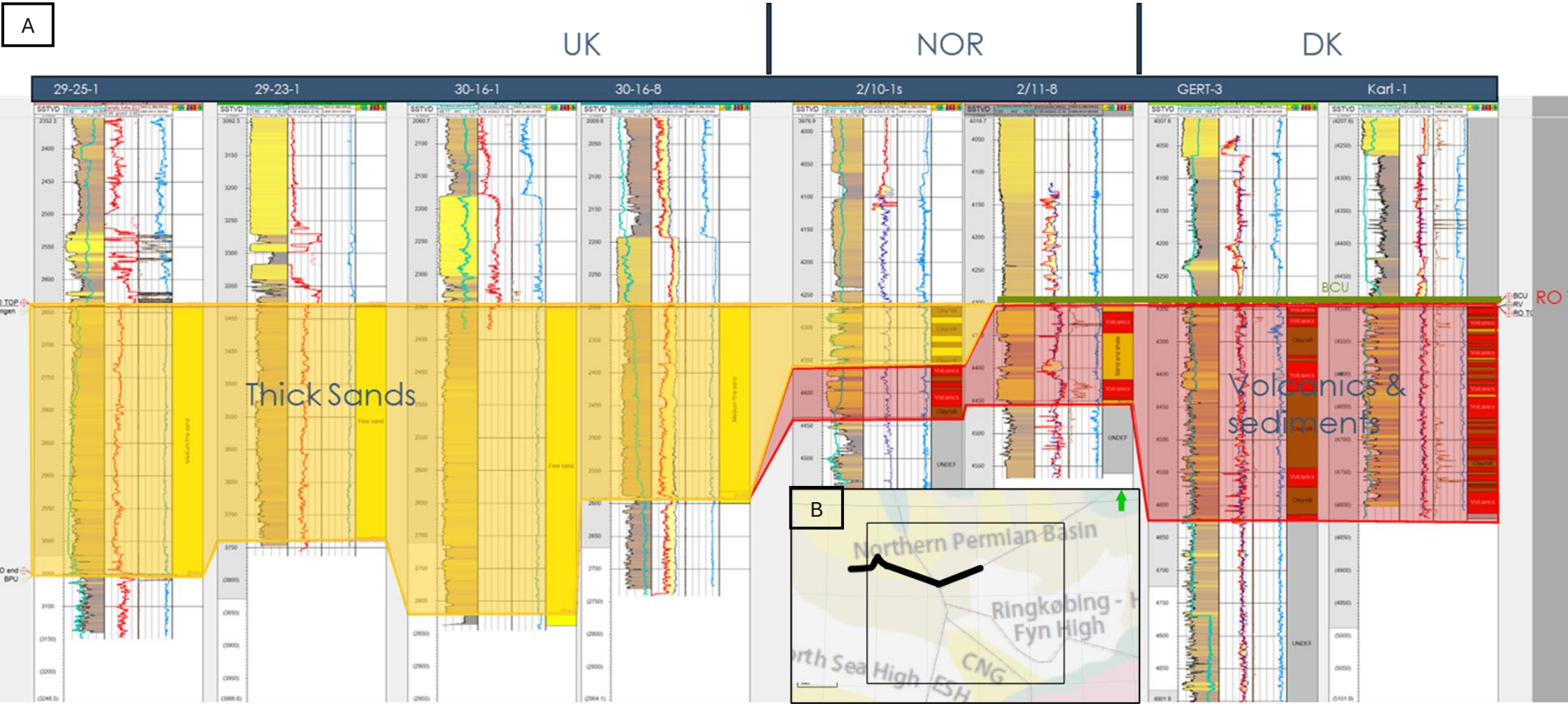

Figure 15(A) Well correlation panel E-W from the UK through Norway to Denmark showing the gradual emergence of Volcanics towards the east, which are cut by the BCU. (B) Map location of the well cross-section.

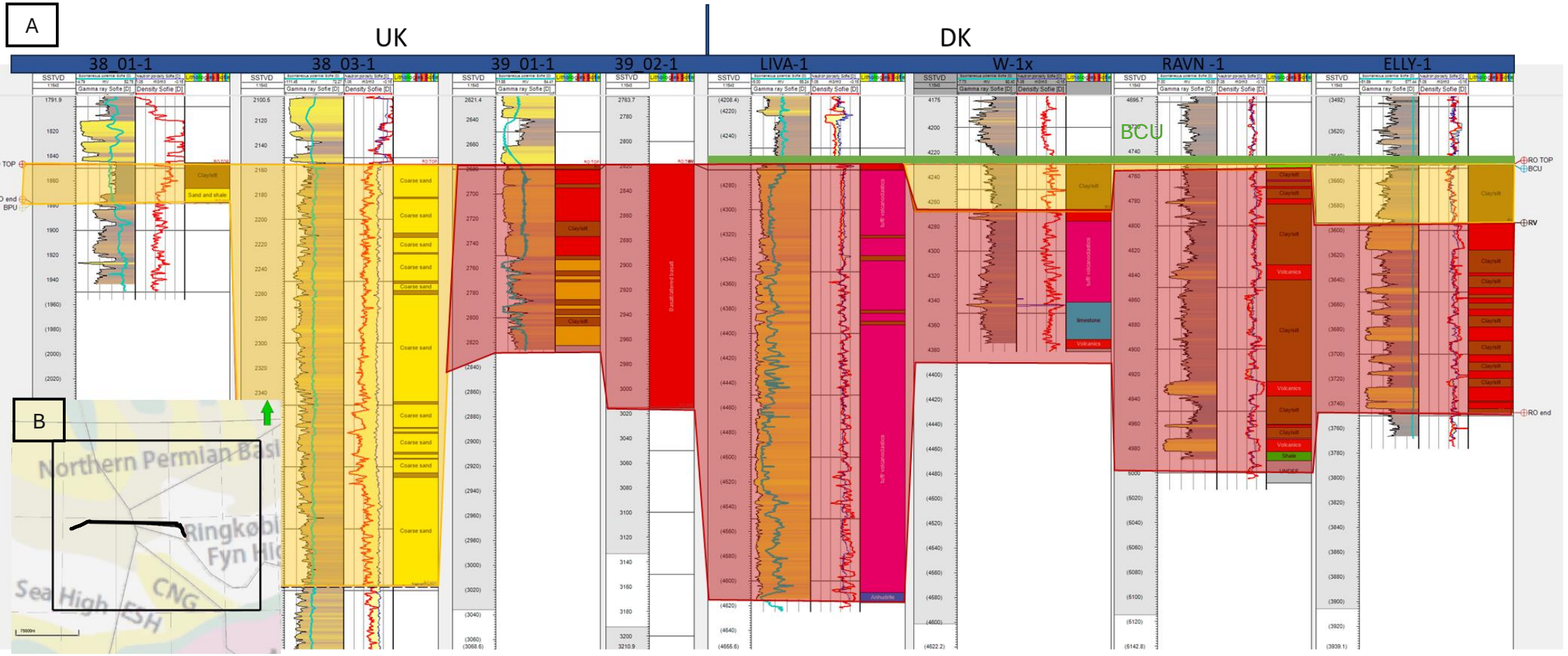

Figure 16(A) Well pane(W-E) from the UK to DK showing the relationship between the Volcanics in the UK and in DK. (B) shows the location of the well panel on the map.

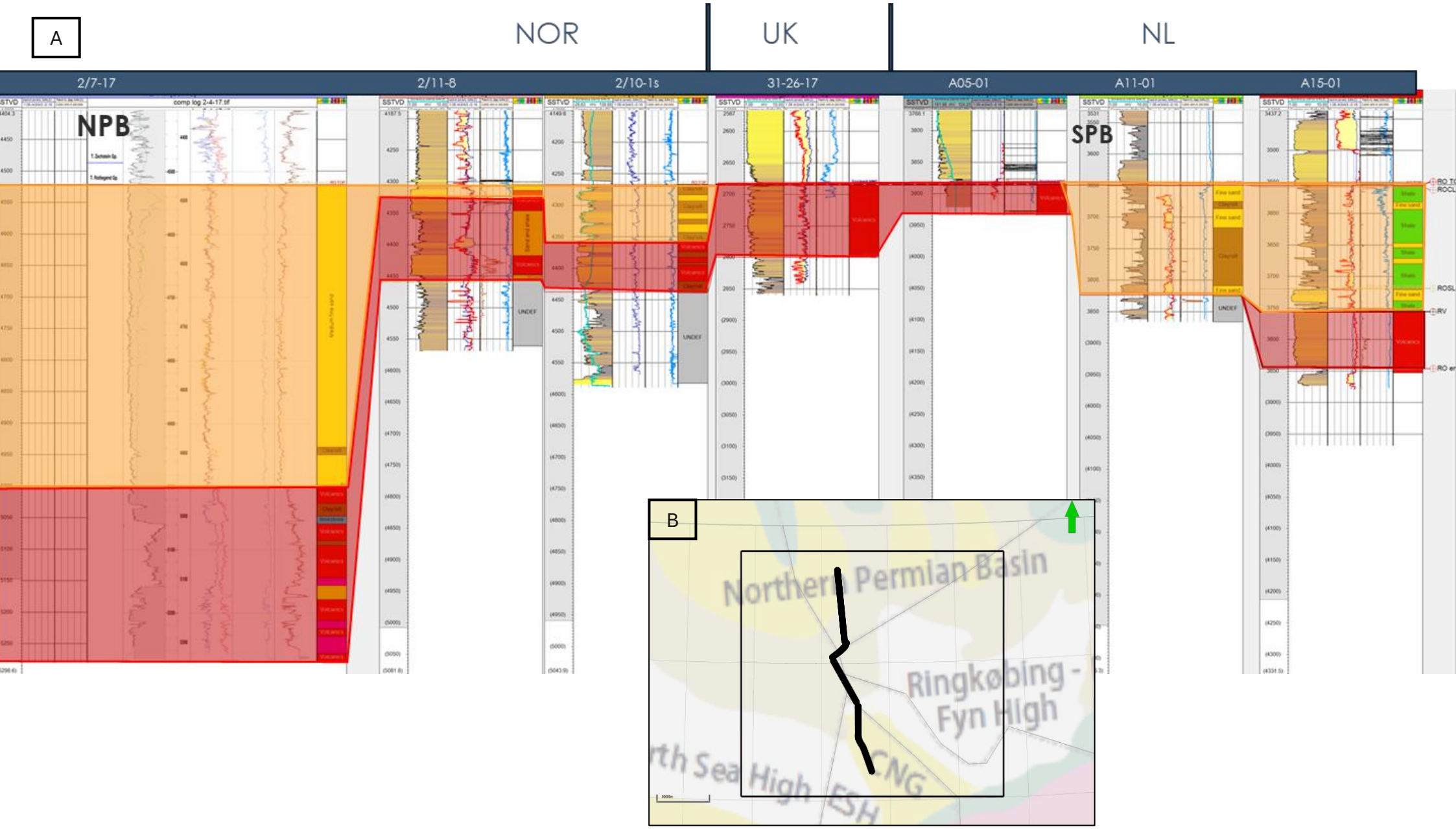

Figure 17 N-S well panel from NOR-DK-GER _NL showing the relation between Volcanics and sediments in NPB and SPB. (B) Shows the location of the well panel on the map.

4.1.3 Rotliegend Sediments:

The Rotliegend sediments had a wider distribution in the project area than the volcanics and are at their thickest in the Norwegian and UK offshore and at their thinnest in areas that have thick volcanics (Figures 14 & 18). On the MNSH, Rotliegend sediments may be completely absent. The Rotliegend sediments generally show a thickening trend away from the volcanics (Figures 15 & 17). In the Netherlands, sediments are absent in the northern tip of the Netherlands (A05-1). Further south, the sediments consist of sands interbedded with clay and become increasingly rich in clay. Outside the project area, the top part of the Rotliegend sediments has repeating layers of salt of the Silverpit formation, which are not present in any other country inside the project area, although also known from wells further south in Germany. Sediments in Germany are scarce, being restricted to a small area in the A block of the German offshore. In the Danish offshore, most of the Rotliegend sediments are absent and are either restricted to areas with no volcanics, or on the RKFH, or are present as thin layers near the areas of well Elly or D1-x. In Norway, the sediments are thickening away northward from the RFKH and the volcanics and becoming less interbedded with clay and silt (Fig.17). The same holds for the sediments in the UK, which are dominated by sands that become increasingly clayey and silty towards the volcanics in Denmark and the highs. In most of the project area, the Rotliegend sediments' top is bounded by either the Coppershale (basal Zechstein) or truncated by the BCU (Fig. 11A).

4.1.3.1 Rotliegend sandstones:

The Upper Rotliegend sandstones are present in both the SPB and NPB parts of the area, with the thickness varying between 0-200 m (Fig. 18B). The sand is at its thickest in the northern part of the UK offshore and the Norwegian offshore. Sands are mainly absent in the Danish offshore, being restricted to the border with Norway, the UK, and Germany. In the Netherlands and the southern part of the UK, offshore, the sands are comparatively thinner. Sandstones in the Netherlands are absent in the most western parts and thickest in the centre of the Dutch offshore. The sandstones in the Netherlands are narrowly connected to parts of the UK and Germany. Some sandstones are also present within the Volcanics in the UK (Grensen Formation; Fig. 12) but are less prominent in the Norwegian, Danish, and Dutch Volcanics.

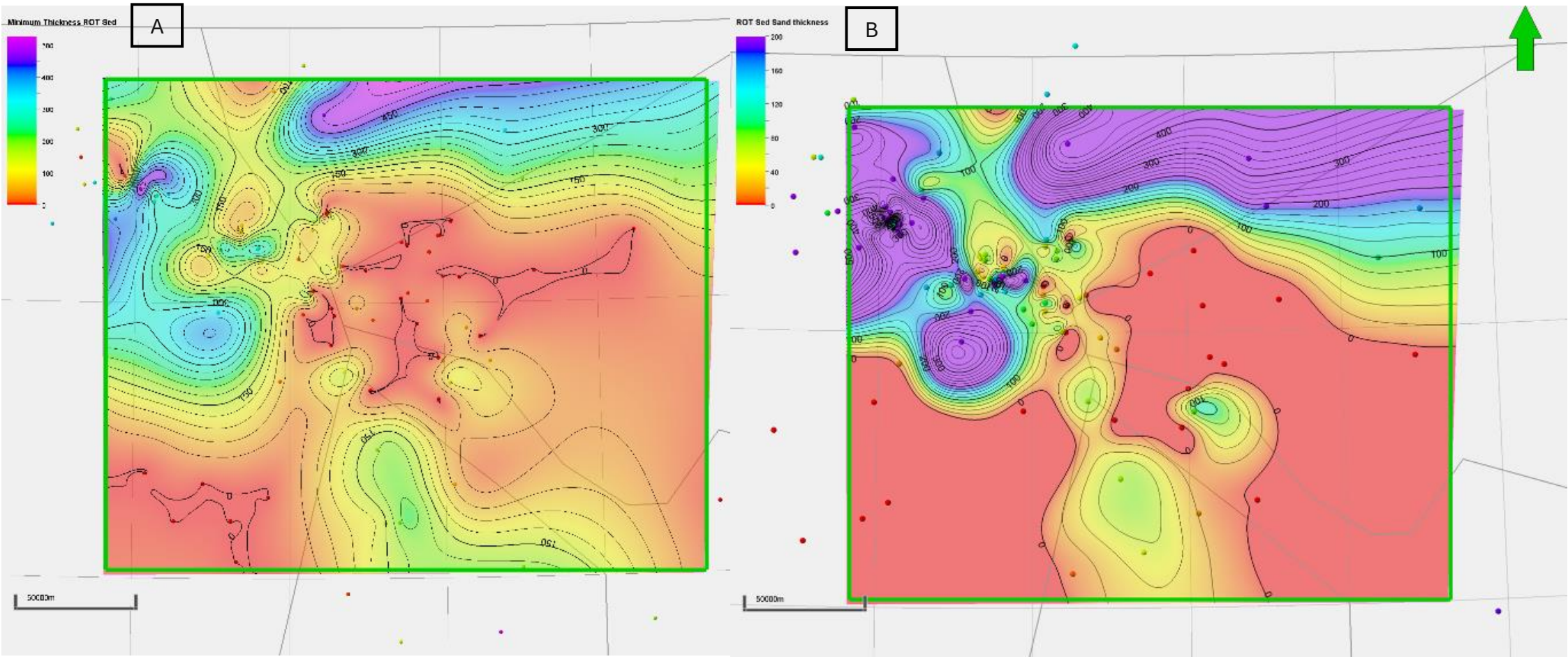

Figure 18(A) Minimum thickness map for the Rotliegend sediments in m colour scale 0-500m. (B) Minimum Thickness of Rotliegend sand from the Upper Rotliegend sediments in m colour scale 0-200m.

4.2 Gross depositional environments and Volcanic distribution:

For all Rotliegend wells within or close to the research area, the Rotliegend Volcanics and Rotliegend sediments were assigned a GDE classification and mapped (Fig. 19). The Rotliegend Volcanics were separated into mafic lavas, felsic lavas, tuff & Volcaniclastic rocks, and undifferentiated Volcanics. The mafic Volcanics showed a correlation with the Bouguer gravity (Figures 7A & 20A), but less so with the total field magnetic anomaly (Figures 7B & 20B). The mafic lavas had 3 areas of deposition. In the Northwestern part of the UK, there is a small centre of mafic Volcanics that has both a positive gravity and magnetic anomaly. Towards the southeast, the next mafic area (2) covers the eastern part of the UK, the southern part of Norway, the far western offshore of Denmark, and northern Germany. This Volcanic area extends from Denmark and Germany to the B blocks in the Netherlands. This area has three centres where both the gravity and magnetic anomaly are positive. The final mafic area is located to the north of the RKFH between wells Stork-1, 3/5-1, and D-1x. Two areas lacked sufficient information to differentiate the Volcanics, one near Dutch well A15-01 and the other in Germany C15-1. The German Volcanics have a positive gravity and magnetic anomaly. Felsic lavas were only found outside the area in the Dutch offshore in well F04-02-A. The Tuffs and volcanoclastic material overlapped with the lavas but had a much wider distribution.

The sediments had a larger distribution. Areas of non-deposition were restricted to the MNSH, RKFH, ESH, and on top of the mafic Volcanics in the centre of the study area. Areas of non-deposition are bordered by mostly alluvial or alluvial-aeolian sediments. The exception to this is in the Netherlands, where tectonic highs and Volcanics are bordered by sandflats or playa/sabkha depositions.

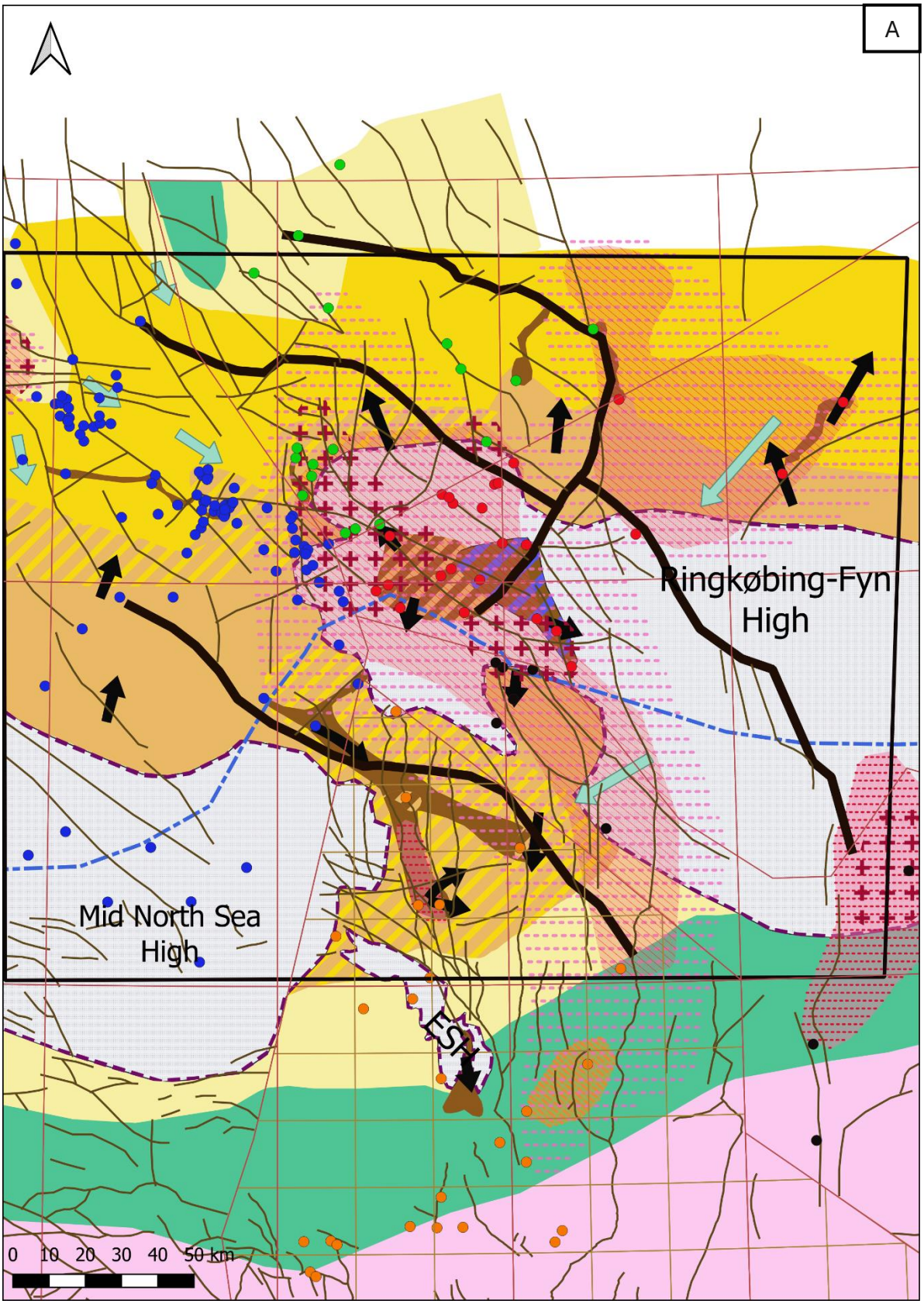
A
Ringkøbing-Fyn
High
Mid North Sea
High
EST
0 10 20 30 40 50 km

Figure 19. (A) Gross depositional environment map (GDE) of the research area. Faults were taken from de Bruin et al., (2015). *Additional maps can be found in the appendix.(B) Legend for all gross depositional maps*

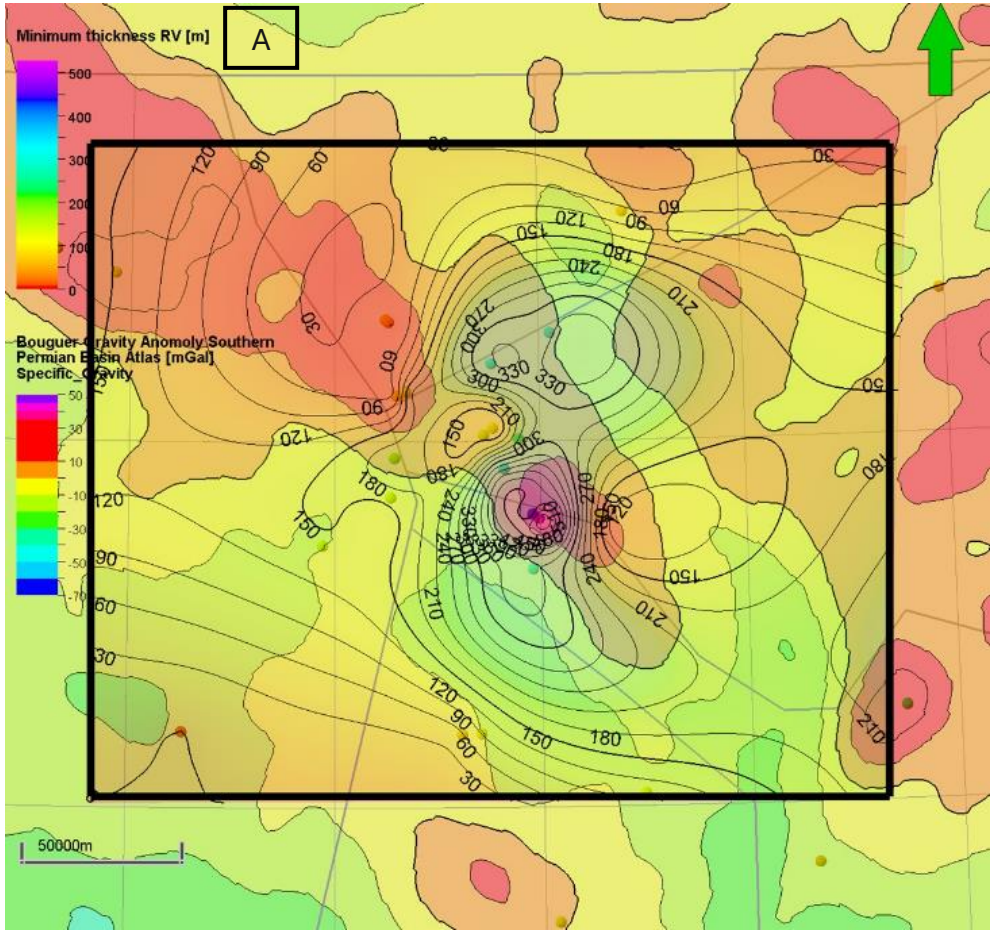

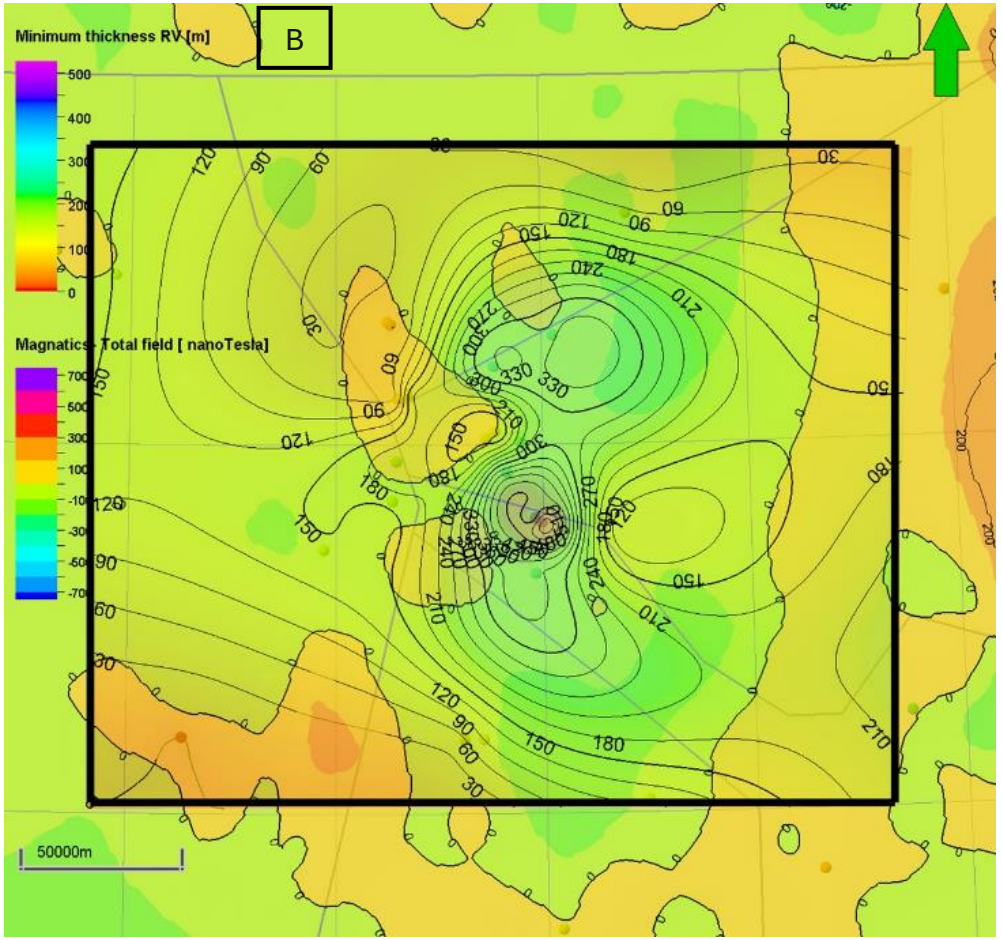

Figure 20. (A) Map showing the Bouguer gravity anomaly versus the thickness of the Volcanics map, and (B) Total magnetic anomaly versus the total RV thickness map. Maps for the Bouguer gravity and total gravity anomaly were taken from.(Guterch et al., 2010)

In addition, sourced from the local highs and volcanic areas, fluvial deposits are present. The largest of these is one that originates in the UK and expands into the Netherlands. In the NPB, the fluvial deposits have a smaller distribution and were transported in the opposite direction to the fluvial deposits in the Netherlands. In general, the alluvial and fluvial deposits were transported away from areas with possible high relief. The Aeolian deposits are dominant in the northern part of the study area, and where the sands thin, they transition into sandflats and playa&/or sabkhas. In the area of the SPB, the playa/sabkha deposits are much more extensive than in the NPB, stretching from Germany through the Netherlands towards the UK. During the Permian, the dominant wind direction was from the Northeast, but dipmeters from the UK instead show a wind direction from the Northwest (Heward, 1991). Based on the distribution of the sand and the deposition of fluvial sediments, it is likely that the SPB and NPB had little exchange of water. A likely watershed boundary was located between the MNSH and RKFH. The most unique sediments are located within mafic lava area 2, fluvio-lacustrine and fluvial&/or alluvial deposits are interfingered with volcanic material. Both of these show evidence for a transport direction away from the centre of the volcanic material.

4.3 Porosity-Permeability-Depth analyses

To determine the reservoir potential of the Dutch offshore, key parameters of porosity, permeability, and depth were analysed. The data were first subdivided depending on the depositional environment. Each measurement was classified as aeolian, alluvial, alluvial-aeolian, playa-sabkha, or fluvial. Based on their classification, they were plotted (Fig. 21). To analyse the depth relationships, the gross depositional environment was disregarded (Fig. 22). For the depth relationships, no clear trend was found between permeability and depth (Fig. 22B) and a poor relationship was found between porosity and depth (Fig. 22A) despite these parameters being known their likely correlation. This poor trend between depth and porosity could be due to sampling bias with the different depths, depositional environments, and number of data points per well not being equally represented. Nevertheless, the poro-depth and perm-depth plots indicate that below 4500 m, the porosity has an increased risk of being lower, whilst the permeability may still be acceptable.

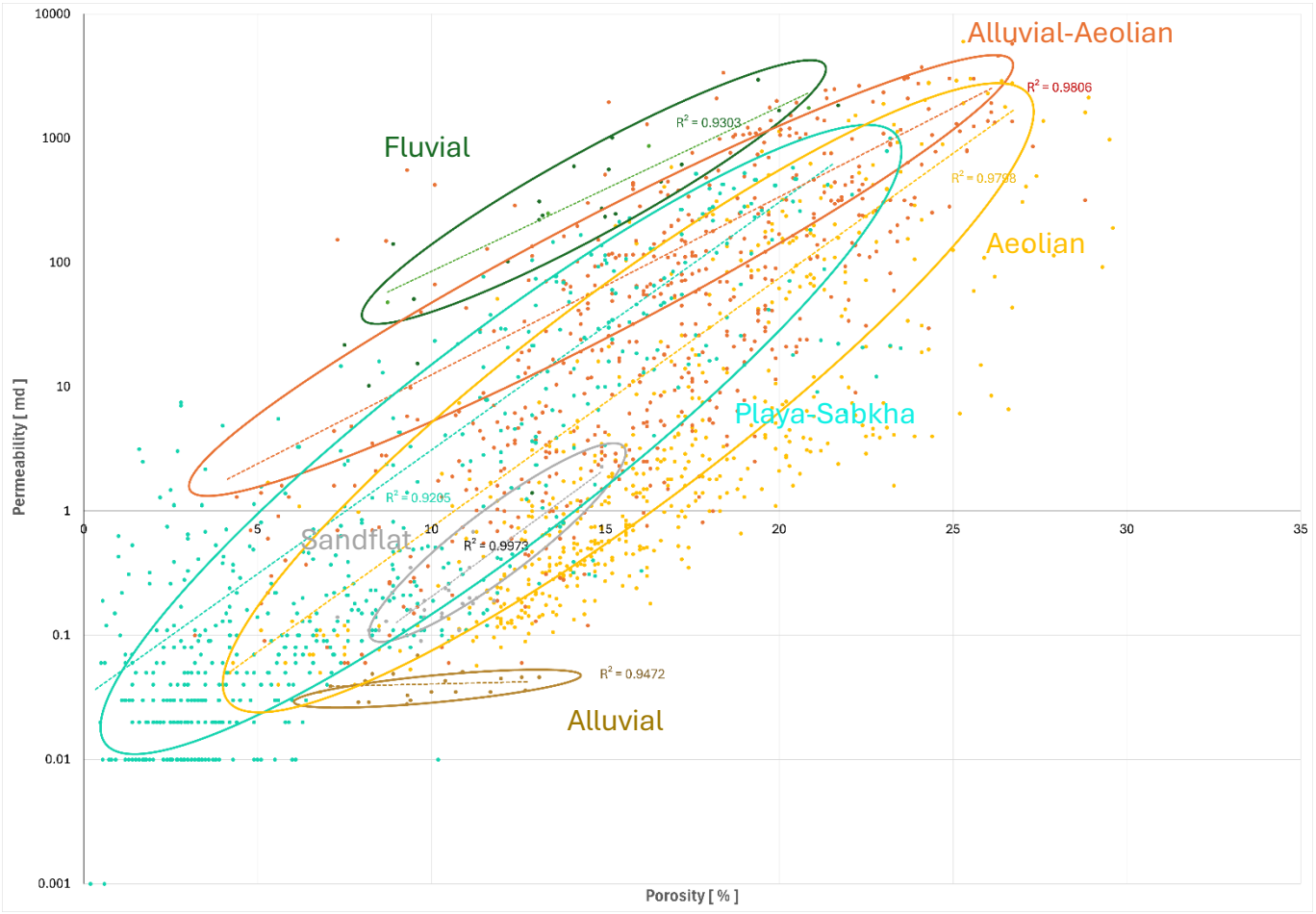

Figure 22 Porosity versus permeability plot for the different deposition environments data points, their trend line and R^2 being marked in their specific colours.

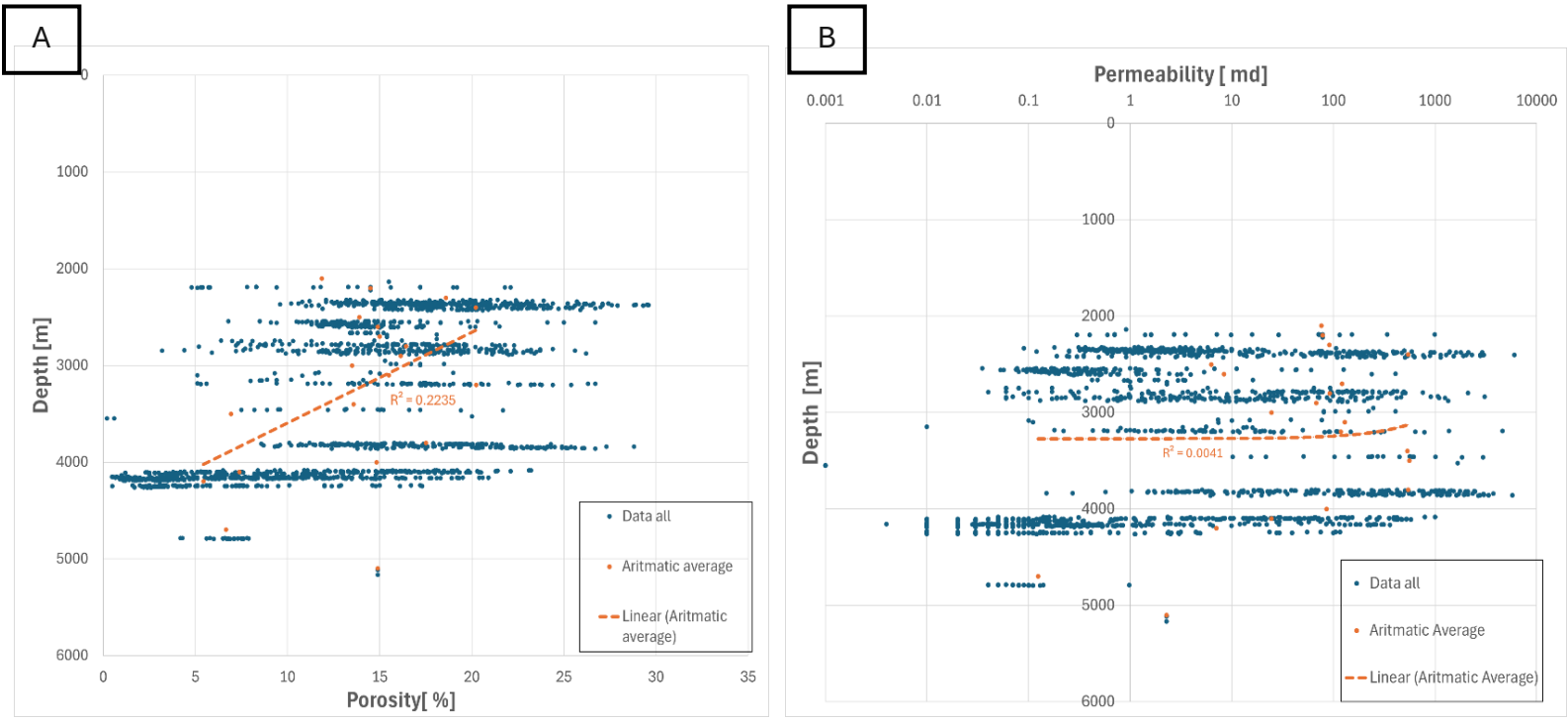

Figure 21 A) Shows the porosity depth plots for all data points regardless of GDE in orange showing the average per 100 m, and the orange line is the trend line. (B) depth permeability plots for all data points. R_2 is shown in orange and is (A) equal to 0.2235, denoting a poor relation, and for (B) R^2 is equal to 0.0541, denoting no relation.

The Aeolian data consisted of 551 data points (Table 3), all of which were located within the UK. Extrapolation towards the Dutch offshore is difficult due to the large distance between the two. The aeolian data showed a clear correlation between porosity and permeability (S1). Alluvial data was scarce, with only 19 data points from a single well in Norway (2-10-2) at depths of ~4155 m. These data points show a clear porosity permeability trend with low porosity and low permeability (S2). The alluvial-aeolian data points consisted of 532 data points, which had a wider distribution that partially overlapped with the Aeolian distribution (S3). The data set was dominated by data from the UK and parts of the Netherlands. The alluvial-aeolian sediments had a good porosity-permeability trend line. Fluvial data mainly originated from Denmark and the UK and consisted of 21 measurements with a clear trendline (S4). Due to the limited measurements, it is unclear what the true extent of the fluvial trend is.25 measurements were classified as sandflat, with the majority originating from the UK offshore northwest of the project area, and the other originating from Norway. The dataset is very shallow, with the UK and Norwegian data originating from two different depth intervals (4100-4200 & 5100-5200), making them the deepest sediments. And showed a clear trendline (S5). 959 data points were used for playa-sabkha and originate from either the Netherlands or Germany. All data points were located outside of the project area, which makes the application inside the project area uncertain. The data points had a clear trendline with lower porosity and permeabilities than the aeolian and alluvial-aeolian data (S6).

Table 3. The Gross depositional Environment classification, the average (μ) porosity and permeability of all data points, with n being the number of data points for that Gross Depositional Environment.

GDE	Porosity μ	Permeability μ	n
Aeolian	16.6584392	127.519343	551
Alluvial	10.0111842	0.040519737	19
Alluvial-Aeolian	16.3730827	276.4127256	532
Fluvial	13.9380952	551.1714286	21
Sandflat	10.388	0.364	25
Playa-Sabkha	8.03727842	29.81755162	959

5. Discussion and Interpretation:

5.1 Volcanics and their influence on sediment distribution:

The Rotliegend Volcanics in the North Sea have been and continue to be intriguing due to the lack of concrete evidence on their composition, timing, and mode of emplacement (van Bergen et al., 2025). Another aspect of the RV in the North Sea is their distribution and how they influenced the deposition of the Upper Rotliegend.

5.1.1 Rotliegend Volcanics emplacement distribution & origin?

The thickness map, based on isochore data, suggests that the Rotliegend Volcanics have a wide distribution, with the thickest parts located in the most western areas of the Danish and German offshore (Fig. 14). GDE mapping reveals that the distribution of the RV is much more limited. The volcanics in the project area consisted of mafic, felsic, tuffs, and volcanoclastic materials. Mafic and undifferentiated volcanic bodies were generally bordered by faults, and a few specific areas had a positive magnetic anomaly. The largest Volcanic body in the area is bordered by the Coffee Soil Fault and the Paleo 5 Fault (Fig. 19). The Felsic Volcanic body to the south of the project area, near well F04-2A, appears to be less influenced by the presence of faults as compared to the mafic volcanic material. Sissing (2004 described these as rhyolites or rhyodacite, which have been strongly altered. Tuffs and/or volcanoclastic material had a much wider distribution. The wider distribution of the tuff and volcanoclastic material is reasonable considering their method of deposition. However, a high amount of uncertainty is associated with interpreting tuff and volcanoclastic material in cores and composite well logs, especially regarding their age. This results in the spread of tuff and volcanoclastic material in some parts of the map being too wide and in other parts too limited.

The proximity of the Rotliegend igneous rocks in relation to the faults points to them having some relationship to each other. One option is that extensional faulting took place simultaneously with the extrusion of volcanics, which would have helped facilitate magma migration to the surface. Heeremans et al (2004b) support this with the observation that the basaltic lavas had relatively short residence times, but also note that syn-sedimentary normal faulting took place after the extrusion of the magmas and that fracture propagation does not require a pure extensional regime. The normal faulting resulted in differential subsidence along the Coffee Soil fault, with relative uplift in the Danish Central Graben and subsidence in the Norwegian-Danish basin (Stemmerik et al., 2000). Due to the presence of sediments during the Saalian unconformity in Denmark and Germany, it is likely that some of the faulting would have taken place during or shortly after the emplacement of the Rotliegend Volcanics, whilst in other parts the faulting would not have started until Upper Permian times. Felsic volcanics did not show a correlation with faults and likely predate faulting.

The origin of the magmatism is heavily debated between lithosphere thinning and a mantle plume (Neumann et al., 2004). The direction and emplacement of positive gravity and Bouguer anomaly show a linear trend. If these centres showed a progressively younger trend, then that would favour the igneous rocks originating from a mantle plume. If no time trend exists, then the lithospheric model would be favourable. The lithospheric model agrees with the proposed model for the temporal evolution of the Thor suture zone, based on seismic refraction data, where thermal relaxation occurred after 330 Ma (Smit et al., 2016). The Volcanics in the area ranged between basalt, trachy-basalt, and rhyolites, making them sub-alkaline (Fig.5). This is supported by Neuman et al (2004), who analysed Sr-Nd isotope data and both major trace elements to further the understanding of the magmatism in the North Sea. Thin sections of volcanics for the Danish offshore do exist, but often lack a scale bar (S23). The general size of the crystals under the microscope leans towards extrusive volcanics. This problem is further enhanced by the eroded and altered nature of the lavas. However, the lack of contact metamorphism in the surrounding sediments does support the hypothesis that most of the volcanics were extrusive.

Most of the thick mafic volcanics correlate with both a positive Bouguer gravity anomaly and some with the total field magnetic anomaly. The exception to this is near German Well C15-1, for which the nature of the Volcanics could not be directly interpreted. However, the presence of the gravity and magnetic anomaly favours the idea that these Volcanics were also of mafic composition.

This interpretation was similarly found by (van Bergen et al., 2025). Their interpretation of the early Permian magmatism is in accordance with the findings of Gast et al., (2010) and notably does not include the southern parts of Norway and most parts of the Danish offshore, including the Karl well in the Danish offshore. This opposes the interpretation of this study and the mapping by Armour et al., 2004, Heeremans, et al., 2004a & Stemmerik et al., 2000). The Volcanics in the UK block 29 are not mapped in any known publication. The igneous rock in block 29 was interpreted based on composite logs of wells in that area and is supported by the fact that the area has both a positive magnetic anomaly and a gravity anomaly, which supports the presence of an igneous body somewhere in the subsurface of block 29. These igneous rocks may not have been interpreted previously due to the old, unreliable composite logs and the relatively small size of the igneous body. Alternatively, this rock could have been wrongly dated in the composite well log and could instead be of Triassic age. Van Bergen et al (2025) also interpreted Permian igneous rock in the German Central Graben. This could not be confirmed in this study due to the lack of wells in the German Central Graben. 3D and 2D basin modelling by Arfai & Lutz, (2017) did not include any Rotliegend in the German Central Graben.

5.1.2 Rotliegend Volcanics and Relationship with the Sediments.

The Rotliegend Volcanics were partly interbedded with sediments. In the UK in block 39 these sediments consisted of sands of the Grensen Formation, whilst towards the east, in Denmark and Norway, the Volcanics were interfingered with more silty and clay-rich material, which are likely part of the Elly or Diamant member, which deposited during and shortly after the majority of the Volcanics were deposited (S22). The interfingering relationship with Volcanics and lacustrine deposition may further support early faulting and basin development simultaneously with the magmatism. Stemmerik et al (2000) proposed that because these Volcanics (276-28 and 261-269 Ma) had younger ages than the Volcanics found in the SPB (~300 Ma), the formation of NPB must postdate the SPB. However, these numbers were dated based on K-Ar ages, whilst Ar-Ar and U-Pb ages argue that they occurred at the same time as the Volcanics in the SPB (van Bergen et al., 2025). Van Bergen et al.,(2025) age determinations indicate an age closer to the late Carboniferous-Early Permian boundary, confirming that the SPB and NPB formed at the same time. The earlier dating would also make the Grensen Formation time equivalent to the sediments in the Danish offshore.

Areas with thick volcanics were lacking in sediment cover, with the best example of this being the Karl well in the Danish offshore (Fig. 15). This lack of sediment cover is either because the Volcanics were relatively elevated or because any sediments on top were eroded. Evidence of erosion is present in alluvial, fluvial, and aeolian depositions in the Norwegian, Danish, UK, and Dutch offshore. These alluvial deposits are often contaminated with volcanoclastic material, making it difficult to determine whether some of these deposits belong to the Lower or Upper Rotliegend due to the lack of a clear definition between the border of the Lower Rotliegend and Upper Rotliegend outside the elusive Saalian unconformity. The half-graben depositional model proposed by Stemmerik et al (2000) would support this and help provide sedimentation space.

As subsidence continued, accommodation space would have continued to be provided, allowing for the sedimentation of the Upper Rotliegend to be deposited (S22C). Stemmerik et al (2000) proposed that this would occur in half-graben-like structures. For the K blocks in the Dutch offshore, it is thought that the erosion-resistant Carboniferous rocks would have helped facilitate basin formation and deposition of the Upper Rotliegend (Fig. 23; Mijnlieff and Geluk, 2011). Seismic sections of the Dutch offshore (de Bruin et al., 2015) show half-graben structures similar to the ones found in Denmark and Norway (Fig. 24). This makes it likely that in the Dutch far offshore, the formation of half-graben would have been the main influence on the deposition of sediments. However, both the Carboniferous rocks and the Rotliegend igneous rocks could also have influenced the paleo relief and the deposition of the sediments.

The Upper Rotliegend was deposited as thinner layers on top of the volcanics and as thick layers in areas where the Volcanics didn't take up accommodation space. These

sediments were thicker and quicker to thicken in the NPB as opposed to the SPB. In the NPB, the sand consisted mainly of aeolian, sandflat, or fluvial deposits. In the SPB, the sediment and sands were much thinner and had larger deposits of sandflats, playa/sabkhas, fluvial, and saline lake deposits. This difference in sand thickness could either be due to differential subsidence rates or due to the Volcanics in the central part of the project area acting as a windshield from the NE wind, paired with a difference in wind energy. Differences in subsidence rates have previously been observed in the SPB, resulting in sands in Germany being ~8 times as thick as the sands in the UK southern North Sea outside of this project's research area (Glennie, 2005 and references therein).On the other hand, winds that generally originated from the north would have had the highest energy in the NPB and lower energy in the SPB. Furthermore, if the Volcanics were relatively elevated, then they could have prevented aeolian sands from reaching the SPB in the project area. To confirm this, subsidence rates between the NPB and SPB during the Permian would need to be researched, but currently, research on the NPB is severely lacking.

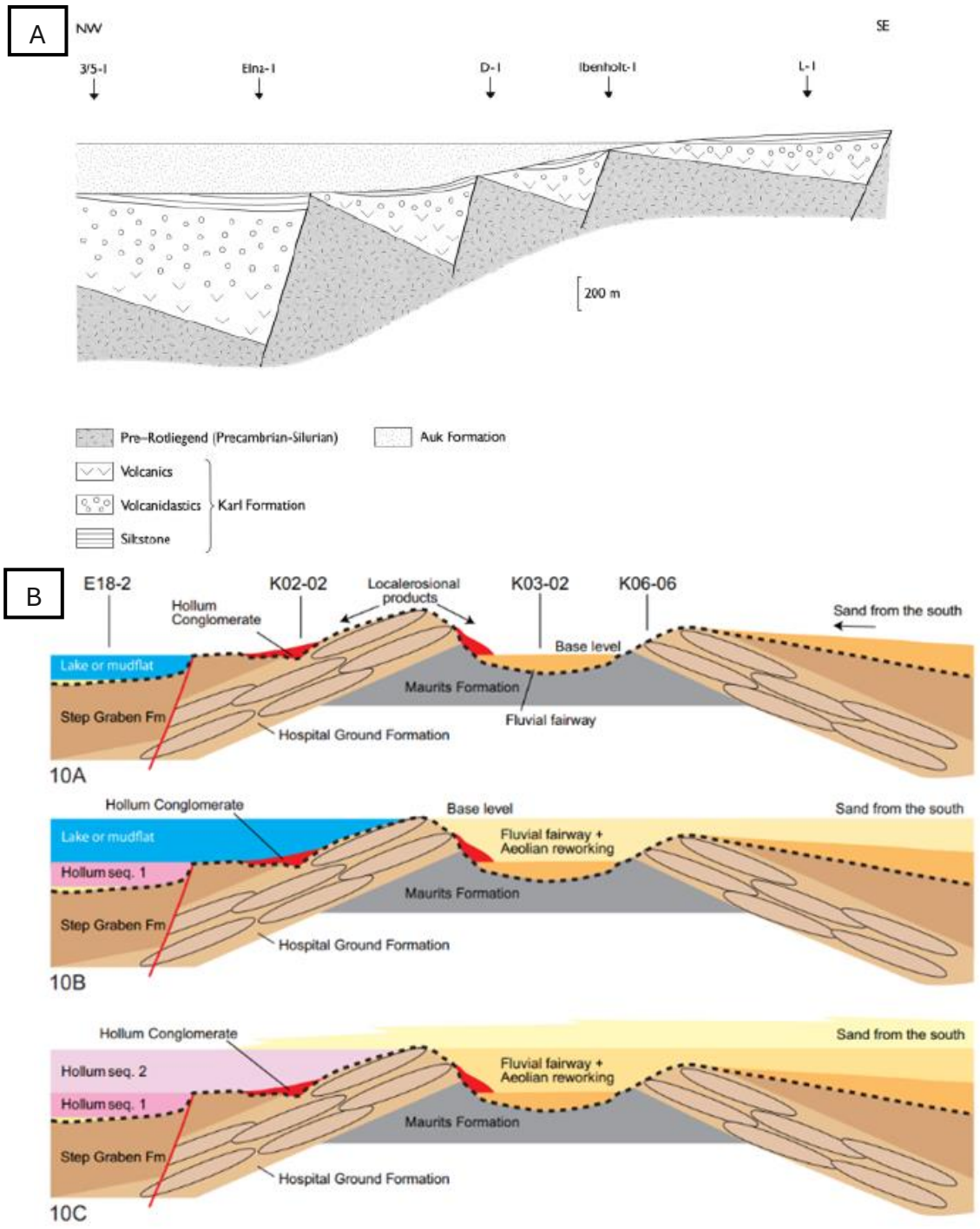

Figure 23 (A) Proposed depositional model by showing the influence of half graben structures(Stemmerik et al., 2000). (B)Proposed model for how paleo relief from the Carboniferous influences the deposition of the Rotliegend Sediments(Mijnlieff & Geluk, 2011).

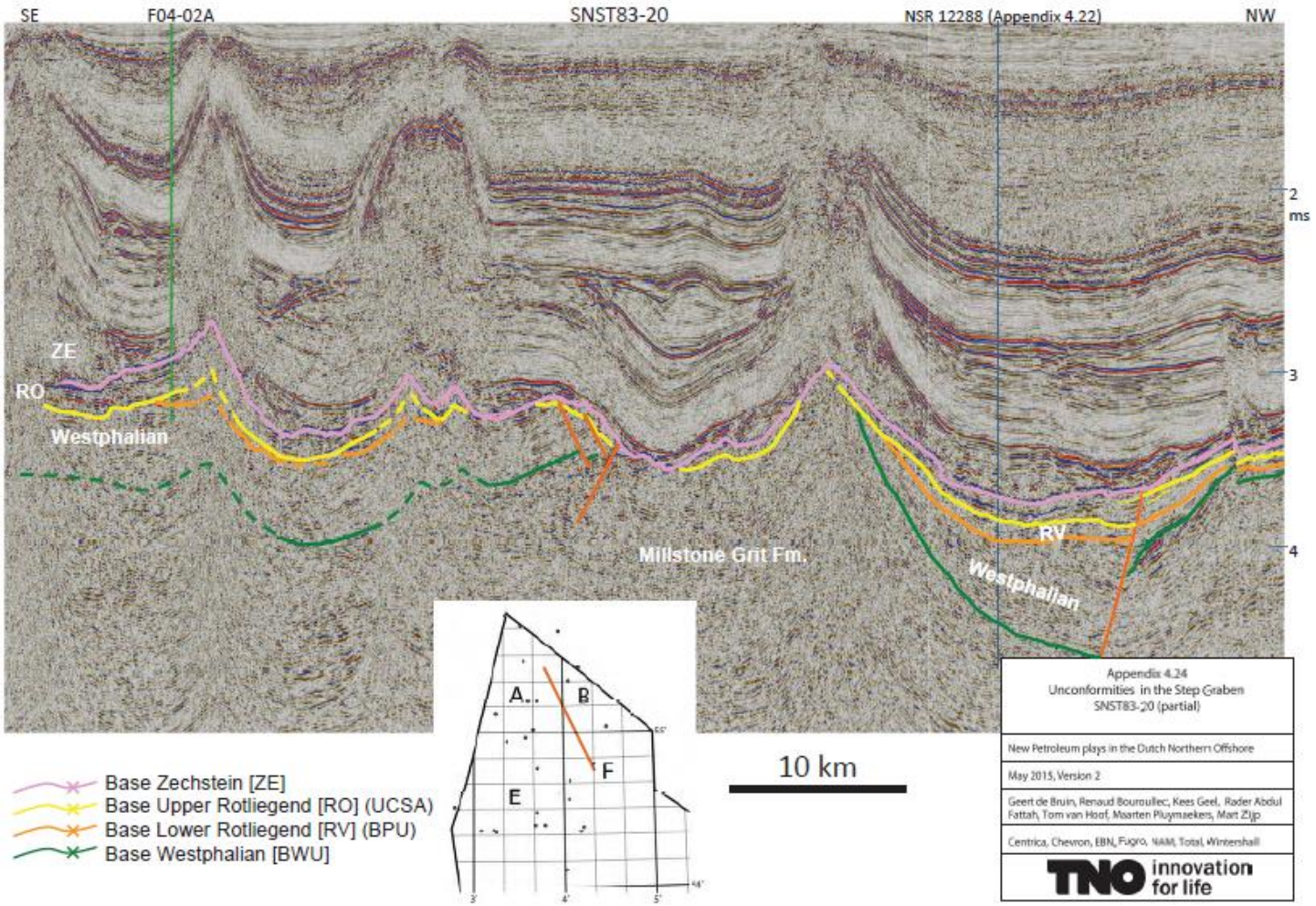

Figure 24 Seismic section of the Dutch offshore showing thick Lower Rotliegend near the fault with Rotliegend sediments on top (de Bruin et al., 2015).

.

Upper Rotliegend was missing on the MNSH and parts of the RKFH. In those areas, Zechstein directly overlies Carboniferous or even Devonian. On parts of the RFKH, Upper Rotliegend was missing due to being cut by the BCU, where the Jurassic overlies the Rotliegend. This shows that the MNSH and RKH during the Permian and following the Permian had different depositional histories, but both were likely never deeply buried again, as evidenced by the low maturity of the Carboniferous source rock (IGI, 2023). Furthermore, the Upper Rotliegend may be missing in the German Central Graben (Arfai & Lutz, 2017). It is uncertain if this is the case for the Dutch central graben as well, but due to the depth of the central graben, it is difficult to confirm. Improved seismics could improve our understanding of the depositional range of the Upper Rotliegend and future thickness maps of the research area.

5.2 Climate and influence of wind and its direction.

5.2.1 Climate variations in the early Permian.

Fluvial, lacustrine, and alluvial sediments, interfingered with the early Rotliegend Volcanics. This indicates that the climate must have been somewhat humid. (Glennie, 2005). Glennie (2005) also noticed this and proposed that this was caused by areas with high local relief. This high relief could have been caused by the formation of half graben, or could have been caused by areas with thick extrusive Volcanics. The Volcanics in the project area reached thicknesses of above 300 m but were likely partly eroded by the Cretaceous erosional event(Fig. 14). Alternatively, the early Permian humidity could be due to the northward drift of Laurasia towards the northern position above the equator. (Glennie, 1998). Much of this drift would have coincided with the Saalian unconformity, and the Arid desert environment associated with the Upper Rotliegend only ensued after.

5.2.2 Transport direction and conflicting wind directions

Based on dipmeter logs, the primary wind direction found in the UK was from the NW, perpendicular to the wind direction that would be expected based on the paleogeographical position north of the equator. North of the equator, between 10-30 °, it would be expected that the trade winds from the northeast would have affected the area. These winds would have varied in strength depending on the size of the icecaps. During Glaciations, the ice caps would have been larger, and high- and low-pressure systems around the equator would have been closer, resulting in faster winds. During periglacial high and low air pressure systems would have been further apart, resulting in weaker winds (Glennie, 1998) (S21). These strong winds explain the large size of the dunes, but fail to explain the dipmeter directions observed in the UK. Glennie (1982) proposed that this perpendicular wind direction was the result of a local high barometric pressure system located on top of the MNSH. This would fit with previously proposed

models on the Cygnus field south of the MNSH (de Bruin et al., 2015). Sneh (1988) completely opposed the idea of winds originating from the Northeast and instead proposed northern winds. Because I found no evidence to disregard the dipmeters or the Northeastern winds, the alternative solution would be that winds originated from both directions. Besly et al. (2018) proposed that the dunes are linear migrating dunes that were able to form due to experiencing two different wind directions. This is further supported by similar dipmeter measurements found in the Dutch onshore.

5.3 Rotliegend Sands in the Netherlands and reservoir potential.

Key parameters to consider for a reservoir are porosity, permeability, and depth. For the Rotliegend, the reservoir rock is the Rotliegend sandstone in the Upper and Lower Slochteren. To confirm this, a thickness map of the Rotliegend sands was constructed based on well correlation. Due to the limited number of wells in the far northern Dutch offshore, the thickness maps lack clear detail. To improve this, new seismics would need to be incorporated in future research. Furthermore, much data from the German A & B blocks has yet to be published, resulting in the thickness and sediment transport direction from Germany towards the Netherlands being highly uncertain. Norwegian wells cause similar uncertainty in the NPB due to the difficulty in obtaining the data. Future research could improve on this study by incorporating the unpublished and difficult-to-obtain data.

The limited number of wells and the sand thickness map show that in the far offshore of the Netherlands, sandstones with a total thickness of at least 80 m exist. The GDE maps show that these sands are either fluvial, alluvial-aeolian, aeolian, or alluvial. The fluvial sediments originate from the UK and were similarly interpreted in Kortekaas et al.(2023). The source of the sediments appears to be either from the MNSH or the mafic Volcanics to the north of the Netherlands. Fluvial sediments likely did not reach the eastern blocks of the B block in the Netherlands due to mafic Volcanics, making it harder for the river to transport itself. Alluvial sediments, due to their transport method, were likely deposited from local areas with high relief, like the ESH, MNSH, from the North of Germany, from thick Volcanics, or as an extension from the RKFH. Aeolian deposits were likely transported from the NE with a possible minor component from the NW due to the dominant wind directions measured in the Area.

5.3.1 Areas with potential reservoir

In the far offshore in the Dutch offshore is dominated by fluvial, aeolian, and alluvial sediments. For this reason, the focus on areas with reservoir potential will be on these depositional environments. The alluvial sediment had a clear trend with poor permeability and porosity. However, the uncertainty for this environment is high due to it being based on data from a single well located in the Norwegian offshore in the NPB. Fluvial data was limited to two wells, both located in the NPB, with both good porosity and permeability. Lastly, aeolian sediments have good reservoir potential, but all data

points originated from the NPB, where the wind originates, likely resulting in slight compositional variations across borders. Alluvial-Aeolian had a similar trend to the aeolian deposits, as they shared similar features. These deposits had the most widespread distribution, including from the Netherlands, providing proof for the potential in the Dutch offshore. Depth analyses showed a poor correlation between porosity and depth, and no correlation between permeability and depth. Depth is a known factor in affecting the porosity, so this poor correlation is likely due to the selection bias of the data, where certain depositional environments and depths are underrepresented. Nevertheless, the porosity depth plot shows that at depth below 5 km, the reservoir potential decreases, whilst the permeability is not affected by depth. To find a good reservoir, the following parameters must be met: sand, a GDE with a good porosity-permeability trend, and above 5 km of depth. Using the Geode playmap for the depth of the base of the Rotliegend areas with depth of 5km or more are marked (Fig. 25A)(Kortekaas et al., 2023). Furthermore, the ESH has no Rotliegend deposits and should thus also be avoided. Combining this with the sand thickness map, prospective reservoir areas are marked (Fig. 25B). Figure 25B shows that prospective areas include blocks A8, A9, A10, A11, A12, A13, A14, A15, A18, B10, and B13. Across the border, the highs and volcanics are usually surrounded by alluvial deposits. Thus, Dutch offshore areas close to those features like blocks A8, A9, A10, A13, and B10 have an increased risk of having poor reservoirs. De Bruin et al (2015) concluded that the most prospective areas were A15 and B13 blocks. This conclusion was based on net sand maps, the presence of a seal, and the maturity of the Carboniferous. Furthermore, de Bruin (2015) also considers the sands in the Lower Rotliegend Volcanics in his analyses and does not disregard areas with depths below 5 km. Reservoirs below 5 km do exist in the Dutch offshore area in the L block in the field at L05-D. Thus, a reservoir at that depth, though less likely, is not impossible, due to the permeability not being affected by the increased depth.

5.3.2 Contamination in Rotliegend Sands

Volcanoclastic rocks contain mineralogically and mechanically unstable components that, during burial, may cause a lower reservoir quality than expected. Generally, secondary alteration of these components may lead to a reduction in permeability. However, under favourable conditions, dissolution of these unstable particles may also increase reservoir quality. The alteration pathways of Volcaniclastic rocks are complex and are thus generally considered unfavourable for reservoir quality. This is confirmed by the well correlation panels, where volcanoclastic material had notably low porosity compared to sands. De Bruin et al. (2015) noted that in well B10-02, the Volcaniclastic rocks may have a zone of high porosity as a result of weathering of the underlying basaltic layer, but other wells in the Danish offshore do not share this trait.

Overall, the components of Volcanic rock will influence the reservoir quality of the Upper Rotliegend sand. The fluvial sediments in the Netherlands originated from the UK

and may have been contaminated with Volcanic material. The dominant wind direction was likely from the Northeast, and the minor wind direction was from the Northwest. Winds from the Northeast may have eroded and transported basaltic material to the aeolian deposits encountered in the Dutch offshore. This can either have a positive effect or a negative effect on the reservoir quality.

A common mineral in mafic rocks is zeolite. Zeolite is a group name for framework aluminosilicates, which are built of corner-linked tetrahedra (Armbruster & Gunter, 2001). Kilhams et al,(2022) noted that a greater abundance of zeolites, compared to secondary clay minerals like smectite, results in better sealing capacities and negatively impacts the reservoir quality. However, if the reservoir's main use is for CO_2 storage(CCS), then the contamination of mafic minerals may improve the effectiveness of the reservoir. CO_2 is either trapped in the pores (residual trapping), dissolved into water(solubility trapping) (Kilhams et al., 2022), or may interact with minerals to form stable carbonate minerals (mineral trapping). The advantage of mineral trapping is that it adds to the security of CO_2 storage. Kilhams et al. (2022) proved that zeolites also interact with CO_2. However, more common heavy minerals like olivine may have a greater impact on the storage capacity for CO_2. Still, it is unknown what the impact would be of these volcanoclastic materials in the sands due to their abundance likely being relatively low due to the length of the transport distance and the likelihood of the minerals being altered, both reducing their effectiveness (Kilhams et al., 2022). The degree to which the potential reservoir will be negatively or positively affected will be determined by the degree of the minerals and the quantity of mafic components.

It is likely that the heavy mineral contamination will be minimal in the Upper Rotliegend but abundant in the sands found in the Rotliegend Volcanics. These sands and clastics correlate with the Grensen Formation in the UK and the Elly member in Denmark. Correlation of the Lower Rotliegend clastics with the Grensen Formation was previously proposed by de Bruin (2015. The idea that the Elly member and the Grensen Formation are related is also commonly pushed (Heeremans et al., 2004b; Pedersen, 2012; Stemmerik et al., 2000). Due to the likely contamination of the Lower Rotliegend, future studies should focus on further exploring the Upper Rotliegend in the far Dutch offshore.

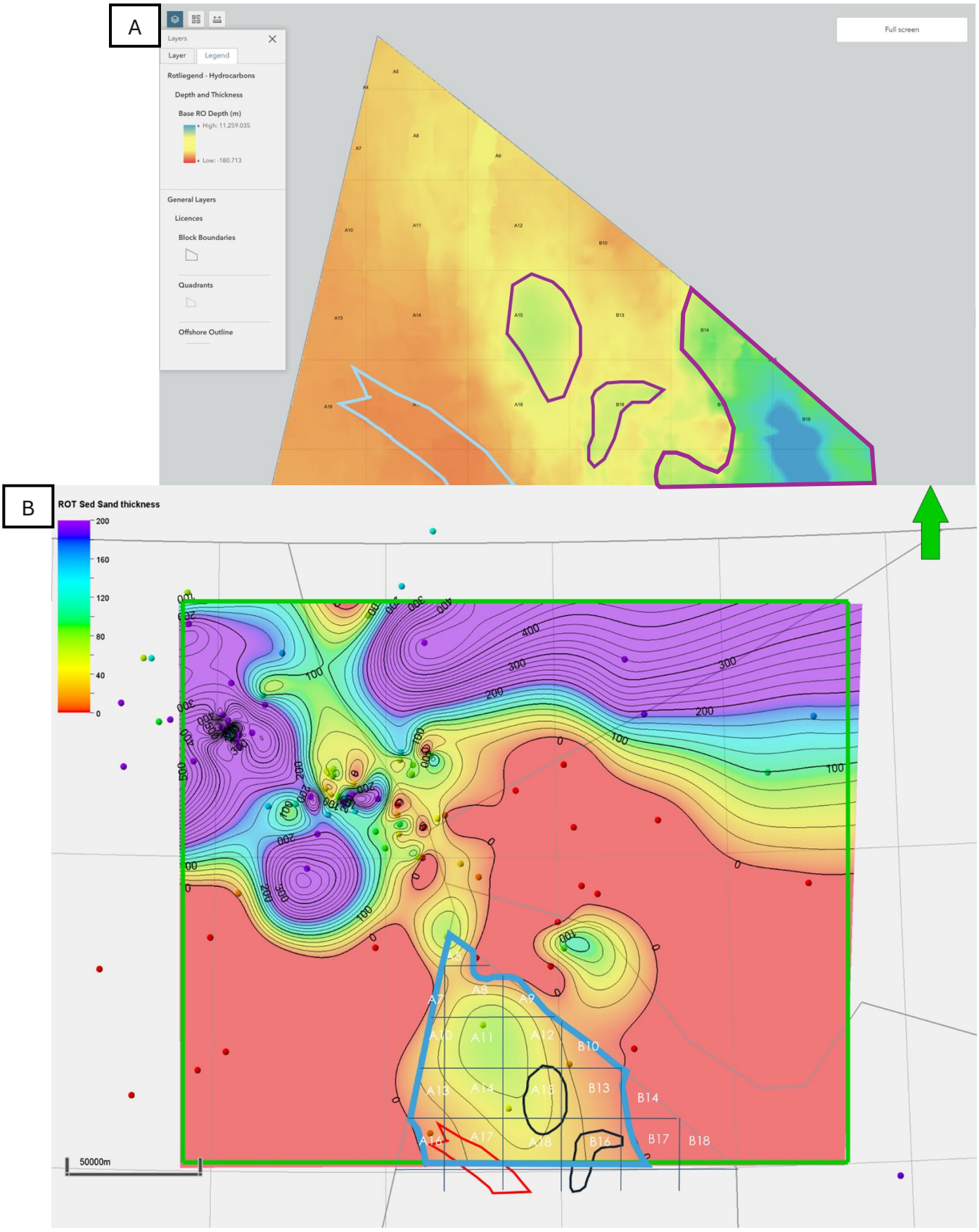

Figure 25(A) Geode map showing the depth of the base of the Rotliegend (Kortekaas et al., 2023) with purple areas outlining depths of below 5 km and the blue area marking the ESH.(B) Thickness map of the Upper Rotliegend sands with the area with potential reservoir in the Netherlands outlines in blue, the areas with depth below 5 km lined in black and the ESH marked in red.

6. Conclusions:

The Rotliegend sandstones have been and continue to be one of the most important potential reservoirs. Due to its importance in the Netherlands and large parts of western Europe, lots of data and research have been done in the past in order to understand the distribution of the Rotliegend. One area where this is not the case is the Dutch far northern offshore in the A-B blocks, where both well data and seismic data are limited. This has resulted in the distribution of the Rotliegend being poorly understood in an area whose geology is further complicated by the presence of the Rotliegend volcanics.

In this report, we successfully improved the understanding distribution of both the Upper Rotliegend clastic and Lower Rotliegend volcanics in the five-nation area. Using well data, core data, and porosity and permeability data, we tried to improve our understanding of the distribution of the Rotliegend, the influence of the Rotliegend volcanics on the deposition of the Upper Rotliegend, and to identify areas in the Dutch offshore with unrealised reservoir potential. The results provide a more detailed look into the distribution and depositional environments in the five-nation area.

The most important findings include:

- The Upper Rotliegend in de Dutch offshore has potential reservoir areas.
- The Upper Rotliegend Sands have a negative correlation with the Lower Rotliegend Volcanics.
- Sands in the NPB are quicker to thicken than in the SPB due to either or a combination of wind direction and differential subsidence.
- The deposition of the Volcanics was facilitated by faults, and basin formation for the Upper and Lower Rotliegend clastics was aided by the formation of Half-Graben structures.
- Two winds were active, a dominant one from the NE and one from the NW.
- Wind and transport directions indicate that the Rotliegend sand may be contaminated with volcanic material, reducing reservoir quality.

7. Recommendations:

This report provides a combination of publicly available literature and data on the Rotliegend in the five-nation area to assess reservoir potential in the Upper Rotliegend. Based on the findings of this research, I would recommend the following:

1. The offshore blocks A11, A12, A15 & B13 hold the most promising reservoir potential and should be prioritized in future research.
2. Areas close to volcanics should be avoided due to the increased risk of rocks with poor reservoir quality.
3. Areas with alluvial deposits or depths below 5 km should be avoided.
4. Future research should include (improved) seismics to provide a more detailed thickness map for the Upper Rotliegend Sandstones.
5. Future studies should consider contamination of volcanic material when considering reservoir quality.
6. To further improve mapping, data that was unavailable during the writing of this report from the German and Norwegian offshore should be incorporated.

Acknowledgements:

I would like to express my gratitude towards EBN for giving me the opportunity to work on this project and to learn about a new subject, obtain new skills, and get to know EBN as a company. I would like to sincerely thank my supervisor, Daan den Hartog Jager, for his guidance throughout the whole process, encyclopaedic knowledge, and compassion. I also like to thank my university supervisor, Professor Fred Beekman, for his help in gathering data. I also appreciate Aart-Peter van den Berg van Saparoea and Sabine Korevaar for their guidance on using software. Furthermore, I would like to thank Bas van der Es, Kees van Ojik, Adriaan Janszen, Henk van Lochem, and Marloes Kortekaas for their suggestions. I also like to thank Joost van den Broek for his help in converting well log data from LIS format to LAS and his aid in analysing porosity and permeability data. I would like to especially thank Esmée Boter for her unrelenting helpfulness and kindness throughout the whole process. Finally, I would like to thank the Federal Institute for Geosciences and Natural Resources (BGR) for their help in obtaining German well data.

References:

Arfai, J., & Lutz, R. (2017). 3D basin and petroleum system modelling of the NW German North Sea (Entenschnabel). *Petroleum Geology Conference Proceedings*, *8*(1), 67–86. https://doi.org/10.1144/PGC8.35

Armbruster, T., & Gunter, M. E. (2001). Crystal structures of natural zeolites. *Reviews in Mineralogy and Geochemistry*, *45*, 1–67. https://doi.org/10.2138/rmg.2001.45.1

Armour, A., Evans, D., & Hickey, C. (2004). The Millennium Atlas : Petroleum Geology of the Central and Northern North S e THE MILLENNIUM ATLAS : of the CENTRAL and. The project to produce the Millennium Atlas was organised by *Petroleum Geology*.

Bas, M. J. L., Maitre, R. W. L., Streckeisen, A., & Zanettin, B. (1986). A chemical classification of Volcanic rocks based on the total alkali-silica diagram. *Journal of Petrology*, *27*(3), 745–750. https://doi.org/10.1093/petrology/27.3.745

Besly, B., Romain, H. G., & Mountney, N. P. (2018). Reconstruction of linear dunes from ancient aeolian successions using subsurface data: Permian Auk Formation, Central North Sea, UK. *Marine and Petroleum Geology*, *91*(February 2017), 1–18. https://doi.org/10.1016/j.marpetgeo.2017.12.021

Bouroullec, R., Geel, C., & Geluk, M. (2025). 4.Permian. In *Geology of the Netherlands* (2nd ed.). Amsterdam University Press. https://doi.org/10.5117/9789463728362

Clark, D. A. (1997). Magnetic petrophysics and magnetic petrology: aids to geological interpretation of magnetic surveys. *AGSO Journal of Australian Geology & Geophysics*, *17*(2), 83–103.

Corfield, S. M., Gawthorpe, R. L., Gage, M., Fraser, A. J., & Besly, B. M. (1996). Inversion tectonics of the Variscan foreland of the British Isles. *Journal of the Geological Society*, *153*(1), 17–32. https://doi.org/10.1144/gsjgs.153.1.0017

de Bruin, G., Bouroullec, R., Geel, K., Fattah, R. A., van Hoof, T., Pluymaekers, M., van der Belt, F., Vandeweijer, V., & Zijp, M. (2015). *New Petroleum plays in the Dutch Northern Offshore*. *TNO 2015 R10920*, 168.

de Jager, J., van Ojik, K., & Smit, J. (2025). 1 Geological development. In *Geology of the Netherlands* (2nd ed.). Amsterdam University Press. https://doi.org/10.5117/9789463728362

Doornenbal, J. C., Kombrink, H., Bouroullec, R., Dalman, R. A. F., DE Bruin, G., Geel, C. R., Houben, A. J. P., Jaarsma, B., Juez-Larré, J., Kortekaas, M., Mijnlieff, H. F., Nelskamp, S., Pharaoh, T. C., Ten Veen, J. H., Ter Borgh, M., VAN Ojik, K., Verreussel, R. M. C. H., Verweij, J. M., & Vis, G. J. (2019). New insights on subsurface energy

resources in the Southern North Sea Basin area. In *Geological Society Special Publication* (Vol. 494, Issue 1). https://doi.org/10.1144/SP494-2018-178

Gast, R., Dusar, M., Breitkreuz, C., Gaupp, R., Schneider, J. W., Stemmerik, L., Geluk, M., Geissler, M., Kiersnowski, H., Glennie, K., Kabel, S., & Jones, N. (2010). Chapter 7 - Rotliegend. *Petroleum Geological Atlas of the Southern Permian Basin Area*, 101–121.

Glennie, K.W. (1972). Permian Rotliegendes of Northwest Europe Interpreted in Light of Modern Desert Sedimentation Studies. *AAPG Bulletin*, *56*(6). https://doi.org/10.1306/819a40ae-16c5-11d7-8645000102c1865d

Glennie, K. W. (1982). Early Permian (Rotliegendes) palaeowinds of the North Sea. *Sedimentary Geology*, *34*(2–3), 245–265. https://doi.org/10.1016/0037-0738(83)90088-X

Glennie, K. W. (1998). Petroleum Geology of the North Sea. In *Sedimentary Geology*. https://doi.org/10.1016/s0037-0738(00)00100-7

Glennie, K. W. (2005). *Regional tectonics in relation to Permo- Carboniferous hydrocarbon potential*.

Gravity and magnetic field | NLOG. (n.d.). https://www.nlog.nl/en/gravity-and-magnetic-field

Guterch, A., Wybraniec, S., Grad, M., Chadwick, A., Krawczyk, C., Ziegler, P., & Thybo, H. (2010). Chapter 2 - Crustal structure and structural framework. *Petroleum Geological Atlas of the Southern Permian Basin Area*, 10–23.

Heeremans, M., Faleide, J. I., & Larsen, B. T. (2004). Late Carboniferous-Permian of NW Europe: An introduction to a new regional map. *Geological Society Special Publication*, *223*, 75–88. https://doi.org/10.1144/GSL.SP.2004.223.01.04

Heeremans, M., Timmerman, M. J., Kirstein, L. A., & Faleide, J. I. (2004). New constraints on the timing of late Carboniferous-early Permian volcanism in the central North Sea. *Geological Society Special Publication*, *223*, 177–194. https://doi.org/10.1144/GSL.SP.2004.223.01.08

Heward, A. P. (1991). Inside Auk—the Anatomy of an Eolian Oil Reservoir. *The Three-Dimensional Facies Architecture of Terrigenous Clastic Sediments and Its Implications for Hydrocarbon Discovery and Recovery*, *3*, 41–56. https://doi.org/10.2110/csp.91.03.0044

Hou, L., Luo, X., Wang, J., Yang, F., Zhao, X., & Mao, Z. (2013). Weathered Volcanic crust and its petroleum geological significance: A case study of the Carboniferous Volcanic crust in northern Xinjiang, NW China. *Petroleum Exploration and Development*, *40*(3), 277–286. https://doi.org/10.1016/S1876-3804(13)60034-8

Houben, S., Bouroullec, R., Nelskamp, S., de Haan, H., Geel, K., Ventra, D., Janssen, N., Verseussel, R., Peeters, S., Veentra, F., Monaghan, A., Keusey, T., Wakefield, O., Vane, C., Hennissen, J., Barron, H., & Stewart, M. (2020). *Paleo-five project: Paleozoic petroleum potential of the five countries area, Southern-Central North Sea*.

IGI. (2023). Basin and Petroleum Systems Modelling Onshore and Offshore the Netherlands. In *Geodeatlas*. Geodeatlas. Geraadpleegd op 6 augustus 2025, van https://prd-ago-items-euw1.s3.eu-west-1.amazonaws.com/09d186100f994b959a28b9f2e4121951/OnshoreOffshore_NL_Basin-PS_Modelling_IGI_November2023.pdf?X-Amz-Security-Token=IQoJb3JpZ2luX2VjEDsaCXVzLWVhc3QtMSJGMEQCIHS9n2KDrZ%2FLAtFoHohDlDc%2Fxln4YtFfuxOtiTcyjdISAiA7pS3idizOR6nYwOF8OC8kTxof6uVs2%2Fs20gOe7RXI0SqzBQh0EAAaDDYwNDc1ODEwMjY2NSIMm1nFtJj7xGoyhMHYKpAFNBQBrgUgJc4W1ggSU87icr3ul7GYyUcew5hGNWTnXtJGTG6YAA3Ph8FhRZVfefNZ5CH9D44lLv4XxZz1pWJAbW6Z6zQex7AF2K1nWiBgKQ5YzIjuD1D7g9yVBi7Oc%2FupbMiEuA18sO54CjVK2HyrcYf4Q8YJnBTsScSUuEykdJOJJUoh1CUrCEcEsWfJbgjvI7XoyYLTBdY8XWte%2BdatgWRjkugRF4D7KEgLmL2mzm62mWi7oX%2BsId4U7YPZR60fMPdQL2cXT%2BdBuSNEy0MZ8yYHYTJbUbId4Ffd6bWfF7IIWSJewECeOW7lURHKUF31SkHTJ82quLQiKZWjs%2BlktjGFjez4Nu2I9XwPAkrflLmljxvLdvdcMo51kmS0T5JWIjhgKgNPJUAO2LWIijqeqSik3%2B8Nev%2FCeWJFYvWE0ZTBe8LQ%2BypJzg8vK3gb3SwVICJLha0wLF6ubxMKwyEu%2FjjCIYRic4ZxtOLq7qPIBWml2BzlGvIffZZhkpshee%2FsFJzuyDpelmU8VxBl453m5sIWZfOYS2PfN1%2BaR%2FmWJIgqqoQn2RMji%2FitvCW55gZQSyjEffF297SqvtAqCT2MlbHnNwBenxtbzN8AU69GWTt9m%2FjtXeEC3%2BSh0M1aC%2Fv%2FOEByveQT%2FHFIG5Sm2Vt5VnCKZ3vwB%2FUfRibLtUK%2Fni2jb3Z4f8puuQvsRTe5avCudmLeEPlhyxP2rTOgsfqwMn2u3E9jRosKnBLRbT0YWNWiFC7ctoeLYjw%2Fb5hhJDDkA8U%2BzKl16MjMSBs2vv2fU5lmz0L%2F5kZJQiW8%2Bpwq5SxlUw%2BfqRRmG8m%2BP9Zl2%2B8ktzNWTt6q9jmO7dKsArIWPAF5%2BiUUxD9o6s5yxBF2SwYwp9rMxAY6sgHt1MX4ytoMK%2Bu3E6YClkzBGxAvg0IujJin8b7CJfcQUeM05VG1QJHFLx3VJoxx8ieBJXoLJL7v1PM4yu1xR26B96Uhu072JxoPSFav3f8LLcTPy1wbSset4aEaqsBWLjcWPaSBNhP%2FjcHqXOtdmfLpTM5%2F%2Bt1GhaxZ8msR677%2BUO1L5mIIDdn3lv4KUxoZ%2B4vo7s3xgWb7JkUtmuykOGbJ4eM4Id1iM6XG0feCRIPaR9Qw&X-Amz-Algorithm=AWS4-HMAC-SHA256&X-Amz-Date=20250806T120619Z&X-Amz-SignedHeaders=host&X-Amz-Expires=10800&X-Amz-Credential=ASIAYZTTEKKE3UFNPDJV%2F20250806%2Feu-west-1%2Fs3%2Faws4_request&X-Amz-Signature=b4515b3759d6f3be41f3922822578b675b1eda225029f08d309d9a7815f58bf8

KGS--Geological Log Analysis--Igneous and Metamorphic Rocks. (n.d.). https://www.kgs.ku.edu/Publications/Bulletins/LA/09_igneous.html

Kilhams, B., Gardiner, S. D., Gozzard, S., Holford, S., Mclean, C., Mcnamara, D., Thackrey, S., & Watson, D. (2022). *The impacts of volcanism on sedimentary basins and their energy resources*. *March*. www.geolsoc.org.uk/energygroup

Kortekaas, M., Bouroullec, R., Peeters, S., van Unen, M., Swart, M., den Hartog Jager, D., Wiarda, E., Nolten, M., & Beintema, K. (2023). *Play 7 Rotliegend*. https://www.geodeatlas.nl/pages/play-7-rotliegend

Malahoff, A. (1969). Gravity A n o m a l i e s o v e r Volcanic Regions1. *Geophysical Monograph Series*, *13*, 364–379.

Marsh, A. (2023). *The North Sea Continental Shelf Cases*. https://sovereignlimits.com/blog/the-north-sea-continental-shelf-cases

Martin, C. A. L., Stewart, S. A., & Doubleday, P. A. (2002). Upper Carboniferous and Lower Permian tectonostratigraphy on the southern margin of the Central North Sea. *Journal of the Geological Society*, *159*(6), 731–749. https://doi.org/10.1144/0016-764900-174

Maynard, J. R., & Dunay, R. E. (1999). Reservoirs of the Dinantian (Lower Carboniferous) play of the Southern North Sea. *Petroleum Geology Conference Proceedings*, *5*(0), 729–745. https://doi.org/10.1144/0050729

McCann, T., Pascal, C., Timmerman, M. J., Krzywiec, P., López-Gómez, J., Wetzel, A., Krawczyk, C. M., Rieke, H., & Lamarche, J. (2006). Post-Variscan (end Carboniferous-Early Permian) basin evolution in Western and Central Europe. *Geological Society Memoir*, *32*(February), 355–388. https://doi.org/10.1144/GSL.MEM.2006.032.01.22

McKie, T. (2011). A comparison of modern Dryland depositional systems with the Rotliegend group in the Netherlands. *SEPM Special Publications*, *98*(98), 89–103. https://doi.org/10.2110/pec.11.98.0089

Mijnlieff, H. F., & Geluk, M. (2011). Palaeotopography-governed sediment distribution-a new predictive model for the Permian Upper Rotliegend in the Dutch sector of the Southern Permian basin. *SEPM Special Publications*, *98*(98), 147–159. https://doi.org/10.2110/pec.11.98.0147

Neumann, E. R., Wilson, M., Heeremans, M., Spencer, E. A., Obst, K., Timmerman, M. J., & Kirstein, L. (2004). Carboniferous-Permian rifting and magmatism in southern Scandinavia, the North Sea and northern Germany: A review. *Geological Society Special Publication*, *223*, 11–40. https://doi.org/10.1144/GSL.SP.2004.223.01.02

Ning, L., Dexing, Q., Qingfeng, L., Hongliang, W., Youshen, F., Lixin, D., Qingfu, F., & Kewen, W. (2009). Theory on logging interpretation of igneous rocks and its

application. *Petroleum Exploration and Development*, *36*(6), 683–692. https://doi.org/10.1016/S1876-3804(10)60002-X

Patruno, S., Kombrink, H., & Archer, S. G. (2022). Cross-border stratigraphy of the Northern, Central and Southern North Sea: a comparative tectono-stratigraphic megasequence synthesis. *Geological Society Special Publication*, *494*(1), 13–83. https://doi.org/10.1144/SP494-2020-228

Pedersen, G. K. (2012). *Sedimentological description of Lower Permian Volcaniclastic sediments in core 1 from the Luna-1 well , Danish North Sea Report for Noreco Sedimentological description of Lower Permian Volcaniclastic sediments in core 1 from the Luna-1 well , Danish North*.

Remmelts, G., Nelskamp, S., & Geluk, M. (2025). 14.Petroleum Geology. In *Geology of the Netherlands* (2nd ed.). Amsterdam University Press. https://doi.org/10.5117/9789463728362

Sissingh, W. (2004). Palaeozoic and Mesozoic igneous activity in the Netherlands: a tectonomagmatic review. *Netherlands Journal of Geosciences*, *83*, 113-134. https://doi.org/10.1017/S0016774600020084

Smit, J., van Wees J., & Sierd Cloetingh, S. (2016) The Thor suture zone: From subduction to intraplate basin setting. *Geological society of America 44* (9), 707–710. https://doi.org/10.1130/G37958.1

Sneh, A. (1988). *Permian Dune Patterns in Northwestern Europe Challenged*. Journal of Sedimentary Research *58*(1), 44–51. https://doi.org/10.1306/212F8D0A-2B24-11D7-8648000102C1865D

Stemmerik, L., Ineson, J. R., & Mitchell, J. G. (2000). Stratigraphy of the Rotliegend group in the Danish part of the Northern Permian Basin, North Sea. *Journal of the Geological Society*, *157*(6), 1127–1136. https://doi.org/10.1144/jgs.157.6.1127

Ter Borgh, M. M., Jaarsma, B., & Rosendaal, E. A. (2018). Structural development of the northern Dutch offshore: Paleozoic to present. *Geological Society Special Publication*, *471*(1), 115–131. https://doi.org/10.1144/SP471.4

van Bergen, M., Vis, G.-J., Sissingh, W., Koornneef, J., & Brouwers, I. (2025). 11. Magmatism in the Netherlands: expression of the northwest European rifting history. In *Geology of the Netherlands* (2nd ed.). Amsterdam University Press. https://doi.org/10.5117/9789463728362

Verdier, J.-P. (1996). The Rotliegende Sedimentation History of the Southern North Sea and Adjacent Countries. *Geology of Gas and Oil under the Netherlands*, 45–56. https://doi.org/10.1306/bdff86d2-1718-11d7-8645000102c1865d

Van Wees, J. Van, Stephenson, R. A., Ziegler, P. A., Bayer, U., Mccann, T., Dadlez, R., Gaupp, R., Narkiewicz, M., Bitzer, F., & Scheck, M. (2000). On the origin of the southern Permian Basin, Central Europe. *Marine and Petroleum Geology*, *17*, 43–59.

Appendix:

A 1. Table showing all wells in the project with their well head coordinate in (ESPG 2303), and whether the well had data useful for thickness mapping and GDE mapping, core description, core photos, or had available porosity and permeability data.

Nation	Well name	Surface X	Surface Y	Thickness mapping	GDE mapping	core description	core photo	poro-perm data
UK	29_05-1	427682	6300191	YES	YES			
UK	29_10-7	428010	6289134	YES	YES			
UK	29_13-2	411617	6277196	YES	YES			
UK	29_14-4	415741	6265418	YES	YES	YES		
UK	29_14-2	414389	6276958	YES	YES	YES	YES	YES
UK	29_18-1	403349	6261017	YES	YES			
UK	29_19-2	417143	6254449	YES	YES			
UK	29_19-3	421246	6255333	YES	YES			
UK	29_20-1	433536	6257912	YES	YES	YES		
UK	29_23-1	404254	6238615	YES	YES	YES		
UK	29_25-1	429646	6240495	YES	YES	YES		YES
UK	30_11-1	443522	6268163	YES	YES	YES	YES	YES
UK	30_12-1	462159	6278775	YES	YES			
UK	30_12-3	455497	6263863	YES	YES			
UK	30_16-1	440031	6252532	YES	YES			
UK	30_16-10	446565	6245631	YES	YES	YES	YES	YES
UK	30_16-12	438686	6255900	YES	YES			
UK	30_16-13	440307	6256101	YES	YES	YES	YES	YES
UK	30_16-15	441815	6257234	YES	YES	YES	YES	YES
UK	30_16-16Y	440506	6258120	YES	YES			
UK	30_16-2	442603	6249701	YES	YES	YES	YES	YES
UK	30_16-3	442545	6252054	YES	YES	YES	YES	YES
UK	30_16-4	442364	6254812	YES	YES	YES	YES	YES
UK	30_16-5	449293	6249557	YES	YES	YES	YES	
UK	30_16-8	445561	6247496	YES	YES	YES	YES	YES
UK	30_16-9	446520	6249881	YES	YES		YES	
UK	30_16-A1	442190	6251190	YES	YES			
UK	30_16-A12	442189	6251186	YES	YES	YES	YES	YES
UK	30_16-A2	442197	6251192	YES	YES			
UK	30_16-A6	442192	6251187	YES	YES			
UK	30_16-A7	442194	6251188	YES	YES			
UK	30_16-A8	442198	6251190	YES	YES			
UK	30_17-a1	451119	6250563	YES	YES			
UK	30_17-12	454021	6250417	YES	YES			
UK	30_17-4	450845	6252603	YES	YES			
UK	30_17-16	455862	6260474	YES	YES			
UK	30_17-8	450827	6257574	YES	YES			

UK	30_21-1	441530	6236598	YES	YES			
UK	30_23-1	467076	6225423	YES	YES			
UK	30_23-2A	466316	6236194	YES	YES			
UK	30_23a-3	472467	6227969	YES	YES			
UK	30_23-4	465297	6233897	YES	YES			
UK	30_24-17	482472	6226250	YES	YES			
UK	30_24-19	479748	6228572	YES	YES			
UK	30_24-2	485550	6225410	YES	YES			
UK	30_24-21	480282	6229228	YES	YES			
UK	30_24-24	479171	6236138	YES	YES	YES		
UK	30_24-26	485818	6228059	YES	YES	YES	YES	
UK	30_24-27	480829	6235775	YES	YES			YES
UK	30_24-28	485468	6227779	YES	YES	YES		YES
UK	30_24-3	487292	6228141	YES	YES	yes		
UK	30_24-31	484616	6225691	YES	YES	YES		YES
UK	30_24-32	478425	6237106	YES	YES			
UK	30_24-33	479119	6226529	YES	YES			
UK	30_24-34	485336	6224833	YES	YES			
UK	30_24-35	480561	6235049	YES	YES	YES		YES
UK	30_24-36	480841	6237766	YES	YES			
UK	30_24-37	485297	6224820	YES	YES			
UK	30_24-38	477801	6230755	YES	YES			
UK	30_24-4	482713	6227817	YES	YES	YES		YES
UK	30_24-5	486709	6227172	YES	YES	YES	YES	YES
UK	30_24-6	485476	6226706	YES	YES			
UK	30_25a-2	487733	6228740	YES	YES			
UK	30_25-4	488088	6232650	YES	YES			
UK	30_25-3	497140	6227163	YES	YES			
UK	30_27-1	456985	6224553	YES	YES			
UK	30_28-1	475031	6214708	YES	YES			
UK	30_29-1	478945	6221622	YES	YES			
UK	30_29-2	479566	6223298	YES	YES			
UK	30_29-3	477309	6219775	YES	YES			
UK	30_30-1	488793	6222914	YES	YES			
UK	30_30-2	496221	6215626	YES	YES			
UK	30_30-3	499646	6209700	YES	YES			
UK	31_21-1	504218	6224918	YES	YES			
UK	31_26-1	507385	6216518	YES	YES			
UK	31_26-11	511547	6206547	YES	YES			
UK	31_26-12	507467	6214803	YES	YES			
UK	31_26c-13	508391	6215598	YES	YES			
UK	31_26-17	508035	6210038	YES	YES			
UK	31_26-2A	509778	6211300	YES	YES			
UK	31_26-3	503661	6224141	YES	YES			
UK	31_26-4	504734	6214808	YES	YES			

UK	31_26-5	504155	6221504	YES	YES			
UK	31_26-8	505041	6218282	YES	YES			
UK	31_26-A9	511535	6206626	YES	YES			
UK	31_26-F1	507853	6214384	YES	YES			
UK	31_27-1	514134	6217201	YES	YES			
UK	37_10-1	435880	6177968	YES	YES			
UK	37_12-1	395450	6166928	YES	YES			
UK	37_23-1	407137	6122336	YES	YES			
UK	37_25-1	431248	6131198	YES	YES			
UK	38_01-1	446132	6193740	YES	YES			
UK	38_02-1Z	456484	6202498	YES	YES			
UK	38_03-1	471207	6202507	YES	YES			
UK	38_10-1	496237	6174576	YES	YES			
UK	38_16-1	441532	6137694	YES	YES			
UK	38_18-1	465032	6133361	YES	YES			
UK	38_22-1	453135	6118263	YES	YES			
UK	38_24-1	476190	6118337	YES	YES			
UK	38_25-1	491483	6127787	YES	YES			
UK	38_29-1	478495	6101653	YES	YES			
UK	39_01-1	505551	6201720	YES	YES			
UK	39_02-1	518162	6201247	YES	YES			
UK	39_02-3	517039	6204142	YES	YES			
UK	39_02-4	516987	6189317	YES	YES			
UK	39_11-1	510506	6166935	YES	YES			
UK	39_07-1	522243	6178526	YES	YES			
NL	A05-01	532731	6170913	YES	YES			
NL	A11-01	535448	6147143	YES	YES			
NL	A14-01	538868	6117385	YES	YES			
NL	A15-01	544753	6117561	YES	YES	YES		
NL	A16-01	516154	6108805	YES	YES	YES		YES
NL	A17-01	542083	6097329	YES	YES			
NL	B10-02-S1	566941	6133197	YES	YES	YES		
NL	B10-02	566941	6133197	YES	YES			
NL	B17-04	594727	6099868	YES	YES			
NL	F04-02-A	585602	6073477	YES	YES			
NL	F04-03	568781	6060433	YES	YES			
NL	F07-02	568695	6046405	YES	YES			
NL	F10-02	578616	6027473	YES	YES			
NL	F10-03	576619	6024319	YES	YES			
NL	F16-03	566178	5997115		YES			
NL	F16-03-S1	566178	5997115		YES			
NL	F16-05	566050	5992581		YES	YES		YES
NL	F16-A-03	566178	5997104		YES			
NL	F16-A-03-S1	566178	5997104		YES	YES		YES
NL	F16-A-05	566174	5997104		YES			

NL	F16-A-06-S1	566176	5997106		YES			
NL	F16-A-07	566174	5997106		YES			
NL	F17-08-S1	601729	6001487		YES			
NL	E02-01	537297	6091503	YES	YES			
NL	E02-02	523748	6088759	YES	YES			
NL	E06-01	545213	6069482	YES	YES			
NL	E09-01	561371	6051807	YES	YES	YES		YES
NL	E10-01-S1	514735	6024611	YES	YES			
NL	E10-02	507283	6024417	YES	YES			
NL	E10-03-S2	516422	6023573	YES	YES			
NL	E11-01	536600	6028600	YES	YES			
NL	E12-02	544026	6028262	YES	YES			
NL	E12-03	545198	6036716	YES	YES			
NL	E12-04-S2	551201	6028394		YES			
NL	E13-01-S2	509007	6016047		YES			
NL	E13-02	510637	6014777		YES			
NL	E14-01	536240	6006679		YES			
NL	E16-01	519127	5996482		YES			
NL	E16-02-S2	509439	5992743		YES			
NL	E16-03	511536	6001680		YES			
NL	E16-04	517932	5992236		YES			
NL	E16-05	506737	6002192		YES			
NL	E17-01	527727	5994204		YES			
NL	E17-02	523478	5992861		YES			
NL	E17-03	538220	5984106		YES			
NL	E17-A-01	523650	5994696		YES			
NL	E17-A-02	523652	5994698		YES			
NL	E17-A-03	523650	5994700		YES			
NL	E17-A-04	523650	5994700		YES			
NL	E17-A-04-S1	523650	5994700		YES			
NL	E17-A-05	523650	5994700		YES			
NL	E17-A-05-S1	523650	5994700		YES			
NL	E17-A-06	523653	5994700		YES			
NL	E17-A-06-S1	523653	5994700		YES			
NL	E17-A-06-S2	523653	5994700		YES			
NL	E18-02	550812	6000777		YES			
NL	E18-03	549333	5991561		YES			
NL	E18-04	564522	6001444		YES	YES		YES
NL	E18-05	561947	6001486		YES	YES		YES
NL	E18-06	560807	5997522		YES			
NL	E18-07	560807	5997519		YES			
NL	E18-A-03	560805	5997525		YES			
GER	B-4-1	570443	6182457	YES	YES			
GER	C-1	711362	6023775	YES	YES			
GER	Q-1	687890	6093843	YES	YES	YES		YES

GER	C-15-1	674239	6126897	YES	YES			
GER	G1-1	647861	6078995	YES	YES	YES		YES
GER	A-9-1	560444	6167704	YES	YES			
GER	A6-A5-3	742972	5966501	YES	YES			
GER	A-6-2	562186	6183114	YES	YES			
GER	A-6-1	560246	6184424	YES	YES			
GER	B-1X duc	565089	6174318	YES	YES			
GER	B-11-02	590696	6138586	YES	YES			
NOR	1/3-5	493529	6292054	YES	YES			
NOR	2/1-7	505764	6302421	YES	YES	YES	YES	YES
NOR	2/10-2	506919	6230600	YES	YES	YES	YES	YES
NOR	2/4-17	514043	6282381	YES	YES			
NOR	2/7-2	509447	6235934	YES	YES			
NOR	2/7-22	509834	6239194	YES	YES			
NOR	2/7-29	505074	6240960	YES	YES	YES	YES	
NOR	2/7-31	505417	6243705	YES	YES		YES	
NOR	3/5-1	587131	6276555	YES	YES	YES		
NOR	3/7-2	565820	6262344	YES	YES	YES		
NOR	8/10-3	517225	6322003	YES	YES			
NOR	17/4-1	515580	6495508	YES	YES			
NOR	16/8-3	475484	6461821	YES	YES			
NOR	2/9-2	557698	6245461	YES	YES			
NOR	2/6-3	550669	6265554	YES	YES	YES		
NOR	16/1-3	445067	6519835	YES	YES			
NOR	16/1-4	459563	6525419	YES	YES			
NOR	16/2-19	470835	6529558	YES	YES			
NOR	16/3-2	488032	6516491	YES	YES			
NOR	16/4-1	449960	6500262	YES	YES			
NOR	25/10-2r	453868	6558400	YES	YES			
NOR	25/11-1	466105	6560687	YES	YES			
NOR	2/10-1s	518766	6220237	YES	YES			
NOR	2/11-9	528225	6222671	YES	YES			
NOR	7/3-1	485085	6411418	YES	YES			
NOR	9/4-5	575683	6393653	YES	YES			
NOR	2/11-8	521523	6221377	YES	YES		YES	
NOR	2/7-21s	515353	6243335	YES	YES			
NOR	2/7-23s	515349	6243340	YES	YES		YES	
NOR	2/6-5	546787	6272540	YES	YES			
NOR	8/3-1	539640	6427604	YES	YES			
NOR	10/5-1	654878	6385173	YES	YES			
NOR	11/5-1	715435	6391482	YES	YES			
NOR	16/2-5	463593	6519673	YES	YES			
NOR	17/12-2	541396	6444526	YES	YES			
NOR	25/12-1	489748	6543526	YES	YES			
DK	D-1x	656115	6256387	YES	YES	YES		

DK	DIAMANT-1	555850	6207298	YES	YES	YES		
DK	ELLY-1	581176	6183324	YES	YES	YES		
DK	ELNA-1	594238	6257140	YES	YES	YES		
DK	GERT-1	545424	6230859	YES	YES			
DK	Gert-2	548456	6228412	YES	YES			
DK	Hejre-1	559928	6233705	YES	YES	YES		
DK	Hejre-2	560966	6234024	YES	YES			
DK	IBENHOLT-1	683624	6253645	YES	YES	YES		
DK	ISAK-1	545115	6208361	YES	YES	YES		
DK	JEPPE-1	556487	6227122	YES	YES			
DK	KARL-1	565202	6239584	YES	YES			
DK	KIM-1	530988	6219409	YES	YES			
DK	L-1X	639319	6236597	YES	YES			
DK	LIVA-1	551570	6198245	YES	YES	YES		
DK	Luna-1	679203	6221010	YES	YES		YES	
DK	Ophelia-1	562094	6217424	YES	YES			
DK	P-1X	547948	6210319	YES	YES			
DK	RAVN-1	577029	6193169	YES	YES			
DK	SAXO-1	527211	6204212	YES	YES			
DK	Stork-1	598882	6219885	YES	YES			
DK	TORDENSKJOLD-1	533860	6199519	YES	YES			
DK	W-1X	571601	6196514	YES	YES	YES		
DK	WESSEL-1	530590	6205875	YES	YES			
DK	GERT-3	547366	6230076	YES	YES			
DK	C-1	786326	6284030	YES	YES			
DK	Q-1X/-ST4	568700	6216978	YES	YES			

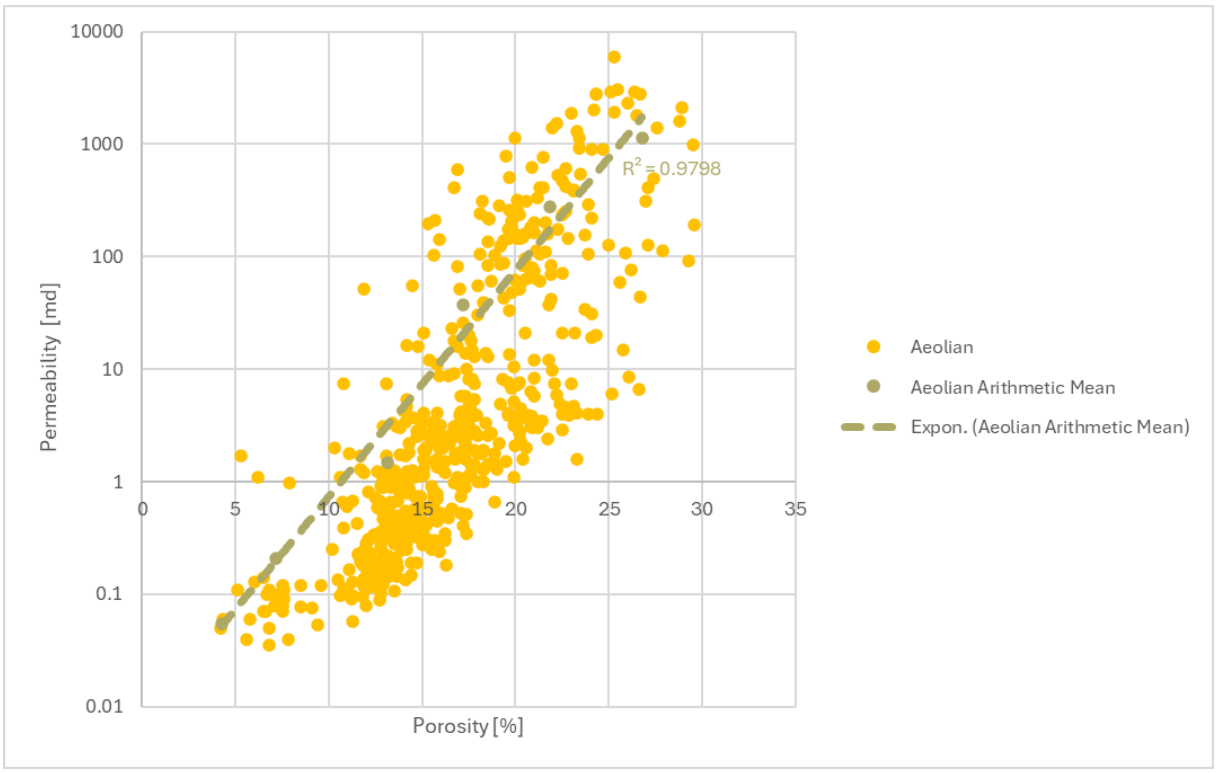

S 1 Porosity permeability plot for the Aeolian data points with the yellow points showing the data points, the green data points showing the arithmetic averages and the line being the trend line for the data set based on binning.

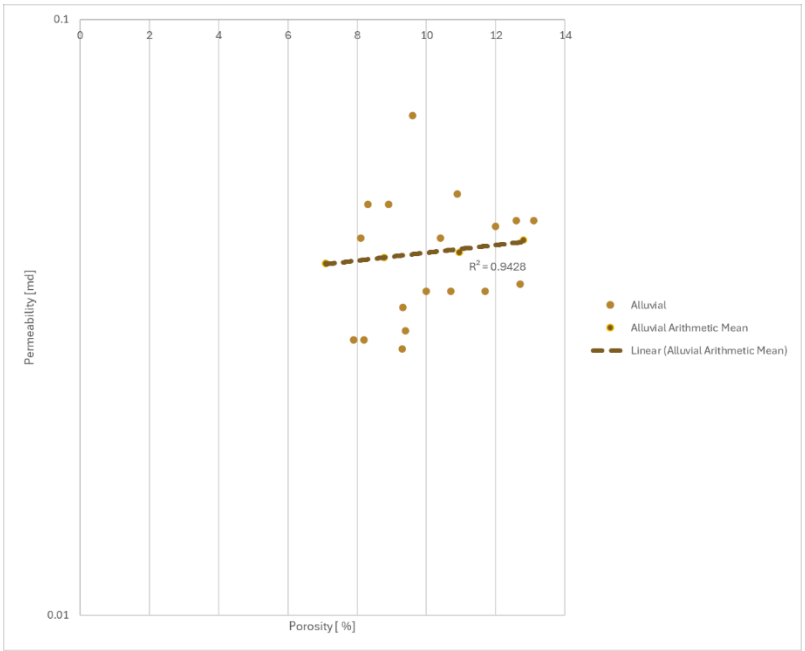

S 2 Porosity permeability plot for alluvial deposits and a trendline based on binning.

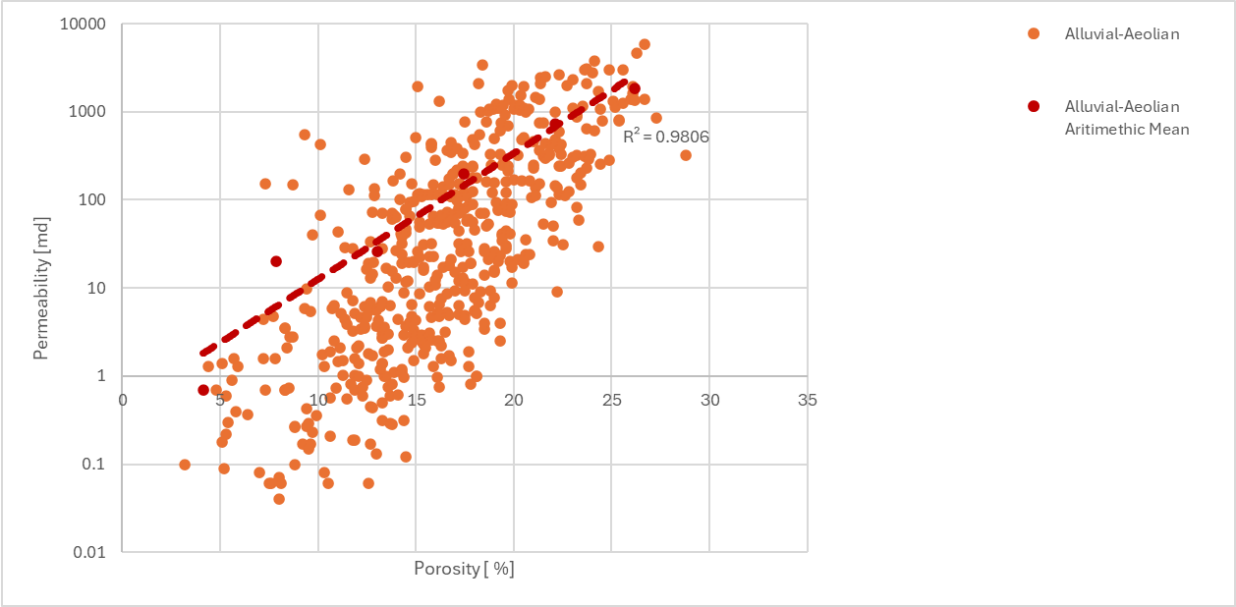

S 3 Alluvial-Aeolian data set with trendline based on arithmetic average from binning

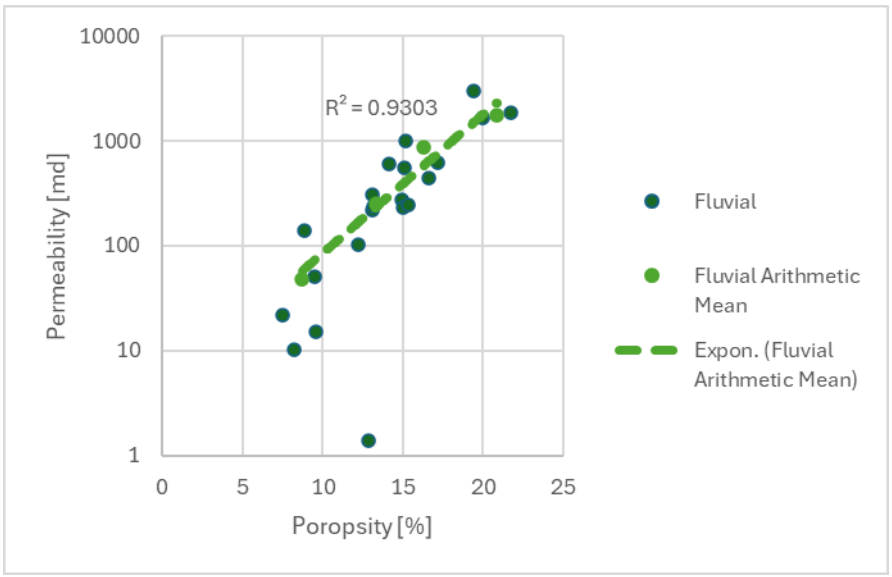

S 4. Fluvial porosity permeability plot with trendline based on arithmetic average

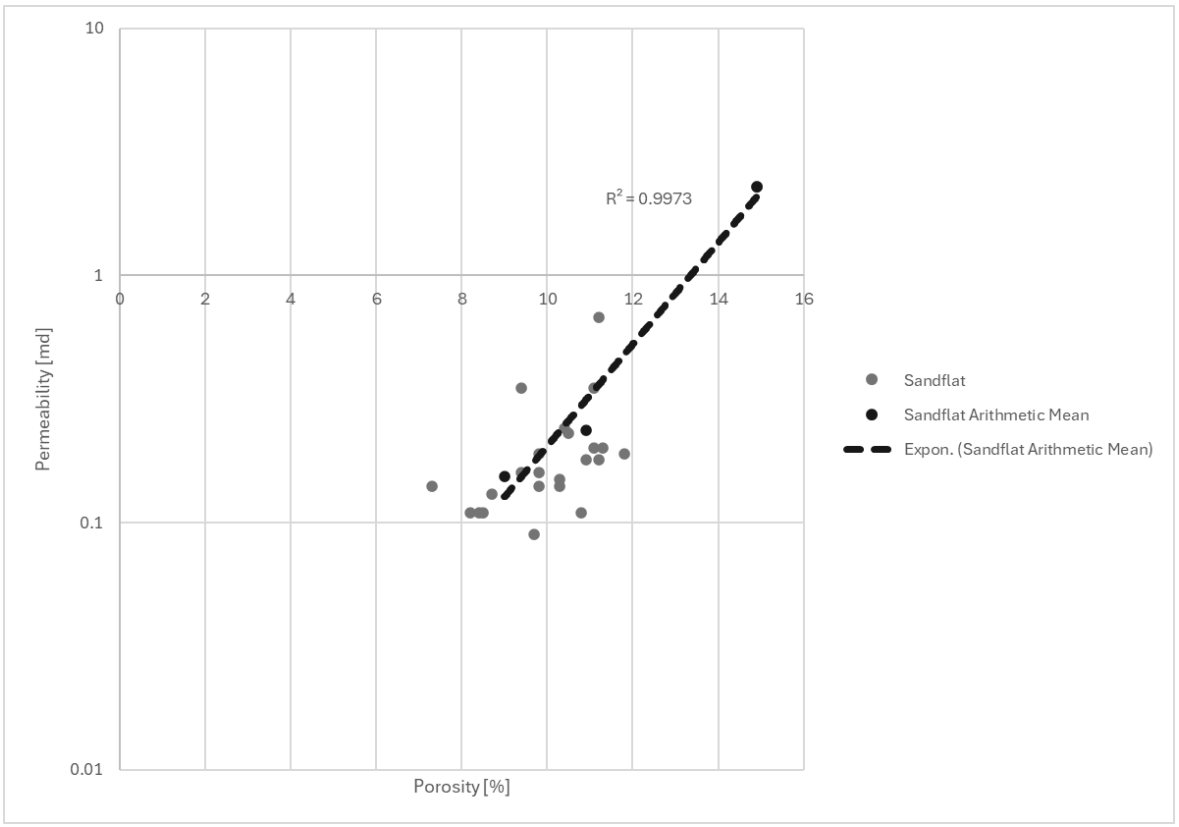

S 5. Sandflat porosity permeability plot

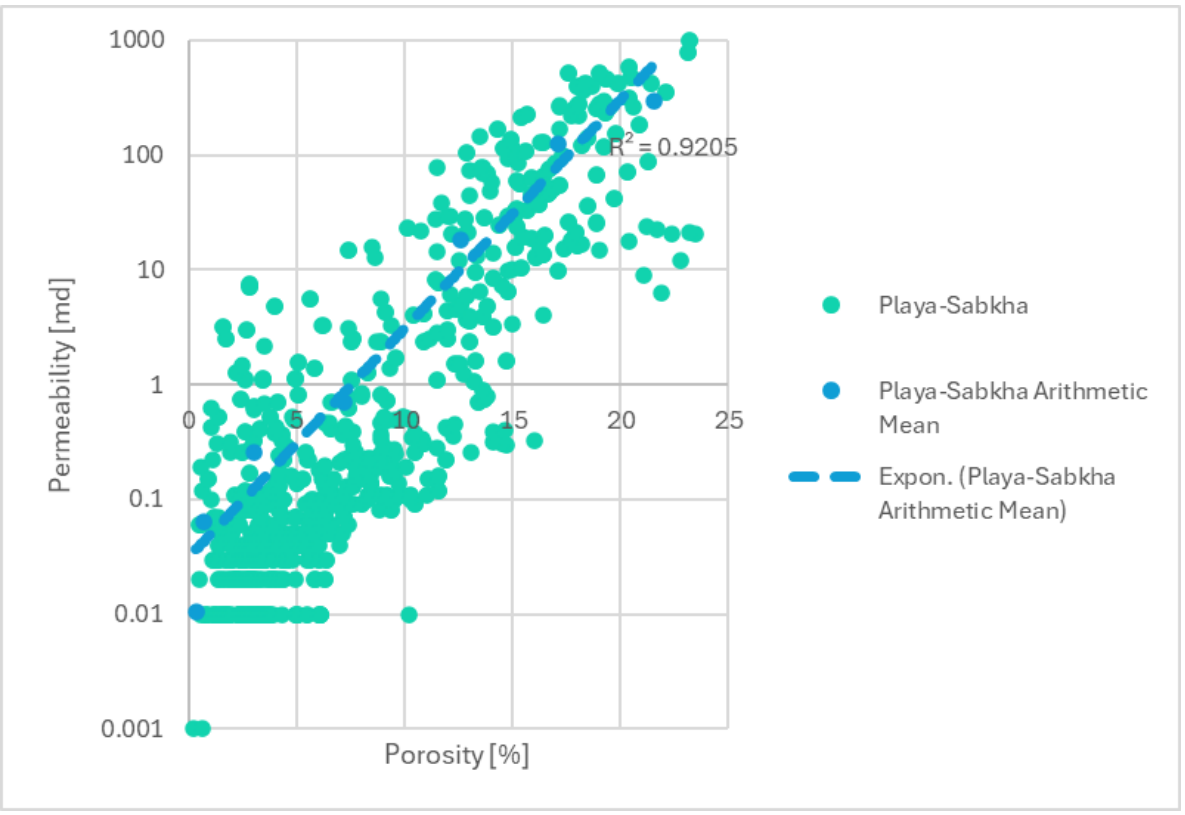

S 6. Playa Sabkha porosity permeability plot.

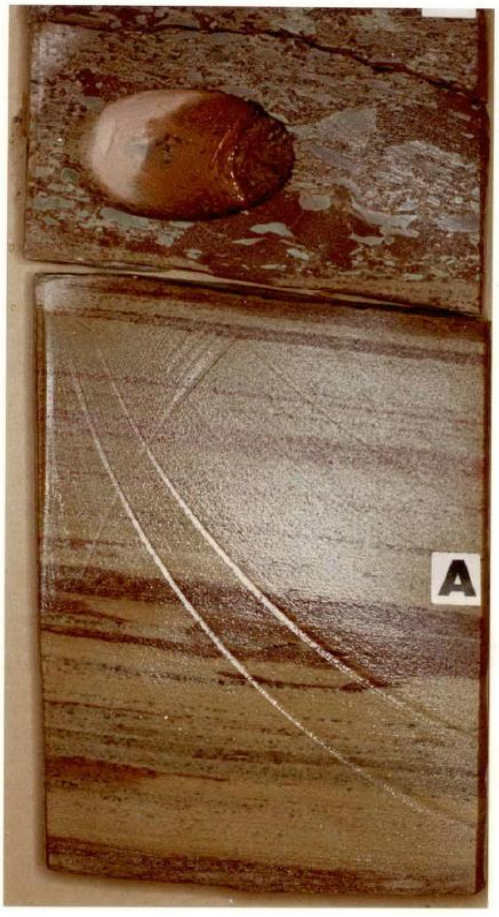

S 7. Core photo30-24-5 of fluvial deposits

S 8.Core photo of 2-1-7 of sandflat deposits

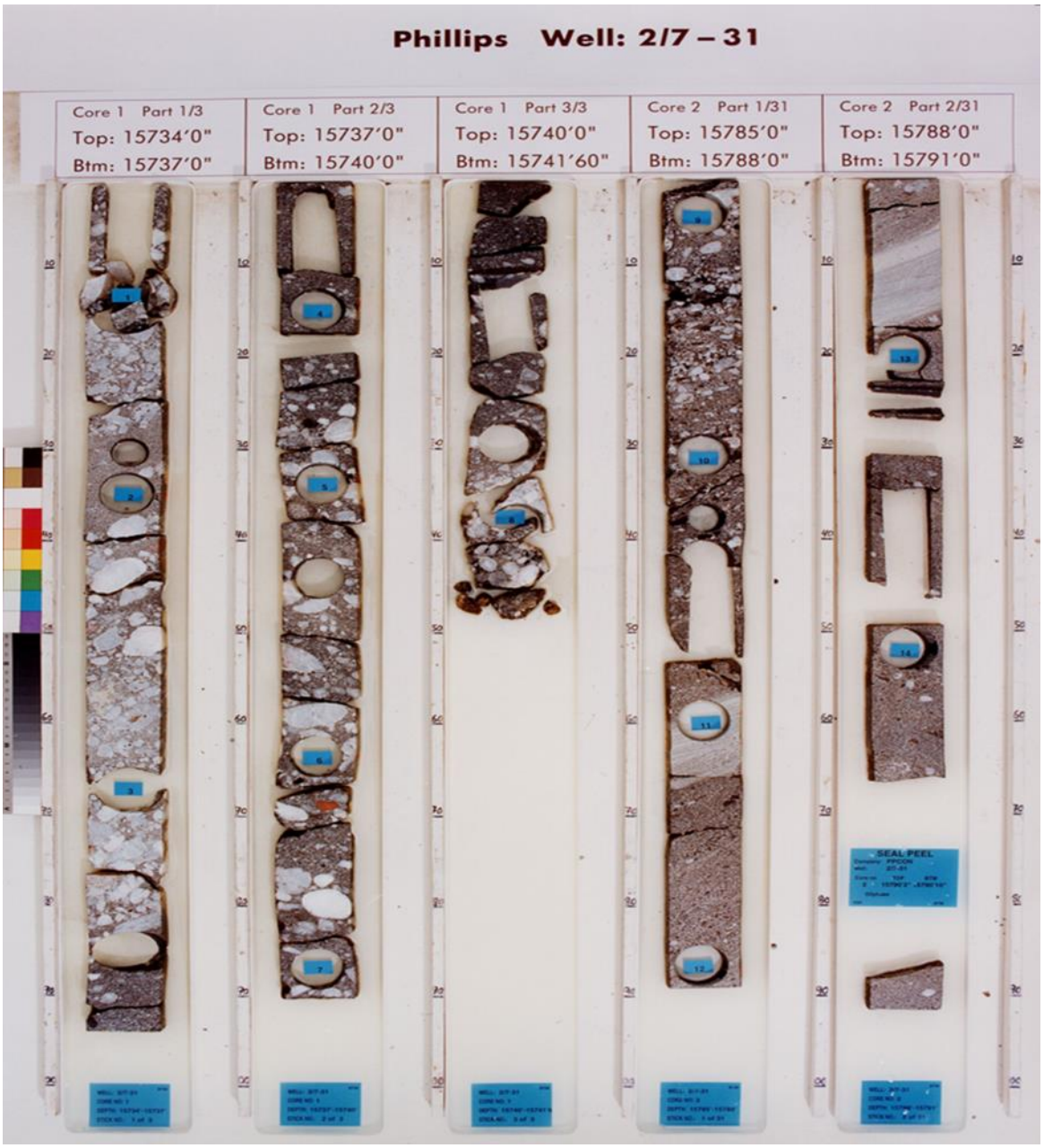

S 9. Core photo from well 2/7-31 of alluvial fan deposits.

S 10. Core photo from well 29-14-2 of Aeolian deposits.

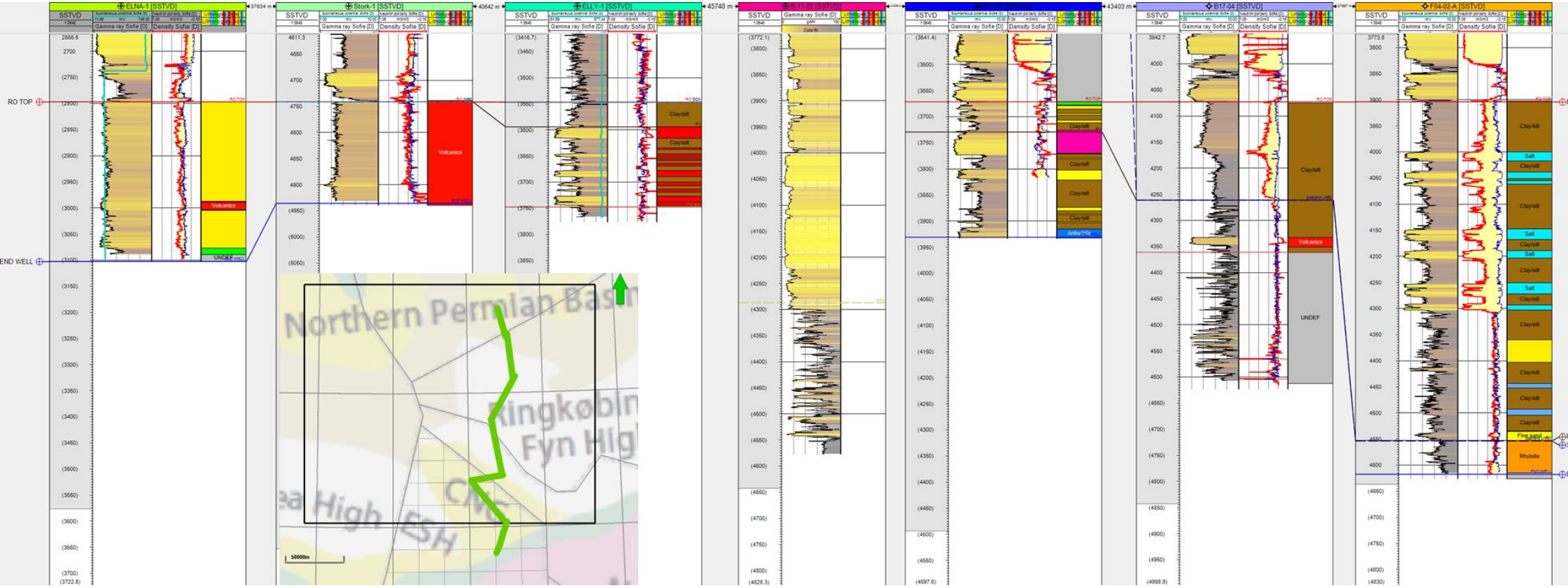

S 11 Well correlation panel N-S from wells Elna 1, Stork, Elly, B11-02, b10-2, b17-04 & F04-02-A., the well path is shown on the map.

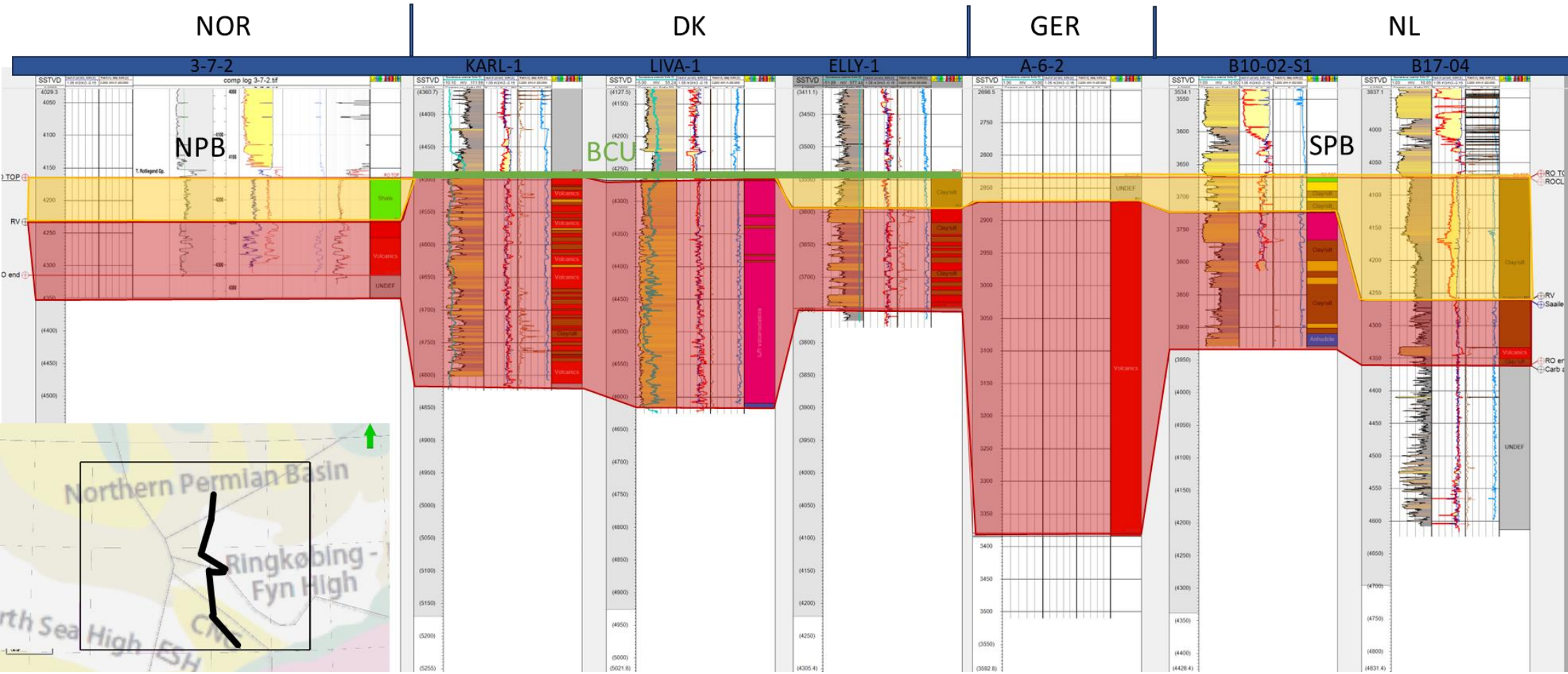

S 12 Well correlation panel N-S NOR-DK-GER-NL showing the NPB and SPB with the position visible on the map.

S 13 Well correlation panel N-S from Karl 1- Diamant 1, Ravn 1, A-6-2, B1x-duc & B10-02. The Map shows were the line crosses the map

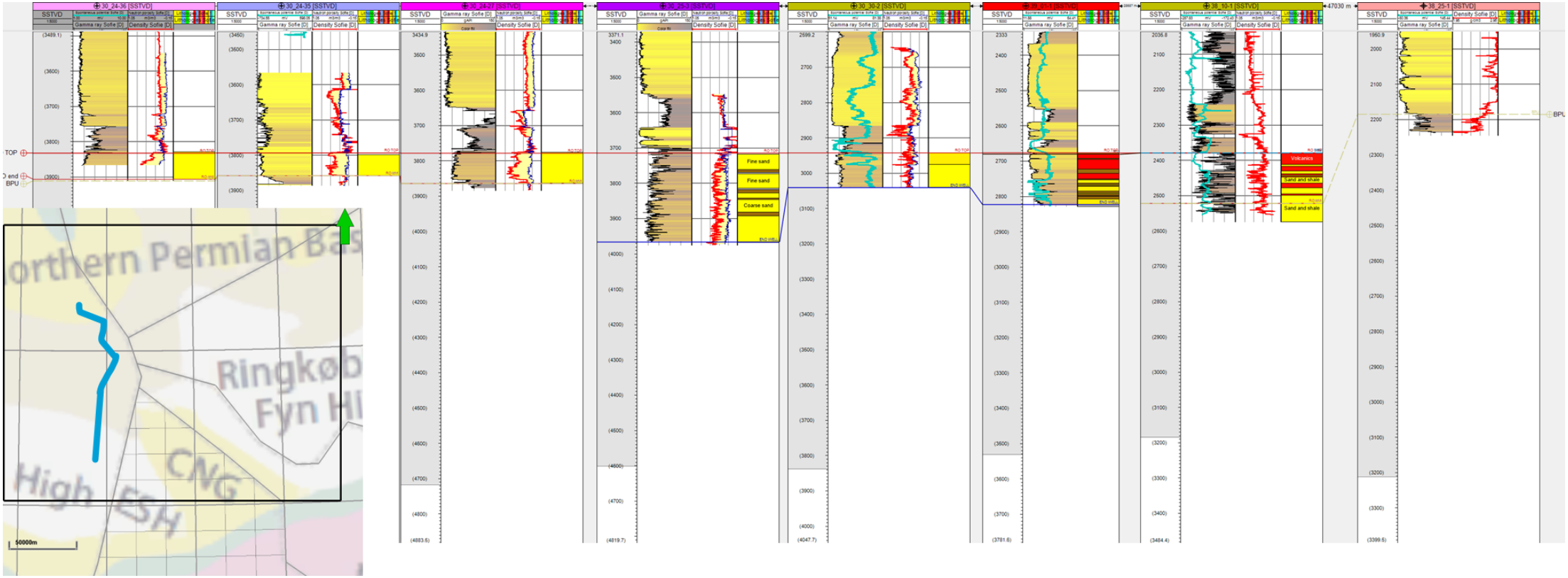

S 14 N-S well panel with the map showing the location of the well pane in the project area.

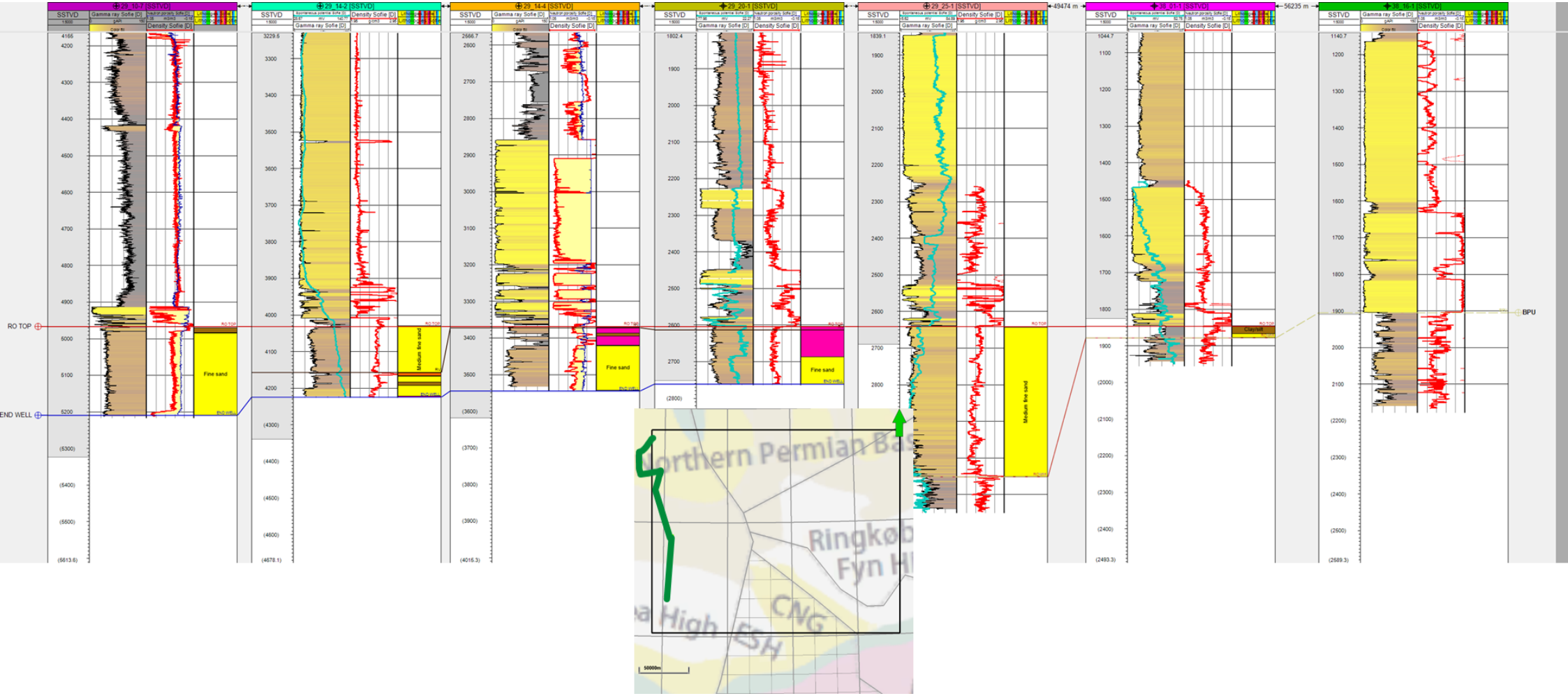

S 15 N-S panel showing in the UK with the location shown on the map with the green line

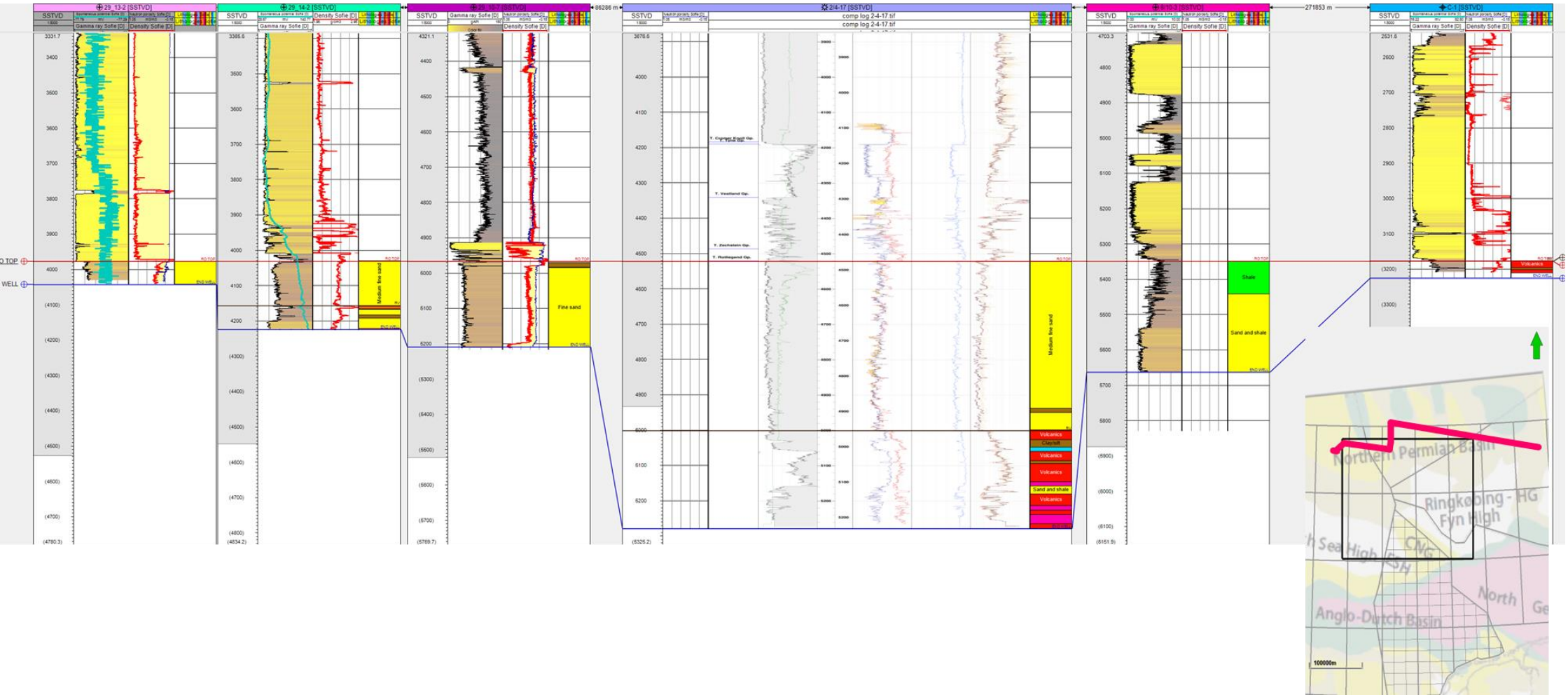

S 16 W-E well panel from the UK to DK with the location shown in pink on the map.

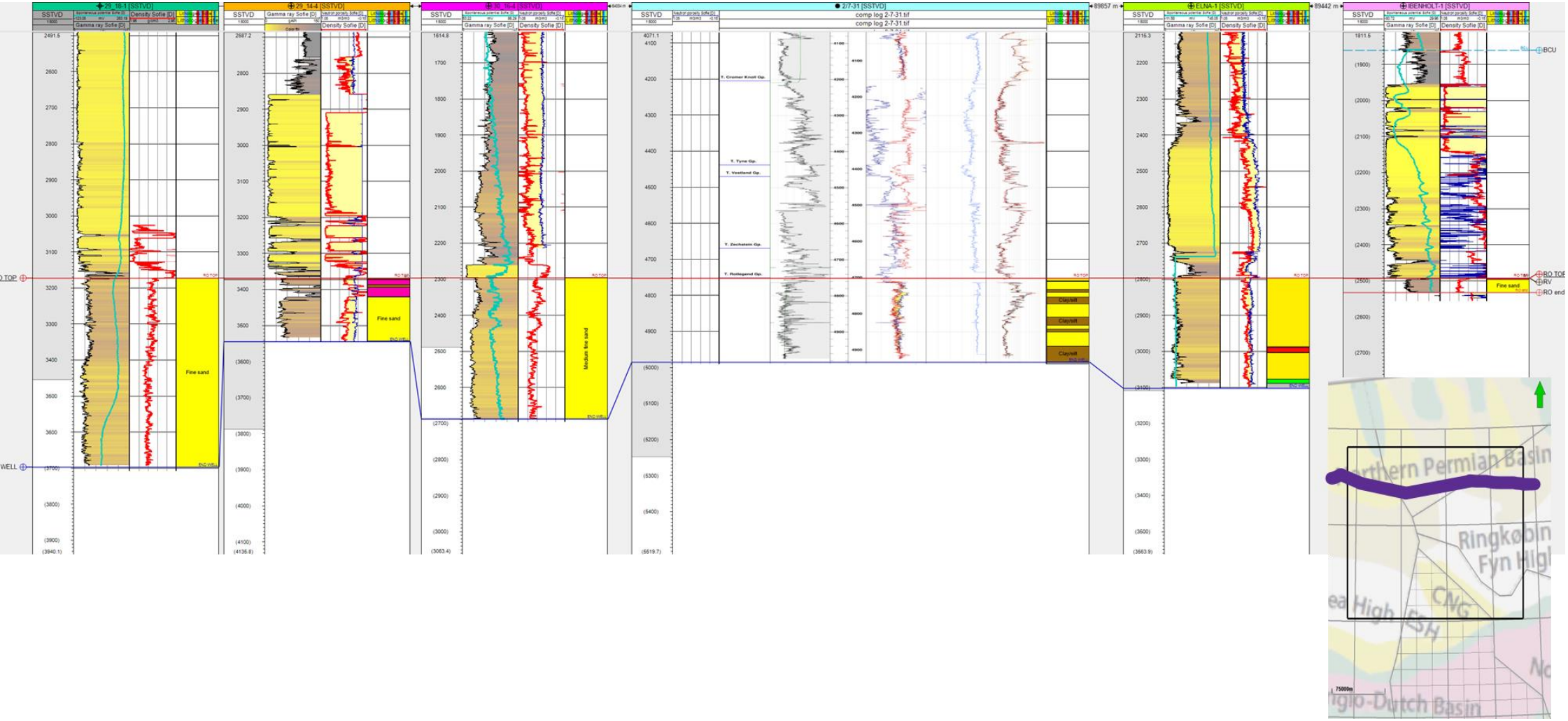

S 17 W-E well panel from the UK to DK. The location of the line is shown on the map

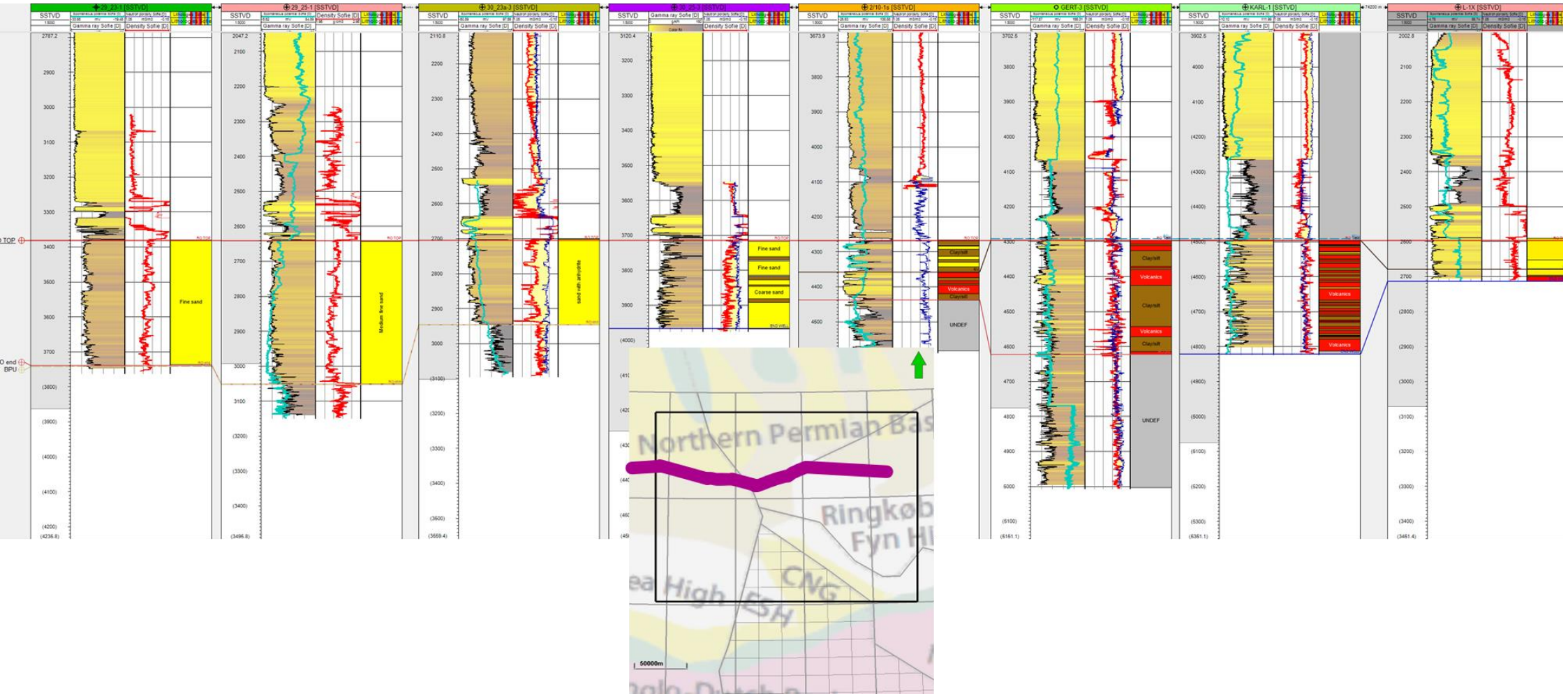

S 18 W-E well panel from UK to Dk. The location is shown on the map

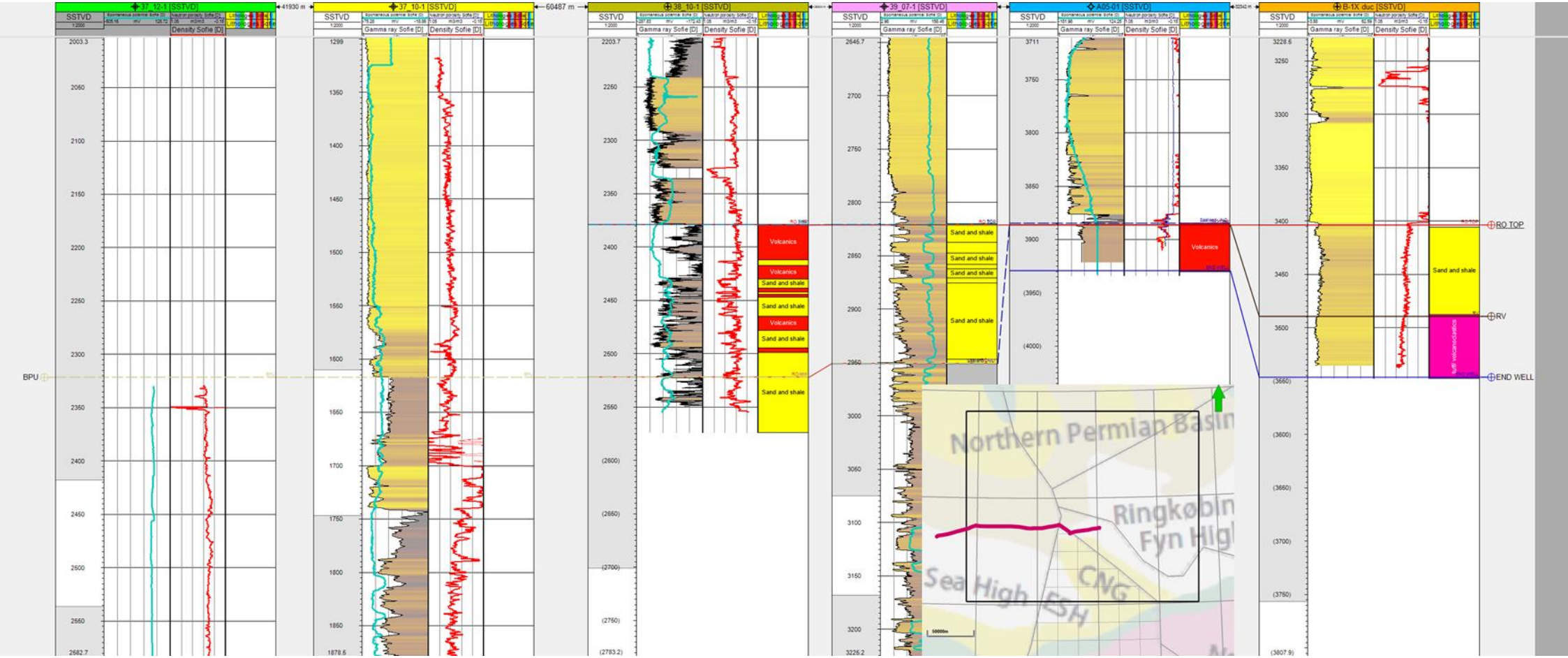

S 19 W-E well correlation panel from UK- NL to Ger. The location is shown on the map.

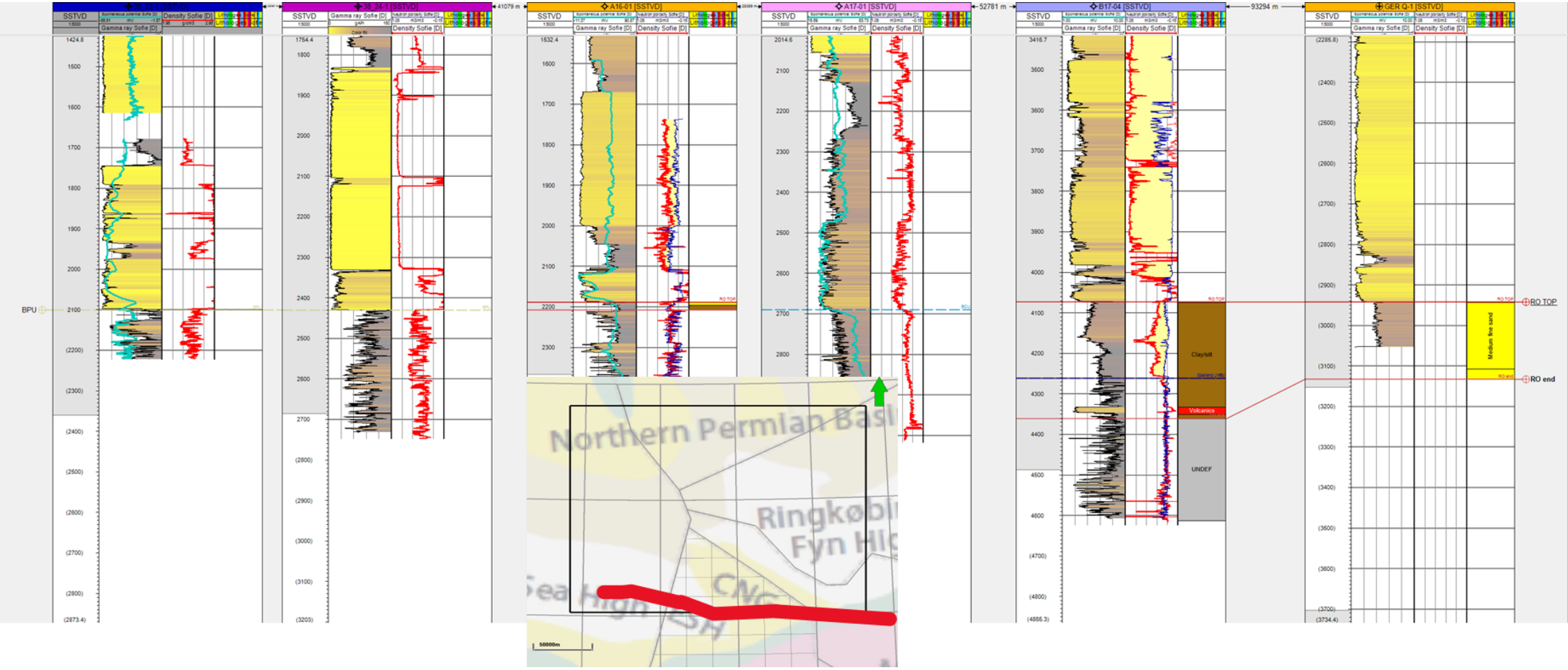

S 20 W-E well correlation panel from UK to NL to GER. Location is shown on the map.

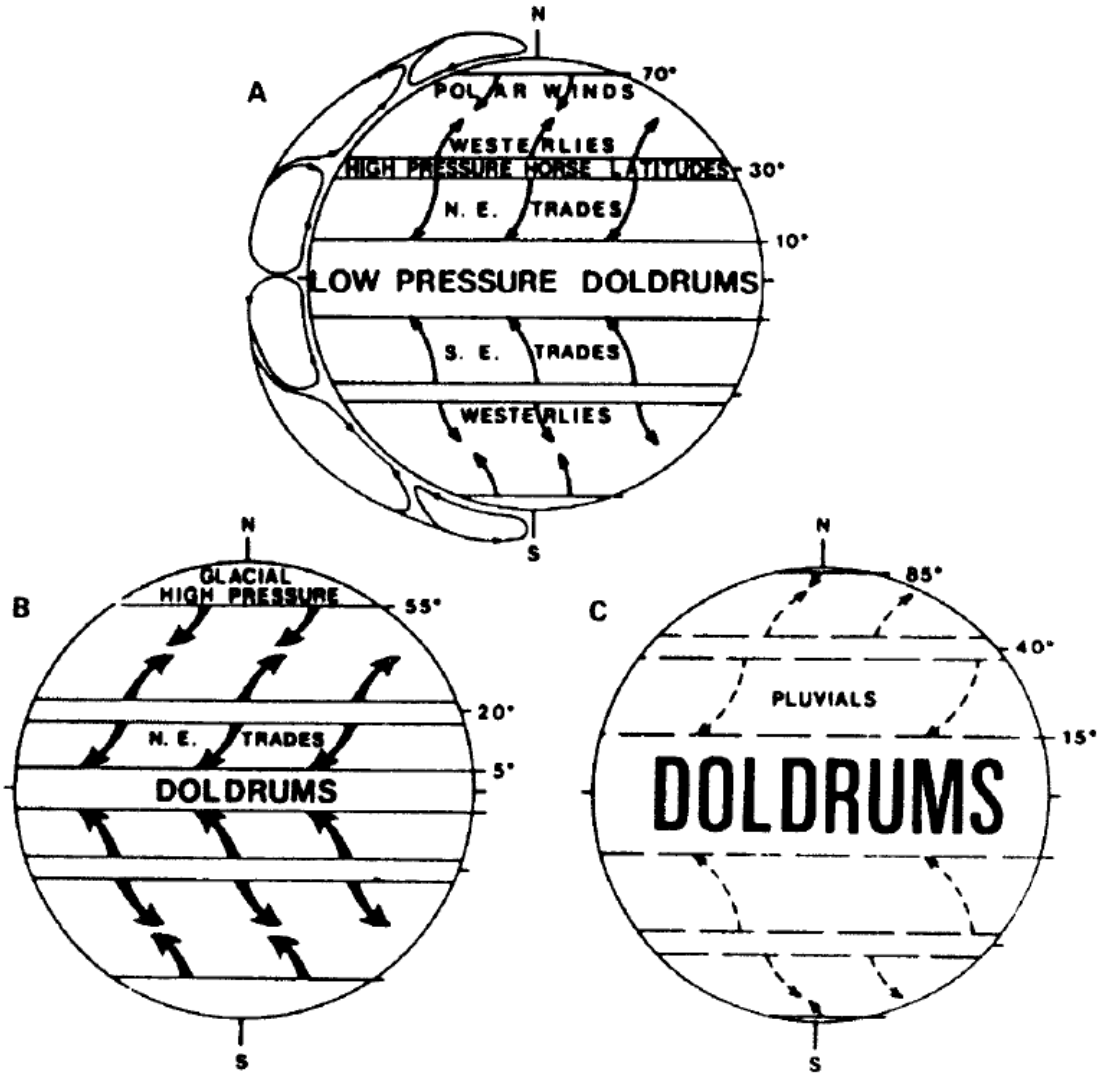

S 21 Conceptual model by Glennie,(1998) showing differences in width and location of Earth's air pressure belts in relation to the size of the polar ice caps (A) shows the present-day wind system, (B). during a Glacial period during the Early Permian, and (C) the wind system during an interglacial.

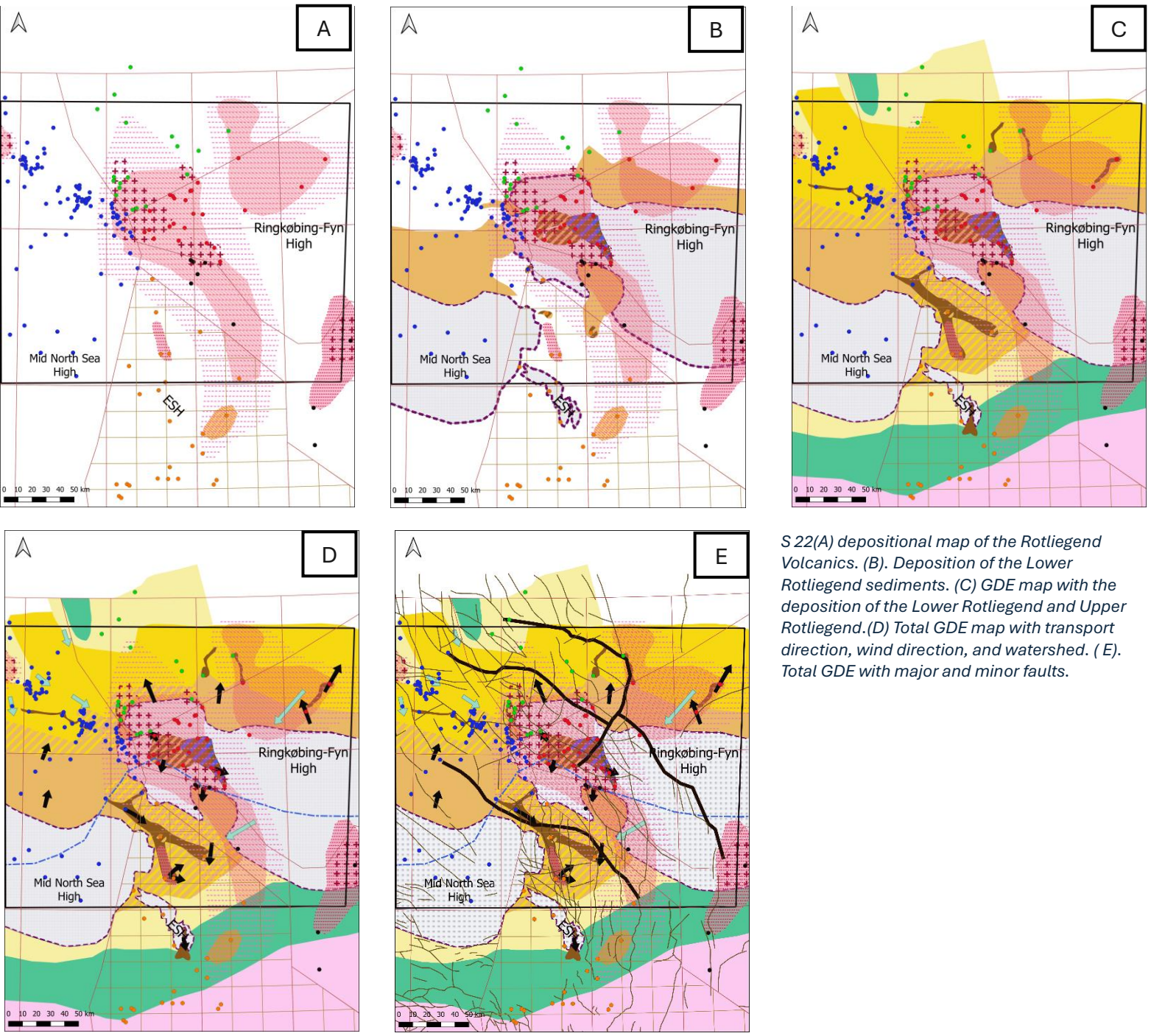

S 22(A) depositional map of the Rotliegend Volcanics. (B). Deposition of the Lower Rotliegend sediments. (C) GDE map with the deposition of the Lower Rotliegend and Upper Rotliegend.(D) Total GDE map with transport direction, wind direction, and watershed. (E). Total GDE with major and minor faults.

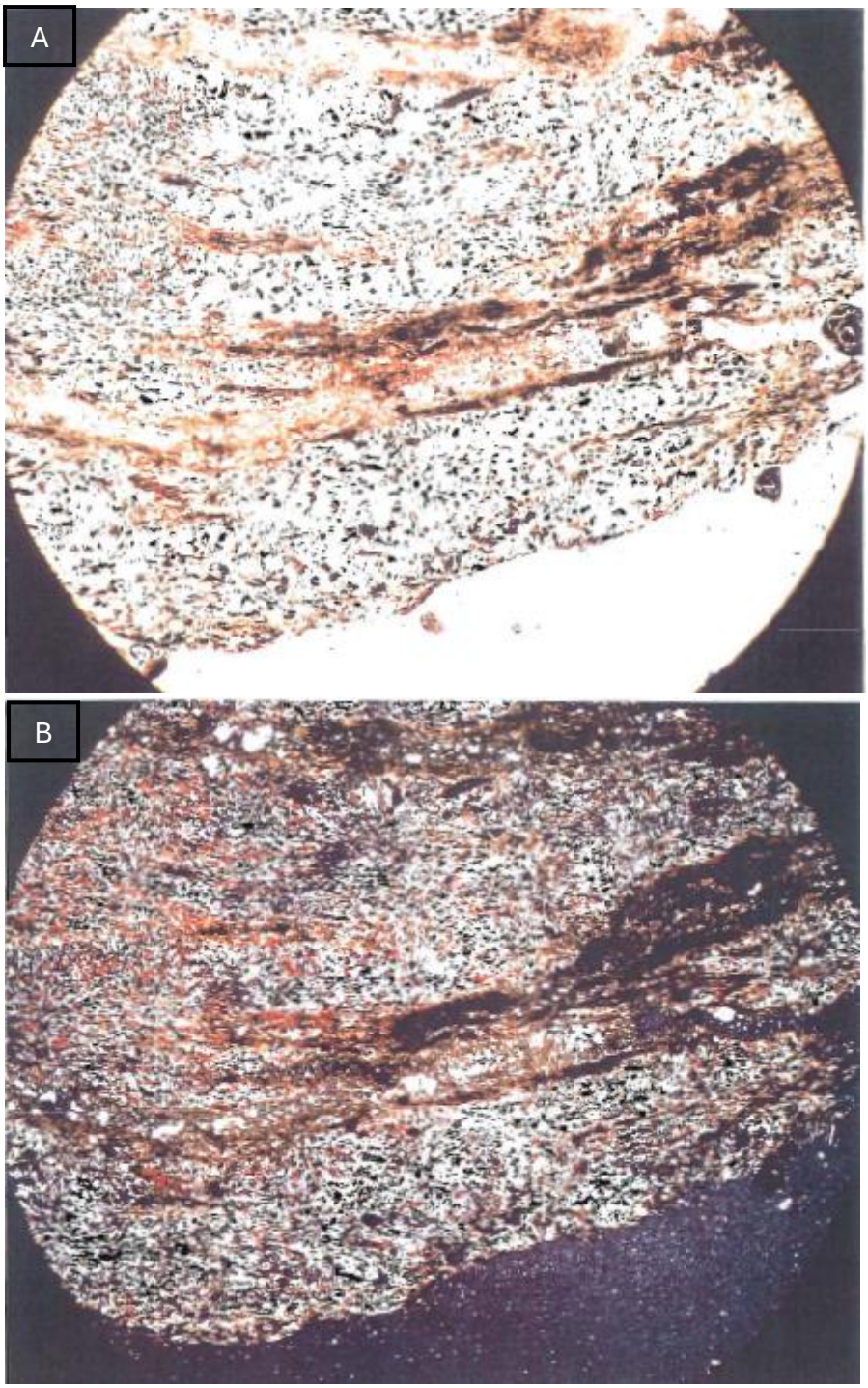

S 23. (A) Thin section image of two sedimentary layers in volcanics(upper and central part) from Heire-1 in plane polarised light (PPL) and in (B) in cross-polarised light (XPL) from GEUS.